

**THERMODYNAMIC STUDY OF
BIOMOLECULES RETENTION
MECHANISM IN CHROMATOGRAPHY**

(クロマトグラフィーにおける生体分子保持機構の熱力学的解析)

令和元年 11 月

João Carlos Simões Cardoso

山口大学大学院創成科学研究科

要旨

近年、抗体タンパク質医薬品をはじめタンパク質医薬品の需要が大幅に増加している。このため、タンパク質医薬品製造プロセスの生産能力の増強が重要な課題となっている。遺伝子組み換え技術の発達により、ここ 10 年の間で培養による生産能力は大幅に増加してきた。しかし、培養液からタンパク質を取り出す工程であるダウンストリームの効率化は十分とは言えず、プロセス全体のボトルネックとなっている。培養液中には目的タンパク質以外に培養細胞や培養細胞由来のタンパク質や DNA が高濃度で含まれる。これらは免疫源性となり重篤な副作用を及ぼす可能性があるため、高度に精製される必要がある。従来、タンパク質医薬品の精製にはクロマトグラフィー分離が用いられてきた。しかし、これまでクロマトグラフィー分離は少量で精度の高い分離を目的として開発されてきており、大容量のサンプルを短時間で処理可能な充填剤の開発は緒についたばかりである。クロマト分離は細孔における拡散抵抗が高速処理において不利となる。このため、従来は数 10 nm 程度であった細孔を 100 nm 程度まで拡大した細孔を有する担体や巨大細孔を有し貫通孔のモノリス担体が開発されている。しかし、細孔径の拡大は吸着面積の減少をもたらし十分な吸着性能が得られない場合がある。このため、細孔構造に加えて、タンパク質の結合を担うリガンド構造を工夫することで吸着性能を向上させる方法も開発されている。従来のリガンドは担体調製後に担体の基材表面近傍に配置されるように基材表面に修飾されてきたが、細孔内においてグラフト重合を行い、グラフト鎖にリガンドを導入することで細孔空間全体にイオン交換基が配置した次世代型のグラフト型クロマト担体が開発されている。グラフト型担体では、リガンドによる閉塞がタンパク質の拡散抵抗を増大させる可能性もあり、リガンド構造の十分な最適化が必要となる。しかし、従来のクロマト担体の評価方法では、クロマト担体の大部分を構成する担体基材の化学的・物理的情報のみが得られるだけであり細孔構造内におけるタンパク質分子の分子レベルでの挙動を解析することは困難である。そこで本研究では、タンパク質の吸着時の反応熱に着目し細孔内における分子レベルでの吸着現象を熱力学的に解析することを試みた。

また、研究対象としてはタンパク質だけでなく分子量が小さく吸着に拡散があまり影響しない低分子化合物も用いており、本論文第 2 章では低分子化合物の吸着現象を、第 3 章では従来型のクロマト担体でタンパク質の吸

着現象を、第 4 章では次世代型のグラフト型担体でのタンパク質の吸着現象を解析した結果をまとめている。以下、各章について述べる。

第 2 章では、カテキンおよびエピガロカテキンを用い、疎水性担体における吸着反応のエンタルピーを求めた。求める手法としては、1)温度毎に測定したクロマト担体における分配係数から反応の自由エネルギー、エンタルピー、エントロピーを計算する方法 2)等温滴定熱量計により反応熱からエンタルピーを計算する方法の 2 種類を行った。2 種類の方法で計算されたエンタルピーはほぼ一致しており、いずれの方法の有効性も示された。またエンタルピー・エントロピーによりカテキンとエピガロカテキンの担体との結合仕様が分子構造の違いを良く反映したものであることが明らかとなった。第 3 章では、第 2 章で確立した解析手法をタンパク質とイオン交換担体との結合の解析に拡張した、分子量・表面電荷の類似した lysozyme および cytochrome C の吸着反応のエンタルピーから、それぞれの反応が発熱反応と吸熱反応と異なることを明らかにした。また、これらの結果はクロマトグラフィーにおけるそれぞれのタンパク質の分配係数の温度依存性を説明するものであり、lysozyme では温度とともに減少し、cytochrome C は温度とともに増加する挙動を示した。

また、担体のリガンドの立体構造が結合に及ぼす違いも熱力学的パラメータを用いて解析しており、リガンドの分岐鎖密度が高い場合は、結合する水の解離や立体障害によりエントロピー支配で反応が進行していることを明らかにした。

第 4 章では、次世代型のグラフト型クロマト担体を用い、牛血清アルブミン BSA を用い担体における相互作用の違いが熱力学的解析により求めたエンタルピーの大きさによく相関できることを明らかにした。また、密にリガンドが配置された場合、エントロピー的に不利になり結合が阻害される可能性があることも熱力学的パラメータを用いて説明することが可能であることを明らかにした。

以上の結果は熱力学的解析手法がクロマト担体細孔のタンパク質の吸着現象を解析可能であることを示すものであり、今後、本解析方法は細孔内におけるリガンド構造を最適化する上で有用な情報を提供可能であると期待できる。

Abstract

Protein adsorption at solid surfaces plays a key role in many natural processes and has therefore promoted a widespread interest in many research areas. Despite considerable progress in this field reviewed in the first chapter, there are still widely differing and even contradictive opinions on how to study and explain observed adsorption phenomena. Thermodynamic analysis of protein adsorption is essential for understanding the binding mechanism and the future design of new separation processes. However, thermodynamic data for proteins adsorption are scarcely available. This study sheds light over the adsorption behavior of molecules onto polymeric chromatography particles.

In the second chapter, temperature effect on the adsorption enthalpy of polyphenols is analyzed. In this chapter, a new method developed in this thesis allows for the enthalpy determination using a linear gradient elution mode, instead of the more commonly used, isocratic elution mode. Resulting in a more robust method and requiring less estimations a priori, while still providing an accurate way to compare enthalpy of adsorption for different molecules. Enthalpy values determined by this novel method are consisting with the values directly measured with isothermal titration calorimetry (ITC), with some exceptions.

In the third chapter, a more complex adsorption mechanism is analyzed. The adsorption of model proteins is analyzed onto ion exchange chromatography (IEC) resins by using ITC to search the answer for the question “why do proteins adsorb?”. As a study system, two similarly charged basic proteins with similar molecular weight, cytochrome c (CytC) and lysozyme (Lys) adsorbing onto cation-exchange chromatography resins was chosen. In a chromatographic column, the retention volume of Lys was larger

than that of CytC. When the temperature increased, the retention volume of CytC slightly increased, whereas that of Lys slightly decreased. This indicates that a more complex mechanism of adsorption may be involved. Large exothermal enthalpies of adsorption were observed when Lys adsorbed onto the cation exchanger. The Lys adsorption was found to be enthalpically driven. On the other hand, endothermic enthalpies were dominant for CytC adsorption, which was entropically driven. This indicates that structural rearrangements, dehydration and release of counter-ions play a major role in CytC adsorption. This is a great example that even similar proteins can have opposite driving forces when adsorption onto the same chromatographic surface. While trying to answer a simple question, a new, more complicated question now emerges “why do similar proteins have different driving forces when adsorbing?”. Each circumstance is a quite unique and we are still very far from a general overarching hypothesis when it comes to the molecular forces that drive protein adsorption.

In the fourth chapter, thermodynamic techniques were used to study more recently devolved chromatography resins: surfaces with grafted-layer ligands. These surfaces were developed to increase the maximum capacity and mass transfer properties in chromatography, with the goal of improving the efficiency and productivity of protein purification. However, a thorough thermodynamic study has yet to be published comparing different types of ligand architecture. In this study, not only the thermodynamic parameters were obtained but these were related with chromatographic data. It was found that the salt needed for protein adsorption on a linear gradient elution is related with the change of enthalpy upon adsorption. Data indicates that bovine serum albumin (BSA) adsorption enthalpy in grafted-layer surfaces varies between exothermic energies ($\Delta H^{\text{ads}} < 0$) and endothermic ($\Delta H^{\text{ads}} > 0$). Solely changing the grafted-layer ligand design, the main interactions between

the protein and the chromatographic surface can vastly differ from being entropic or enthalpically driven.

However, despite the extensive effort of the scientific community, the understanding of protein adsorption remains incomplete. Discrepancies, contradictions and even conflicting views persist concerning such fundamental issues as the nature of driving forces of protein adsorption. Which main reasons have been thoroughly pointed out in this study. Because of its vital significance, protein adsorption is studied here, both experimentally and theoretically. The present study may be useful, but not limited to, the development of new chromatographic surfaces and develop novel downstream processing systems.

Table of Contents

要旨 (Abstract in Japanese)	iii
Abstract.....	vii
Table of Contents.....	xi
Chapter 1: General Introduction	1
1.1 Adsorption.....	2
1.2 Methods for protein adsorption studies.....	4
1.3 Protein Liquid Chromatography	6
1.4 Grafted chromatographic surfaces	8
1.5 Thermodynamics on the study of adsorption	11
1.5.1 Indirect methods.....	13
1.5.2 Direct methods.....	16
1.5.3 Infinite dilution and reference state.....	20
1.5.4 Discrepancies between direct and indirect calorimetric methods	21
Chapter 2: Thermodynamic study of small molecular weight compounds adsorption on chromatographic surfaces	27
2.1 Introduction.....	27
2.2 Material and methods	29
2.2.1 Chemicals	29
2.2.2 Chromatography experiments	29
2.2.3 Isocratic elution.....	30
2.2.4 Linear gradient elution (LGE)	30
2.2.5 Isothermal Titration Calorimetry (ITC).....	31
2.3 Theory.....	31
2.3.1 Isocratic elution.....	32
2.3.2 Linear gradient elution	32
2.3.3 Van't Hoff analysis.....	33
2.3.4 Isothermal titration calorimetry	34
2.4 Results	35
2.4.1 Elution curves	35
2.4.2 Thermodynamics of adsorption.....	38
2.5 Discussion	43

2.6	Conclusions.....	44
2.7	Summary	45
Chapter 3: Adsorption thermodynamics of proteins with similar charge and size onto conventional cation exchange chromatography resins		47
3.1	Introduction	47
3.2	Materials and Methods	49
	3.2.1 Chemicals.....	49
	3.2.2 Linear Gradient Elution.....	51
	3.2.3 Adsorption isotherm experiments	51
	3.2.4 Isothermal titration calorimetry	52
3.3	Theory.....	54
	3.3.1 Thermodynamic analysis	54
3.4	Results and Discussion.....	55
	3.4.1 Gradient elution retention.....	55
	3.4.2 Equilibrium adsorption isotherms.....	58
	3.4.3 Driving force of adsorption.....	60
	3.4.4 Effect of salt and pH conditions near protein isoelectric point	67
3.5	Conclusion	68
3.6	Summary	69
Chapter 4: Grafted ligand architecture effect on protein adsorption enthalpy.....		71
4.1	Introduction	71
4.2	Experimental.....	72
	4.2.1 Ion exchange chromatography	72
	4.2.2 Equilibrium adsorption isotherms.....	75
	4.2.3 Isothermal titration calorimetry	76
4.3	Results and discussion	79
	4.3.1 Linear gradient chromatography and equilibrium adsorption isotherms.....	79
	4.3.2 Thermodynamic analysis	84
4.4	Conclusion	87
4.5	Summary	87
General conclusions.....		89
List of Publications		91
List of Figures.....		93
List of Tables		98

List of Common Abbreviations	101
References	103
Acknowledgments	118

Chapter 1: General Introduction

For the best and safest method of philosophizing seems to be, first to inquire diligently into the properties of things, and establishing those properties by experiments and then to proceed more slowly to hypotheses for the explanation of them. For hypotheses should be subservient only in explaining the properties of things, but not assumed in determining them; unless so far as they may furnish experiments.

Excerpt from Isaac Newton's letter to the Editor P.Pardies. May 21st, 1672. (Bernard Cohen 1958)

In 1672, Isaac Newton's view of science was that we should start by observing the *properties of things*, and then formulate hypotheses that can explain every or most observed facts. Almost 300 years later, Karl Popper, a notorious science philosopher, suggested that before explanations we should have *points of view and theoretical problems*. According to Popper, the researcher should have a hypothesis or a point of view before starting experimenting to confirm or, even more honorable, refute the same hypothesis. Problem and hypothesis are the two links between theory and experiment. Modern science philosophers now attempt to find a middle term between Newton's *explanatory hypothesis* and Popper's *predicting hypothesis*.

To obtain an *explanatory hypothesis* is usually a lot more difficult than it is to obtain a predicting one, besides its rewards are not immediately obvious. *Predicting hypothesis* are paramount for scientific breakthroughs, they are of utmost importance for the success of the scientific projects and programmes. Although this may be true, academia and the industry focus on the *predicting* one and often neglects to search for *explanatory hypotheses*. By understanding a process much knowledge can be gained however, which can be turned into several predicting hypothesis, leading to future discoveries and inventions, and eventually changing the scientific paradigm (Pogany 1985).

All things considered, from both Newton's and Popper's perspective, the current thesis aims to understand the fundamentals of protein adsorption to better understand the intrinsic factors that affect and drive this process.

1.1 ADSORPTION

Almost two decades ago, protein adsorption on solid surfaces was considered a common but very complicated phenomenon (Nakanishi, Sakiyama, and Imamura 2001). In recent years, in the face of the recent advances in the field of protein adsorption, this phenomenon can be considered even more complicated.

Knowledge on the binding behavior of proteins provides valuable insight into the molecular mechanisms of protein interactions in a biological context. Protein adsorption at solid surfaces plays an important role in a number of fields such as biology, medicine, biotechnology and food engineering, and has therefore promoted a widespread interest in different research areas. Due to the nature of each field, each focuses on studying different aspects of protein adsorption. The most significant factors in protein adsorption, summarized in **Table 1.1**, have different relative significance depending on the field of study.

Table 1.1. Various fields or events in which adsorption of proteins onto solid surfaces plays an important role. The open circle symbol (○) indicates the factors that are primarily important in the function or efficiency of the events. Adapted and transformed from (Nakanishi et al. 2001).

Fields or processes	Significant factors				
	Adsorbed amount	Selectivity for adsorption	Orientation and conformation of the adsorbed proteins	Affinity/Distribution coefficient of adsorption	Mass transfer
Enzyme immobilization	○		○		○
Enzyme-linked immunoassay			○		
Design of biocompatible materials	○	○			
Liquid Chromatography	○	○	○	○	○
Filtration	○				
Food manufacturing processes	○				○
Biosensors	○			○	
Cultivation of animal cells and tissue models	○	○			
Drug delivery systems	○			○	
Reaction using soluble enzymes	○				
Blood-material interactions	○			○	

While in some processes one seeks to hinder protein adsorption (e.g. the design of biocompatible implants) because protein adsorption can trigger adhesion of particles, bacteria or cells possibly promoting inflammation cascades or fouling (Elofsson, Paulsson, and Arnebrant 1997; Kalasin and Santore 2009). In immobilized enzymatic reactors, a stable and irreversible adsorption based on covalent bounds is desirable to improve the stability of certain type of reactors.

Further, as an example, to purify a specific protein from a pool of different proteins, preparative liquid chromatography is widely used. In the most common types of liquid chromatography, proteins adsorb to the solid phase but this time via a reversible reaction and then desorb with different conditions. These conditions depend on the type of solid phase, target protein and the purpose of separation. In the field of liquid chromatography, separation selectivity, affinity and mass transfer that different proteins have with the solid phase are the most important aspects for a successful separation. These adsorption factors may not be as relevant in the design of biocompatible implants.

An adsorbent surface can be defined as a thermodynamic phase boundary, where the physical and chemical properties of the adjacent phases change abruptly. Adsorption is the adhesion of a molecule, or adsorbate, from a liquid phase onto an adsorbent surface. Adsorption results from forces between individual atoms, ions, or molecular regions of an adsorbate and the adsorbent surface. Despite the accuracy of this description, this point of view is too simple when it comes to protein adsorption in liquid chromatography. There is an equilibrium between an adsorbed molecule and free molecule on the liquid phase. But in addition, other relevant equilibria are present, as shown in **Figure 1.1**. Important equilibria that are often overlooked when discussing protein adsorption include:

- Water molecules, salt ions interact with both the solid phase and the protein surface. These play a major role in the adsorption process and have a high impact on the adsorption process.
- Proteins, polyclonal anti-bodies, DNA and other biomolecules due to its size and structure, have some degree of flexibility that change upon adsorption.
- Depending on the concentration, proteins can interact with other proteins, adsorbed or not.
- Free ions in the solution also interact with water. Different ions interact with bulk water properties in different ways and consequently change protein charge, conformation and activity (Yang 2009).

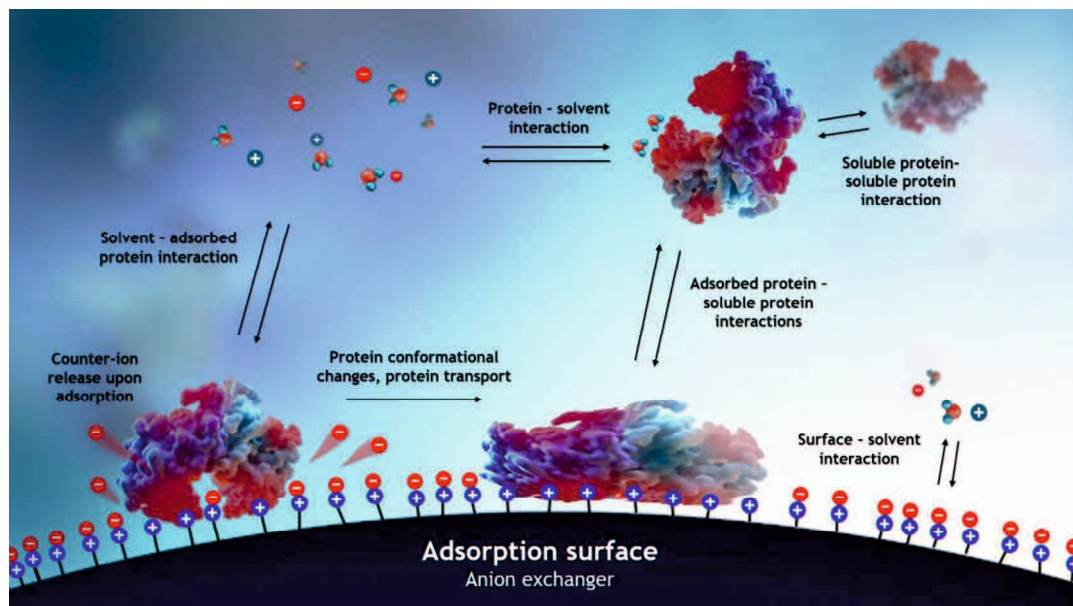


Figure 1.1. Adsorption equilibria. This is a simplified scheme of the equilibria and interactions that are present on protein adsorption onto an anionic surface. Despite most adsorption models taking into consideration some of the overall equilibria, overarching general mechanistic models are still lacking.

1.2 METHODS FOR PROTEIN ADSORPTION STUDIES

Due to the diversity of applications of protein adsorption, there are several techniques that are used to investigate this phenomenon. While some techniques focus on simply measuring the amount of protein that was

adsorbed, others can give us more information at the atomic level. **Table 1.2** summarizes most of the techniques that have been applied to study adsorption.

Table 1.2. Summary of main techniques that can be used to study adsorption. Adapted from (Nakanishi et al. 2001).

¹Search results obtained on scopus.com by searching the technique name followed by the word “adsorption” from 1989 to 2019.

Technique	Principle	Information to be obtained	¹ Popularity in the last 30 years	References
Depletion / Mass balance	Measurement of the decrease in solute concentration over time after incubation with a solid surface.	Amount of adsorbed molecule	3635	(Liu et al. 2012; Oberholzer and Lenhoff 1999; Wang et al. 2019)
Radiotracer	Decrease in concentration of radioisotope-labeled molecules in solution. Radioactivity on surface due to radioisotope-labeled molecules adsorbed.	Amount of molecules adsorbed from single- and multi-component solutions. Amount of irreversibly adsorbed molecules.	1685	(Ubiera and Carta 2006)
Quartz crystal microbalance (QCM)	Change in oscillating frequency of piezoelectric devices upon mass loading	Courses of adsorption and desorption. Amount of irreversibly adsorbed molecules.	3709	(Kaufman et al. 2007)
Enzyme-linked immunosorbent assay (ELISA)	Epitope recognition by primary antibodies	Amount of irreversibly adsorbed molecules	1280	(Salim et al. 2007; Zhou et al. 2012)
Ellipsometry	Change in the state of polarized light upon reflection	Amount of adsorbed protein and thickness of the protein layer.	2508	(Seitz, Brings, and Geiger 2005)
Total internal reflection fluorescence	Fluorescence due to surface-adsorbed molecules excited by evanescent field	Amount of fluorophores adsorbed on surface	253	(Arima and Iwata 2007)
Neutron reflection	Reflectivity of neutrons at solid-water interface	Amount of adsorbed protein and thickness of the protein layer. Multi or mono-layer adsorption.	503	(Lu, Zhao, and Yaseen 2007; Zhao, Pan, and Lu 2009)
Fourier transform infrared spectroscopy (FTIR)	Change in infrared absorption spectrum of protein on adsorption	Conformation of protein adsorbed on surface	28716	(Tsai et al. 2011; Wang et al. 2019)
Fluorescence correlation spectroscopy	Change in fluorescence spectrum of protein on adsorption	Conformation of protein molecules on surface	4218	(Röcker et al. 2009; Tsai et al. 2011)
Atomic force microscopy (AFM)	Images the topography of a sample surface by scanning a cantilever over a region of interest.	High-resolution images of adsorption surfaces. Determination of interaction forces between biological molecules and surfaces.	9045	(Servoli et al. 2008; Willemsen et al. 2000)
Dynamic light scattering	Measurements of particle size analysis in the nanometer range.	Change in hydrodynamic radius and diffusion constant. Used to study adsorption on nanoparticles	23018	(Tsai et al. 2011)
Nuclear magnetic resonance (NMR)	Atomic interaction between surface and molecule	Relative distance of atoms compared with the native state	7871	(Hao et al. 2016)
Isothermal titration calorimetry (ITC)	Heat changes upon adsorption. Batch process	Adsorption thermodynamic parameters	419	(Baker and Murphy 1996; Beyer and Jungbauer 2018; Blaschke et al. 2011; Blaschke, Werner, and Hasse 2013; W. Y. Chen et al. 2007; Chen et al. 2003; Cliff, Gutierrez, and Ladbury 2004; Gill et al. 1995; Huang et al. 2000; Kabiri and Unsworth 2014; Lin et al. 2001a, 2001b, 2000; Mirani and Rahimpour 2015; Ueberbacher et al. 2010; Werner, Blaschke, and Hasse 2012; Werner, Hackemann, and Hasse 2014)
Flow Microcalorimetry (FMC)	Heat changes upon adsorption. Dynamic process	Adsorption thermodynamic parameters	223	(Desch, Kim, and Thiel 2014; Dias-Cabral et al. 2005; Dias-Cabral, Queiroz, and Pinto 2003; Esquibel-King et al. 1999a, 1999b; Katiyar et al. 2010; Phillips and Pinto 2004; Rosa et al. 2018; Silva et al. 2014; Thrash and Pinto 2001)
Monte carlo simulations	Computerized mathematical technique that allows the calculation of one optimal solution.	Estimation of thermodynamic parameters, equilibrium simulation and diffusion	6305	(Ustinov 2019; Vuong and Monson 1996; Zhang et al. 2014)
Molecular dynamics simulation	Computational simulation at atomic level.	Estimation of patterns, properties of protein behavior, conformational changes that a protein or molecule may undergo	12535	(Ganazzoli and Raffaini 2019; Zhang et al. 2014)

Still many problems exist at present that need to be solved or clarified, such as the difficulties in experimental examination and regulation of protein orientation or conformational transitions at surfaces, the effect that ligand architecture has on adsorption, and the micro-scale elucidation of surface transport mechanisms. The study of protein dynamics in the lab is a very complicated, expensive, and time-consuming process. Therefore, a lot of effort and hope lies with the computers and the *in silico* study of protein structure and molecular dynamics (Vlachakis et al. 2014). We should keep in mind the molecular dynamics view and be careful about general conclusions. Protein behavior is very unique, and adsorption is specific to the interacting domains of the protein and to the surface.

Some of the technological problems are being studied by using molecular simulations combined with theoretical and experimental investigations (Yu, Zhang, and Sun 2015). Especially in the field of liquid chromatography, a deep combination of theoretical approaches, experimental data and computer simulation are paramount to elucidate the mechanism of adsorption.

1.3 PROTEIN LIQUID CHROMATOGRAPHY

Production of therapeutic proteins and monoclonal antibodies have seen a substantial increase in productivity over the last decades. However, this rapid development of fermentation is not being followed by development of large scale separation and purification processes, also referred as downstream processes. Downstream processes are now the main bottleneck of the protein production with costs reported to account for 50 to 90% of the overall production costs for most recombinant therapeutic proteins (Kawai, Saito, and Lee 2003; Müller 2005). This process requires multiple steps of filtration and chromatography and some proteins undergo as many as ten different

procedures to achieve its final purified form. Preparative chromatography, i.e. chromatography used in downstream processing, is widely used as a final separation technique in the pharmaceutical industry (Marston, Hostettmann, and Hostettmann 1986).

Especially in preparative chromatography, the physical properties of the chromatographic surface dictate the efficiency of the overall process. These surfaces are designed so that the backbone is compatible with biomolecules, and separation can be performed in aqueous buffers.

Alternatively, another use of chromatography relies on analytical applications. Analytical chromatography objective is the separation of molecules with the final goal of analysis, quantification, identification (Cherry 1988) as well as studies of the protein's structure (Alberts et al. 2002), post-translational modifications (Huang et al. 2014) and function (Alberts et al. 2002; Matsuda et al. 2012).

The industry usually use the type of ligand to define chromatography modes. The ones that are compatible with preparative chromatography are the following:

- Affinity chromatography (AC) or Biospecific chromatography (BIC)
- Ion exchange chromatography (IEC); anion (AEC) or cation (CEC)
- Hydrophobic interaction chromatography (HIC)
- Size exclusion chromatography (SEC)
- Mixed-mode chromatography or multi-modal chromatography (MMC)
- Metal chelate chromatography (MIC)

Depending on the impurities, the selectivity of each mode varies and usually more than one chromatography mode is used in sequence in a multi-step downstream process. For example, HIC and IEC are often used sequentially to process complex mixtures. Moreover, purification can be achieved by binding the protein of interest and then elute it (classic elution chromatography) or by binding the impurities and allowing the target

molecule to flow-through the chromatographic particles (flow-through or frontal chromatography).

Even with the recent developments in the field of adsorption, chromatographic surfaces have been developed mainly by trial-and-error methods. In order to perform a rational design of new chromatographic surfaces for biomolecule separation, researchers from different fields have been conducting research in order to understand different parts of the adsorption process, shown in **Table 1.3**. The present work focusses on the molecular level of the adsorption process. This is essential for the rational ligand design of new chromatographic surfaces.

Table 1.3. Adsorption mechanisms subtopics applied to chromatography

Adsorption mechanism sub-topics applied to chromatography
Molecular interactions between protein and surface
Characterization of chromatographic surfaces
Protein binding orientation
Protein conformational alterations and protein aggregation
Mass transfer

1.4 GRAFTED CHROMATOGRAPHIC SURFACES

The rational design of chromatographic surfaces applied to macromolecules date back to 1956, when Peterson and Sober developed a cellulose bead in which proteins could enter and diffuse (Peterson and Sober 1956). Now, commercially available protein chromatography surfaces are usually carefully produced porous beads with diameters between 15-200 μm and pore sizes between 20-0.003 μm that are then packed into a column. Chromatography particles, without pores or monolithic columns are occasionally used in cases in which is difficult for the target molecule to get in/out the pore, for example, for large proteins or macroparticles like viruses, phages or even cells. These bead pores can be functionalized by the surface manufacturer with the desired ligand depending on the desired chromatography mode. If the ligand is

negatively charged this will result in cation-exchange chromatographic beads with charged ligands covalently bound to the pore walls. Alternatively, the beads pores can be partially or completely filled either with a cross-linked gel or with grafted polymers, which provide a net of tentacles or “hydrogel” features for macromolecule capture (**Figure 1.2**).



Figure 1.2. Pores of grafted chromatography surface beads. (A) conventional type with charged ligands covalently bound to the pore walls, (B) grafted polymers as spacers, (C) cross-linked gel polymer network.

Verlaan, Bootsma and Challa reported the first application of a grafted polymer on spherical beads in 1982. Although the original goal of this functionalization was mainly heterogenous catalysis for the oxidative coupling of phenols, it ended up being used in separation science in an attempt to increase the maximum binding capacity of chromatographic surfaces. Maximum binding capacities and mass transfer properties have been the main focus point of optimizations by the chromatography industry (Müller 2003, 2005; Verlaan, Bootsma, and Challa 1982).

Whether the protein transference from the liquid phase to the grafted layer can be considered *adsorption* is the cause of some disagreement in the field. Instead of adsorption, some authors consider this as a partition effect from one medium to another. As an example, ionic liquid separation of proteins is never called adsorption from one liquid phase to another. However, since the grafted layer has distinct thermodynamic properties than the aqueous solution, this transference will be considered *adsorption* in this work. Depending on the length and density of the grafts, this can be more or less similar with conventional adsorption onto a surface.

Grafting is usually applied to ion exchange chromatography because equally charged polymer chains repel each other providing a three-dimensional space for proteins to travel into the “forest” of the extended polymer chains. Grafts were applied to HIC surfaces but there was no significant changes in the maximum binding capacity of these resins, because at high salt concentrations, the hydrophobic tentacles attract each other and collapse, leaving no water molecules or ions between the arms, preventing the formation of an hydrogel structure and the protein penetration (Kawai et al. 2003; Müller 2003).

Subprocesses of protein adsorption

In the present, there is no technique that single handed can explore the dynamics of protein adsorption, which restricts not only the adsorption mechanism understanding, but the ligand design and process optimization (Moo-Young 2011). Nevertheless, some light has been shed on this from a theoretical point of view. According to Yamamoto et al. and Lin et al., the binding process of different biomolecules onto respectively, ion exchange and hydrophobic resins are similar and can be divided into at least five subprocesses (Ee 1996a, 1996b; Huang et al. 2000; Lin et al. 2000, 2001b; Lin, Chen, and Hearn 2002):

1. Dehydration or/and removal of the protein electrical double layer (EDL);
2. Dehydration or/and removal of the solid phase EDL;
3. The interaction between the protein and the solid phase;
4. The structural rearrangement of the protein upon adsorption;
5. Rearrangement of the excluded water or/and ion molecules in bulk solution.

Although these subprocesses are shown in order, it is hard to believe that proteins molecules wait for other proteins to be dehydrated before adsorption. Latest thermodynamic results indicate that there is no clear boundary of one process to another and these subprocesses can be simultaneous and overlap with each other (Aguilar et al. 2014; Marques et al. 2014; Silva et al. 2014).

1.5 THERMODYNAMICS ON THE STUDY OF ADSORPTION

Thermodynamics has been used successfully applied to the study of biomolecule interactions and hence, protein adsorption studies. **Table 1.2** shows some of these studies in which calorimetry is used. The main advantage of these methods is that there is no requirement for labels or molecular markers. The heat released, or needed, upon adsorption can be obtained with proteins and surfaces at real adsorption conditions. However, data interpretation can be an arduous task due to all the interconnected subprocesses and equilibria explained above.

Thermodynamic parameters of adsorption such as change in enthalpy ΔH , free energy ΔG , entropy ΔS , and heat capacity Δc_p can be determined either with direct methods or indirect methods. Direct methods are calorimetric methods that measure the enthalpy of adsorption directly in real time such as ITC and FMC. When the thermodynamic parameters are derived from experiments that do not measure heat, these are called indirect methods, i.e. indirectly applying van't Hoff analysis to chromatographic experiments.

For a reaction to occur spontaneously like adsorption, the Gibbs free energy of the initial state ($G_{initial}$) is necessarily higher than that G_{final} of the state towards which the reaction is heading. In an equation form:

$$\Delta G = G_{final} - G_{initial} \leq 0 \quad (1)$$

where ΔG is the amount of energy available for chemically driven work. The change in Gibbs free energy differs from the enthalpy change (ΔH) in that it

does not include contributions to energy arising from volume or pressure changes, nor does it include the entropic contributions ($T\Delta S$).

In liquid chromatography of biomolecules, temperature, pressure and chemical potential of the solvent usually remain constant. Under these conditions, Gibbs energy of the adsorbing protein (G_i) is related to its molar concentration (C_i) and protein activity coefficient (γ_i) by the following equation (adapted from (Winzor and Jackson 2006a)):

$$\Delta G_i = \Delta G_i^0 + RT \ln(C_i \gamma_i) \quad (2)$$

where G_i^0 is the standard free energy defined under the constraints of constant temperature and solvent chemical potential (reference state); R is the gas constant and T is the absolute temperature.

A simple protein adsorption reaction can be written as $L \rightleftharpoons S$ where L and S is the free protein in liquid phase and solid phase, respectively. The free energy change, $\Delta G = G_S - G_L$ can be written as:

$$\Delta G = \Delta G^0 + RT \ln\left(\frac{C_S \gamma_S}{C_L \gamma_L}\right) \quad (3)$$

In practice the ratio of activity coefficients may be taken as unity ($\gamma_S/\gamma_L \approx 1$) if we use sufficiently dilute solutions for the system to approach thermodynamic ideality. Assuming, infinite dilution conditions, in equilibrium, $\Delta G = 0$ in equations 2 and 3, the standard free energy change under conditions of thermodynamic ideality is related to the equilibrium concentrations of participating species by the following expression

$$\Delta G^0 = -RT \ln\left(\frac{C_S^e}{C_L^e}\right) \quad (4)$$

where the superscripts e are used to identify concentrations at adsorption chemical equilibrium. Since the distribution coefficient K is, by definition, the ratio of equilibrium concentrations, equation 4 can be expressed as

$$\Delta G^0 = -RT \ln K \quad (5)$$

On the other hand, if described with the dissociation ratio $K_d = C_L^e / C_S^e$, the relationship becomes

$$\Delta G^0 = RT \ln K_d \quad (6)$$

Although ΔG^0 is enough to define the energetics of protein adsorption, there are considerable advantages in its breakdown into enthalpic (ΔH^0) and entropic contributions (ΔS^0) that can be represented by the generally known Gibbs-Helmholtz equation,

$$\Delta G^0 = \Delta H^0 - T\Delta S^0 \quad (7)$$

The behavior of proteins in adsorption is a net result of various types of interactions already mentioned in previous section. If the entropy term contributes to ΔG in such a way that it becomes negative, the process is called entropy driven; if exothermic enthalpy values are dominant, leading to a negative ΔG^0 , the process is termed enthalpy driven.

From enthalpic contributions, we can gain molecular insight on the nature of the predominant noncovalent interactions responsible for adsorption. For example, hydrogen bonding and ionic interactions are generally enthalpically driven (negative ΔH^0) whereas hydrophobic interaction derive their strength from a positive ΔS^0 that outweighs the consequences of any enthalpic contributions.

Currently there is no list or detailed separation between enthalpically driven events from entropically driven ones due to their inseparable nature. The enthalpy change depends on the entropy change and vice versa. A common outcome of thermodynamics studies is the widely discussed enthalpy-entropy compensation, the occurrence is a conclusion in several studies, but it is already an obligatory consequence when using equation (7) used to calculate the thermodynamic parameters.

1.5.1 Indirect methods

Combining and rearranging expressions (5) and (7) gives:

$$\ln K = -\frac{1}{T} \frac{\Delta H^0}{R} + \frac{\Delta S^0}{R} \quad (8)$$

also known as the van't Hoff equation. Considering standard entropy and enthalpy change to be temperature independent, then allows the determination of ΔH^0 and ΔS^0 for a combination of experiments in which K varies with temperature. From the slope ($-\Delta H^0/R$) and ordinate intercept ($\Delta S^0/R$) of a linear dependence of $\ln K$ upon $1/T$ (**Figure 1.3**).

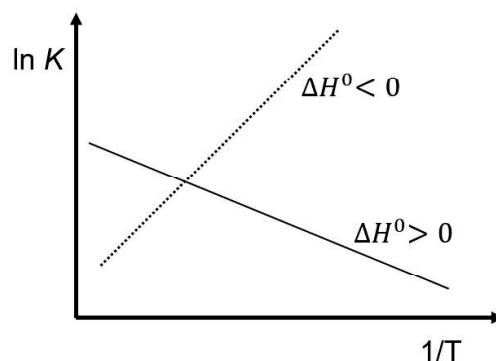


Figure 1.3. van't Hoff plot. By plotting $\ln K$ versus $1/T$, standard enthalpy change can be directly determined from the slope of the obtained curve ($-\Delta H^0/R$), and standard entropy change from ordinate intercept ($\Delta S^0/R$).

In order to apply the van't Hoff equation to biological sciences, we must have in mind all the assumptions that were needed to derive the equation.

Table 1.4 summarizes the assumptions that were done for the obtention of the expressions leading to the van't Hoff equation. Especially noteworthy, entropy-enthalpy compensation cannot be concluded or confirmed when using van't Hoff analysis, since it is a central prior assumption.

Table 1.4. Assumptions for linear van't Hoff expression in chromatography

Assumptions for linear van't Hoff expression in chromatography
The system is in equilibrium $\Delta G=0$
ΔH^0 is temperature independent
ΔS^0 is temperature independent
Δc_p^0 is temperature independent
Enthalpy and entropy are interconnected (entropy-enthalpy compensation)
Infinite dilution system ($\gamma_s/\gamma_t \approx 1$)

On the same chromatographic surface, there are different binding sites with different local energy minimums, i.e. not all proteins adsorb in the same exact conditions on the same surface. The thermodynamic quantities associated the van't Hoff are believed to represent average values due to the heterogeneity of the chromatographic surface (Haidacher, Vailaya, and Horváth 1996).

Temperature affects physical properties of the chromatographic media and the protein (Huang et al. 2000; Silva et al. 2014; Tilton, Dewan, and Petsko 1992; Werner et al. 2014). Thus, is it correct to use the linear van't Hoff expression assuming ΔH^0 and ΔS^0 are temperature-independent? When ΔH^0 and ΔS^0 are temperature dependent, the integrated form of Kirchoff's law is used to evaluate the thermodynamic quantities resulting in a quadratic equation:

$$\ln K = a + \frac{b}{T} + \frac{c}{T^2} \quad (9)$$

where

$$\Delta H^0 = -R\left(b + \frac{2c}{T}\right) \quad (10)$$

$$\Delta S^0 = R\left(a - \frac{c}{T^2}\right) \quad (11)$$

$$\Delta c_p^0 = \frac{2Rc}{T^2} \quad (12)$$

Here, the linear equation assumes constant Δc_p^0 , equation (9) allows for the determination of ΔH^0 and ΔS^0 for cases that are temperature dependent.

The quadratic fit is more commonly used in hydrophobic exchange chromatography because it is assumed that temperature affects this mode in more significant ways and HIC often exhibits nonlinear van't Hoff plots (Chen et al. 2003; Rodler et al. 2019; Rowe et al. 2008; Ueberbacher et al. 2010). But it has also been applied to ion exchange chromatography in non-linear van't Hoff plots (Marques et al. 2014). It is still lacking a study on the differences

between the thermodynamic parameters determined from linear and quadratic expressions in the case of protein adsorption.

1.5.2 Direct methods

Direct methods for thermodynamic parameters determination include Isothermal titration calorimetry (ITC) and Flow microcalorimetry (FMC). Although sharing a similar goal, ITC works with two cells and measures heat compensation as it will be explained further in this section, FMC works in a continuous mode and does not need a reference cell and measures heat transfer directly. Since this study uses ITC as the only direct method, FMC mode of operation will not be extensively addressed in this chapter.

But why are these techniques capable of measuring thermodynamic parameters of chemical reactions? The enthalpy change of a system is defined as the sum of the change in internal energy of that system (ΔU) and the change in the total volume (ΔV):

$$\Delta H = \Delta U + \Delta V \quad (13)$$

Protein adsorption occurs in virtually incompressible aqueous media ($\Delta V = 0$), this renders ΔH essentially synonymous with the change in internal energy ($\Delta H = \Delta U$). By definition:

$$\Delta U = \Delta Q - \Delta W \quad (14)$$

where ΔQ is the heat exchange of the adsorption reaction and ΔW is the change in work which is approximately 0 in molecular reactions. Leading to

$$\Delta H = \Delta Q \quad (15)$$

ITC, which directly measures ΔQ , can effectively measure the change of enthalpy of protein adsorption.

ITC application to biological systems is mostly used in studies between proteins and ligands (Baker and Murphy 1996; Cliff et al. 2004; Connelly et al. 1994; Duff, Grubbs, and Howell 2011; Færgeman et al. 1996; Moo-Young 2011;

Winzor and Jackson 2006b), aggregation or folding (Kabiri and Unsworth 2014; Makhatadze and Privalov 1993), conformational alterations and adsorption. It does not rely on the presence of chromophores or fluorophores, nor does it require an enzymatic assay. Because the technique relies only on the detection of a heat effect upon binding by measuring the heat compensation needed to maintain two cells at the same temperature.

Figure 1.4 shows a simplified scheme of the ITC system. In the case of protein adsorption studies, in the beginning of the calorimetric titration experiment, the reference cell is usually filled with distilled degassed water (Solution B in **Figure 1.4**). The main cell is filled with slurry resin suspension, i.e., chromatography resin mixed with buffer (Solution A in **Figure 1.4**). The syringe is then filled with the protein solution (Solution C in **Figure 1.4**). The system is closed and the chromatographic surface is kept under suspension by agitation.

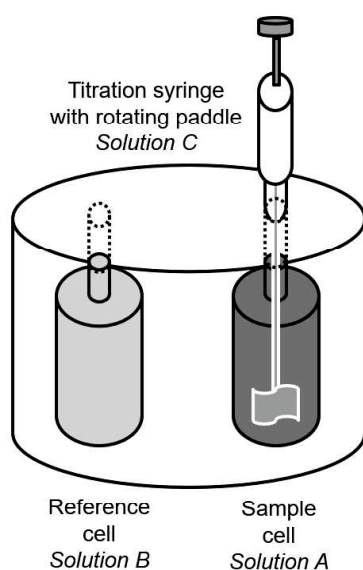


Figure 1.4. Isothermal titration calorimeter scheme. reference cell is usually filled with distilled degassed water (Solution B). The main cell is filled with slurry resin suspension, i.e., chromatography resin mixed with buffer (Solution A). The titration syringe is containing the protein solution (Solution C) which then is injected periodically

Approximately forty years ago, Norde and Lyklema applied ITC to the study of protein adsorption to solid surfaces and it has been used since then. ITC measures the heat effect when an aliquot of ligand solution is added to a

protein solution. When the binding is of moderate affinity, ITC can be used to determine an observed binding constant, K , and an observed enthalpy change, ΔH^0 . When the binding is of high affinity ($>10^8$), ΔH^0 can still be determined with high precision, even though K cannot be determined (Baker and Murphy 1996; Freire, Mayorga, and Straume 1990; Norde and Lyklema 1979; Wiseman et al. 1989).

A typical ITC thermogram, for moderate K obtained with ITC is shown in **Figure 1.5**. In the beginning, protein/ligand is injected into the cell and it will react with the other protein/ligand suspended on the sample cell. During the interaction, heat is released, or absorbed by the protein-ligand system. As more injections continue, the heat released/absorbed start to decrease due to the lack of more available binding sites. Finally, we have small constant peaks because interaction is no longer occurring due to the lack of reaction species. Only the dilution heat of the protein/ligand being injected in the cell is measured. If the peak area is represented versus time, a typical thermogram results in a curve with a sigmoidal shape.

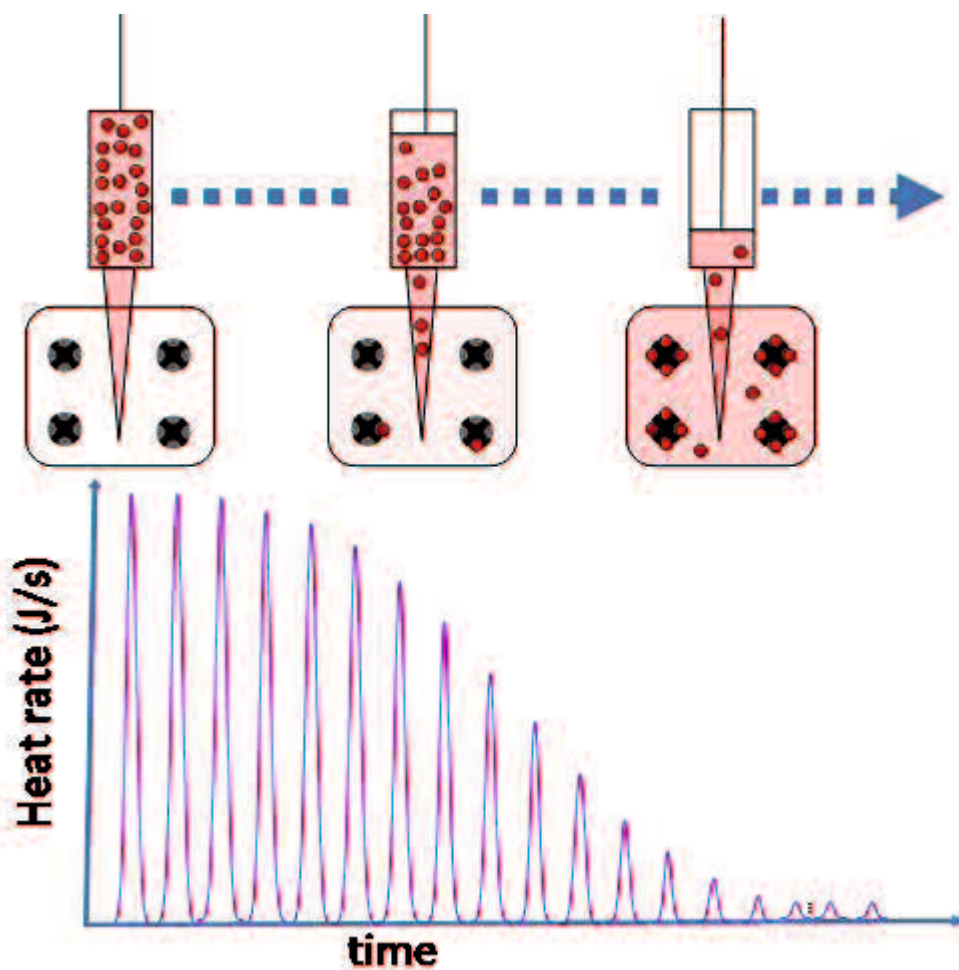


Figure 1.5. Typical thermogram for a reaction with a moderate K value. The enthalpy of adsorption can be directly determined from the area of the first peaks. The area of the smaller, later peaks occur due to dilution heat.

In the case of protein adsorption in ionic exchange surfaces, K is usually very high. **Figure 1.6** shows a thermogram obtained in a reaction with a high K . This leads to high peaks that never reach a saturation of the total binding sites. Making the obtention of a curve with sigmoidal shape more difficult. However, it is also possible to obtain dilution heat and adsorption heat in different experiments as also shown in **Figure 1.6**. After subtracting the dilution heat, also called *blank trials*, from protein into surface injections, we can determine the effective adsorption heat that is released or used upon adsorption. Finally, assuming infinite dilution conditions, we can determine the molar enthalpy change of adsorption for any given protein/surface system.

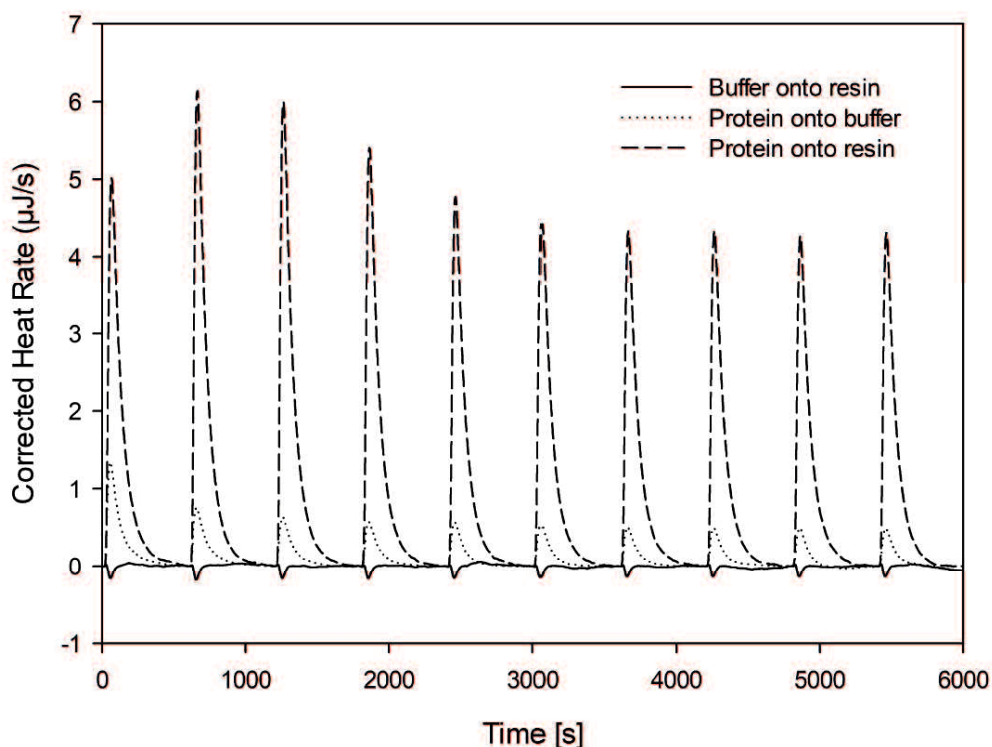


Figure 1.6. Typical thermogram for a reaction with a high K value. Thermograms obtained titrating BSA monomer at 20 mg/mL onto Toyopearl Q600AR and the respective blank trials. Buffer was 10 mM TRIS, 30 mM NaCl at pH 7, 25°C.

1.5.3 Infinite dilution and reference state

As explained in beginning on this section, infinite dilution conditions are a main assumption of most thermodynamic equations used for data interpretation. The following well known fundamental thermodynamic relation is used in the subsequent derivations already derived by previous authors (Atkins and De Paula 2010; Blaschke et al. 2011):

$$\left(\frac{\partial \left(\frac{\mu}{T}\right)}{\partial T}\right)_{p,n} = \left(\frac{\partial \left(\frac{G}{T}\right)}{\partial T}\right)_{p,n} = -\frac{H}{T^2} \quad (16)$$

where the subscripts p and n refer to constant pressure and constant composition (closed system). The chemical potential in aqueous solutions (μ) can be described by

$$\mu = \mu^0 + RT \ln(C_i \gamma_i) \quad (17)$$

For infinite dilution ($\gamma_i = 1$), this equation formally reduces to

$$\mu^\infty = \mu^0 + RT \ln C_i^\infty \quad (18)$$

where

$$C_i^\infty = \lim_{C_i \rightarrow 0} C_i \quad (19)$$

Dividing equation 18 by T results in

$$\frac{\mu^\infty}{T} = \frac{\mu^0}{T} + R \ln C_i^\infty \quad (20)$$

And differentiating with respect to the respect to T under consideration of equation 16, it follows

$$-\frac{H^\infty}{T^2} = -\frac{H^0}{T^2} \quad (21)$$

And thus,

$$H^\infty = H^0 \quad (22)$$

Hence, if the enthalpy obtained calorimetrically was obtained in infinite or close to infinite dilution equals the enthalpy in the reference state we have:

$$\Delta H^\infty = \Delta H^0 \quad (23)$$

In practice, this means that in order to use and compare thermodynamic parameters with enthalpy obtained using van't Hoff analysis we should determine the adsorption enthalpy at low concentrations ($C_s \rightarrow 0, C_l \rightarrow 0$) or take data points at several concentrations and extrapolate the observed ΔH^0 to infinite dilution (Werner et al. 2012, 2014).

1.5.4 Discrepancies between direct and indirect calorimetric methods

Theoretically, thermodynamic parameters, being state properties, should not depend on the method of determination. Nevertheless, discrepancies between direct and indirect calorimetric methods are extensively reported in the literature. **Table 1.5** summarizes most of these studies. However, the reason of the discrepancy is still subject of some controversy. The main hypotheses on the reason why direct methods vary from indirect are as follows.

Direct methods include more contributions. Some authors state that direct methods includes other contributions of buffer protonation and desolation

that are not considered in van't Hoff analysis (Castellano and Eggers 2013; Chen et al. 2003; Færgeman et al. 1996; Liu and Sturtevant 1995). Nevertheless, Liu et al. (Liu and Sturtevant 1995, 1997) associated the calorimetric methods with the true enthalpy value and associated the van't Hoff analysis results with the apparent enthalpy value because the Gibbs free energy and K , lacks contributions to the system thermodynamics. They also mentioned the possible role of desolation, which is not included in van't Hoff analyses, while noting the inherent difficulty in measuring changes in hydration. On the other hand, Færgeman, et al. also noted a discrepancy between $\Delta h^{\text{ads,ITC}}$ and $\Delta h^{\text{ads,vH}}$, and chose to refer to $\Delta h^{\text{ads,vH}}$ as the intrinsic value instead. Also stating that $\Delta h^{\text{ads,ITC}}$ as being the sum of $\Delta h^{\text{ads,vH}}$ and all possible concomitant reactions which may accompany the binding reaction but do not directly influence the intrinsic binding constant K (Færgeman et al. 1996).

Different experimental conditions. Horn et al. concluded that discrepancies between $\Delta h^{\text{ads,ITC}}$ and $\Delta h^{\text{ads,vH}}$ arise from different experimental conditions, and that for closed systems, in theory, $\Delta h^{\text{ads,ITC}}$ and $\Delta h^{\text{ads,vH}}$ should be the same, regardless of the type or degree of linked equilibrium (e.g., conformational changes, ion binding, dehydration) (Horn, Brandts, and Murphy 2002)

Protein conformational changes. Protein conformational changes upon adsorption which are not accounted for by van't Hoff analysis in liquid chromatography but are accounted in ITC experiments (Chen et al. 2003; Rodler et al. 2019; Ueberbacher et al. 2010).

The thermodynamic equilibrium is not reached. In order to determine enthalpy changes with indirect methods we have to assume that the system is in equilibrium, this assumption is not needed when using calorimetric methods. There is no guarantee that the thermodynamic equilibrium is reached, hence the deviation between these two methods (Werner et al. 2014);

Linear van't Hoff equation does not account for heat capacity. The linear form of van't Hoff equation (equation 8) does not account for changes in enthalpy with different temperatures (Chaires 1997; Liu and Sturtevant 1995).

Indirect methods do not correctly determine changes in entropy. van't Hoff equation overlooks the contribution for total entropy of the system (Weber 1996).

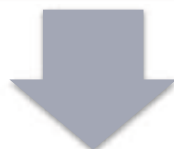
Table 1.5. Summary of discrepancies found in literature between indirect and direct methods for enthalpy determination. Note that not all of them apply to adsorption studies.

Reference	Analysis method	Model system	Simple description of results and hypothesis
(Werner et al. 2014)	Van't Hoff (chromatography), Van't Hoff (adsorption equilibrium isotherms), ITC	Lysozyme, HIC	Pegylated lysozyme adsorption onto HIC media is endothermic. Van't Hoff analysis was conducted using K determined with two different techniques, chromatography and equilibrium isothermal adsorption curves. Resulting ΔH agreed well, but there were discrepancies when comparing with direct methods (ITC). ΔH^{direct} was higher than $\Delta H^{indirect}$. The discrepancies were higher for longer and more PEG chains on the protein. Despite the absolute values were different, trends with increasing PEG size were similar. Discrepancies were because thermodynamic equilibrium is not reached.
(Ueberbacher et al. 2010)	Van't Hoff (adsorption equilibrium isotherms), ITC	BSA, β -Lactoglobulin, HIC	BSA and β -Lactoglobulin adsorption onto HIC media is endothermic. The discrepancies between ΔH^{direct} and $\Delta H^{indirect}$ were higher at higher temperatures, where the thermal destabilization of proteins is higher. Both absolute ΔH^{direct} and $\Delta H^{indirect}$ values and trends with increasing temperature were discrepant. Discrepancies were explained by the protein conformational changes. For this reason, ITC is the superior method to van't Hoff analysis when analyzing enthalpy involving protein conformational changes.
(Chen et al. 2003)	ITC vs Van't Hoff (isotherms)	Lysozyme, myoglobin and α -amylase adsorption on HIC	Higher the temperature, more endothermic adsorption enthalpy between protein and HIC media. ΔH^{direct} was 10-15 kJ/mol larger than $\Delta H^{indirect}$. The discrepancy was explained by possible conformational changes, heat capacity changes with temperature, and that direct methods include more contributions.
(Freiburger, Auclair, and Mittermaier 2012)	ITC	Acetyl-coenzyme A	In ITC, equilibrium is not fully reached, hence, results of van't Hoff analysis, based on equilibrium isotherms, cannot be the same.
(McCann, Maeder, and Hasse 2011)	Van't Hoff and ITC	Carbate formation reaction	ΔH^{direct} was compared with $\Delta H^{indirect}$ from previous literature, the results were in good agreement despite some minor discrepancies.
(Naghibi, Tamura, and Sturtevant 1995)	Van't Hoff and ITC	Interaction between 2'-CMP and ribonuclease	ΔH^{direct} and $\Delta H^{indirect}$ was slightly different, especially at lower temperatures. The discrepancy was explained as the measured enthalpy values include additional contributions from buffer interactions (temperature-dependent ionization of buffer ions etc.).
(Liu and Sturtevant 1995)	Van't Hoff and ITC	18-crown-6 ether reaction with BaCl ₂	Nonlinear least-squares fitting of the binding constants to the integrated van't Hoff equation, including a temperature-independent change in heat capacity, leads to van't Hoff enthalpies that differ significantly from the observed calorimetric enthalpies. This discrepancy appears at present to be very widely occurring.
(Liu and Sturtevant 1997)	Van't Hoff and ITC	Reactions of heptylamine with heptanoic acid and α -cyclodextrin with sodium heptanoate	$\Delta H^{indirect}$ was higher than ΔH^{direct} at all tested temperatures. The discrepancies led the authors to conclude that chemical reactions are quite generally more complex than indicated by the simple chemical equation (that does not account for entropy or water molecules). The authors decided not to choose between ΔH^{direct} and $\Delta H^{indirect}$ methods.
(Haidacher et al. 1996)	Van't Hoff	Aminoacids adsorption on HIC	Van't Hoff analysis was successfully applied to chromatography of aminoacids. Linear equation X and quadratic equation X were compared and the differences between the resulting enthalpy change were small.
(Chaires 1997)	Monte carlo simulation	n.a.	Even small heat capacity (Δc_p) values make a hidden contribution to the van't Hoff plots. It is difficult to analyze with the human eye if van't Hoff plots have curvature or not for small values of heat capacity. The apparent differences between ΔH^{direct} and $\Delta H^{indirect}$ are most likely a result of the difficulty in the determination of statistically reliable ΔH and Δc_p values from van't Hoff plots that cover a narrow temperature range, and are unlikely to indicate physically significant differences in the two quantities.

ITC measures the heat effect when an aliquot of ligand solution is added to a protein solution. When the binding is of moderate affinity, ITC can be used to determine K , and an observed enthalpy change, ΔH . When the binding is of high affinity ($K > 10^8$), ΔH can still be determined with high precision, even though K cannot be determined (Baker and Murphy 1996).

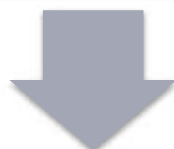
Chapter 2. Thermodynamic study of small molecular weight compounds adsorption on chromatographic surfaces: Comparison of adsorption enthalpy obtained by isothermal titration calorimetry and by van't Hoff plots using isocratic and linear gradient elution

- Van't Hoff's linear equation application to isocratic and gradient elution chromatography
- Temperature influence on the adsorption of catechin and EGCG on hydrophobic exchange chromatography



Chapter 3. Adsorption thermodynamics of proteins with similar charge and size onto conventional cation exchange chromatography resins

- Temperature effect on the adsorption of Lysozyme and Cytochrome c on ion exchange chromatography
- Determination of the adsorption driving force of similar proteins adsorbing onto negatively charged surface
- Discussion on the original reasons that may rule if adsorption is entropically or enthalpically driven



Chapter 4. Grafted ligand architecture effect on protein adsorption enthalpy

- Spatial disposition of ligands effect on BSA monomer adsorption enthalpy
- Mass transfer of BSA monomer on chromatography resins with grafted layer
- Comparison of ligand attachment technologies effect on BSA monomer adsorption at different pH
- Relation between driving force of adsorption of proteins and difference on the ligand structural design
- Novel relation between salt at elution concentration and energy released upon adsorption

Figure 1.7. Flow chart of the present study

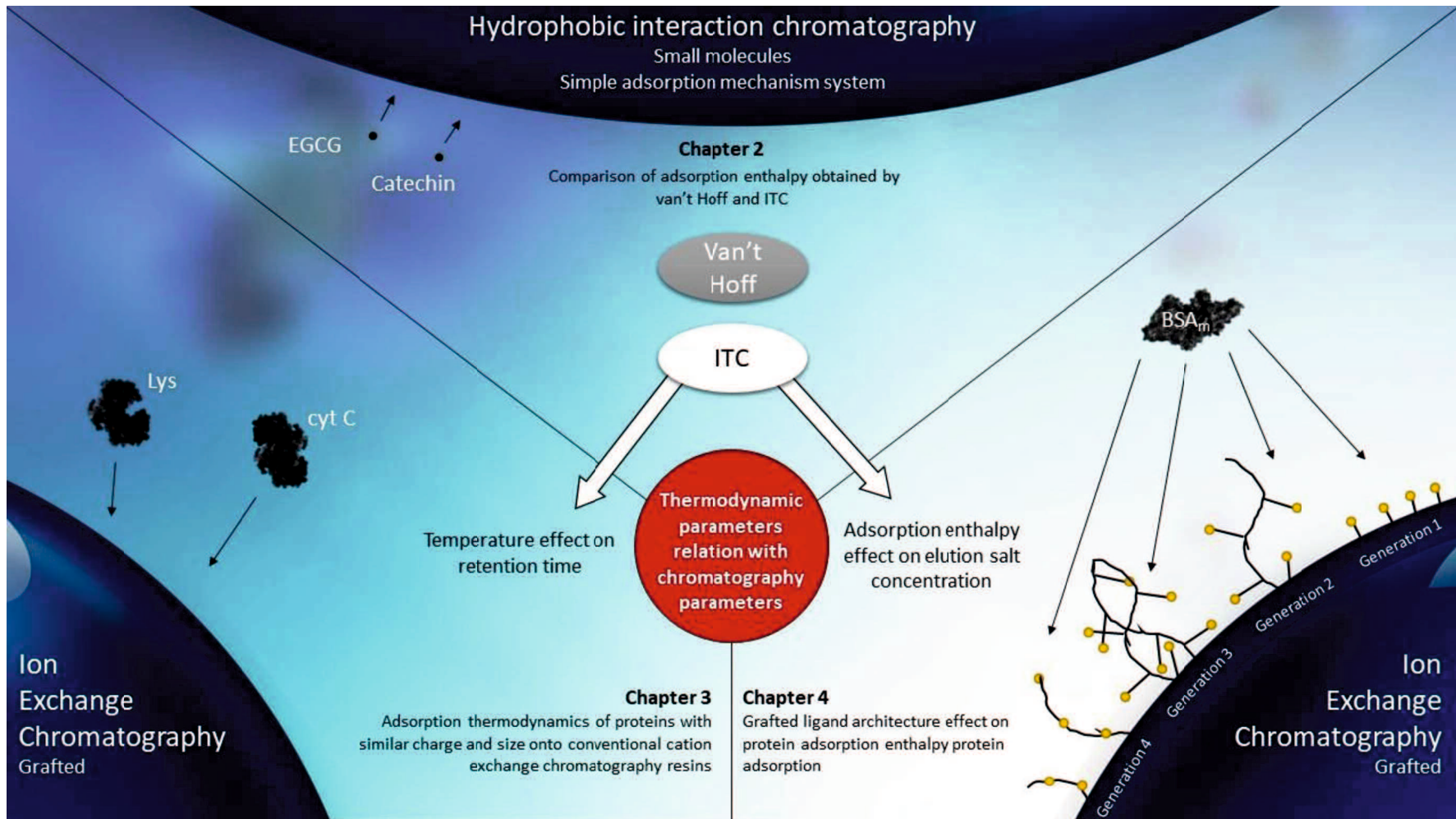


Figure 1.8. Summary schematics of the present study

Chapter 2: Thermodynamic study of small molecular weight compounds adsorption on chromatographic surfaces

2.1 INTRODUCTION

Chromatography separation processes are important for both biopharmaceutical and food industry. Although temperature is one of the important parameters affecting the chromatographic separation (Aguilar and Hearn 1996; Haidacher et al. 1996; Ladisch 2001), it is not examined in detail in most cases. This is because most biopharmaceutical products such as protein drugs are not stable at higher temperatures. Similarly, food industries are concerned with the quality loss at high temperature processes. Consequently, most cases chromatography processes are carried out at or near room temperature.

Understanding the temperature dependence of chromatography processes is important not only for process understanding/optimization but also for thermodynamic analysis of interaction between solute and ligand of the stationary phase, which is the basic principle of chromatography. Thermodynamic analysis is essential for understanding and enlighten complex adsorption mechanisms in liquid chromatography based on adsorption enthalpy (Blaschke et al. 2013; Lin et al. 2001a).

There are direct and indirect ways to determine the enthalpy of adsorption, ΔH^{ads} . The most commonly used indirect method is to use van't Hoff (vH) plots (Lin et al. 2002; Ueberbacher et al. 2010; Werner et al. 2014) with the retention data as a function of temperature. This can be done as follows, the distribution (partition) coefficient K values are determined from the retention volume in isocratic elution at different temperatures. Then, $\ln K$

is plotted against at $1/T$ where T is the absolute temperature. Thermodynamic quantities such as the enthalpy and the entropy can be determined from the slope and the intercept of $\ln K$ vs. $1/T$ curves, respectively. As a direct method, Isothermal titration calorimetry (ITC) is known to provide accurate information on binding energies between a molecule and the ligand (Blaschke et al. 2013). Although ITC is usually used to study homogeneous systems, several researchers applied ITC to measure the adsorption enthalpies between a molecule and chromatography packing materials (Blaschke et al. 2013; Chen et al. 2003; Lin et al. 2001a; Ueberbacher et al. 2010; Werner et al. 2014). ITC measurements are carried out at a specific temperature in order to determine the enthalpy $\Delta h^{\text{ads,ITC}}$.

Discrepancies between $\Delta h^{\text{ads,ITC}}$ and $\Delta h^{\text{ads,vH}}$ have however been widely reported in the literature (Castellano and Eggers 2013; Chaires 1997; Chen et al. 2003; Freiburger et al. 2012; Haidacher et al. 1996; Liu and Sturtevant 1995; Mizoue and Tellinghuisen 2004; Naghibi et al. 1995; Ueberbacher et al. 2010; Weber 1995; Werner et al. 2014; Winzor and Jackson 2006b) with respect to the interactions involving macromolecules such as proteins and also small molecule compounds (Castellano and Eggers 2013; Naghibi et al. 1995; Winzor and Jackson 2006b). Therefore, a chromatographic approach which allow reasonably estimation of the thermodynamic parameters for the adsorption processes needs to be developed. We have shown that the K values can be determined by linear gradient elution (LGE) chromatography experiments (Hosono et al. 2012). This method of analysis using so-called $GH-I_R$ curves (GH : normalized gradient slope, I_R : retention modulator concentration), is useful because one can precisely predict the K values at various modulator (salt for ion-exchange chromatography, ethanol in this study) concentrations without performing multiple chromatographic runs. Until now, LGE experiments at different temperatures for Van't-Hoff plots have not been carried out.

In this study, we compare the adsorption enthalpy values obtained by ITC experiments with those determined by LGE as well as isocratic elution experiments. The model separation system in this study was polyphenols separation by polymer-based resin chromatography with an ethanol-water mobile phase. Catechin and epigallocatechin gallate (EGCG) were used as model polyphenol samples. The stationary phase was composed of porous beads composed of polystyrene-divinylbenzene resins.

2.2 MATERIAL AND METHODS

2.2.1 Chemicals

The polyphenol samples were catechin hydrate (Catalog no. C1251, $C_{15}H_{14}O_6$, MW = 290 g/mol) from Sigma (St. Louis, MO, USA) and epigallocatechin gallate (Catalog no. 059-05411, $C_{22}H_{18}O_{11}$, MW = 458 g/mol) abbreviated as EGCG from Wako (Osaka, Japan). As the solid phase, polystyrene-divinylbenzene (PS-DVB) resin particles (Diaion HP20SS, Mitsubishi Chemicals, Tokyo, Japan) were used. HPLC grade ethanol (Wako, Osaka, Japan) and Mili-Q pure water were employed as the mobile phase solutions.

There are indications in the literature that catechin structure becomes unstable at temperatures higher than 352 K (Komatsu et al. 1993). Since this temperature was not reached, it is assumed that the polyphenols structure was stable throughout the experimental procedure.

2.2.2 Chromatography experiments

The chromatographic experimental setups and protocols were essentially the same as in our previous studies (Yamamoto and Kita 2006). Standard HPLC setups (JASCO PU980 pumps and a 6-way injection valve) were employed with the UV detection at 280 nm (JASCO UV970, Tokyo, Japan). HP20SS resins were packed into a column having an adjustable flow-adaptor (Millipore,

Vantage, diameter $d_c=1.1$ cm). Since the packed bed height changes with the mobile phase compositions (ethanol-water mixture), the top flow adaptor was adjusted in order to minimize the dead volume between the top of the packed bed and the flow adaptor. The packed bed height was between 4 and 5 cm for isocratic elution and 4.1 cm for linear gradient elution mode.

The column void volume V_0 was determined from the peak retention volume of a completely excluded solute. Dextran of 2,000,000 molecular weight (Sigma-Aldrich) was used. The column bed void fraction ($\varepsilon = V_0/V_t$ was ca. 0.39). The sample (catechin and EGCG) was dissolved in the mobile phase (ethanol-water mixture). The flow-rate was 1mL/min throughout all experiments and it was assumed that the columns were operated under the linear zone of the adsorption isotherm.

2.2.3 Isocratic elution

The sample was dissolved in the 20% ethanol mobile phase with a concentration of 1.0 mg/mL and 0.1 mL were injected. Each chromatographic run was repeated twice. Experiments were performed with a column oven (JASCO CO1560, Tokyo, Japan) maintained at a specified temperature (283, 293, 298, 303, 308 and 318 K).

2.2.4 Linear gradient elution (LGE)

The column was equilibrated with mobile phase A (10% ethanol). The sample was dissolved in the mobile phase A. The concentration was 0.25 mg/mL (Catechin) and 0.125 mg/mL (EGCG). LGE experiments were performed by changing the ethanol concentration linearly [from mobile phase A to B (40% ethanol solution)]. Experiments were carried out using at least four different gradient slopes. Each chromatographic run was repeated twice at 288, 298, 308 K.

2.2.5 Isothermal Titration Calorimetry (ITC)

ITC experiments were carried out by using ITC SV (TA Instruments, New Castle, DE, USA). The specification of this equipment was as follows. At the beginning of the ITC experiment, the reference cell was filled with previously degassed pure water. The sample cell with a total volume of 1.3 mL was filled with the slurry-resin suspension (1.225 mL of 20% ethanol and 0.075 mL of solid phase). The ITC syringe was filled with catechin or EGCG solution in a concentration of 1 mg/mL in 20% ethanol. After resin sedimentation by gravity in the sample cell, the excess liquid was removed, and the cell was closed and agitated at 300 RPM at 288, 293 and 298K. After a 5400 second timeout, for the thermal equilibrium, ten injections of 10 μ L were titrated with a 100 μ L Hamilton syringe. Injections of 1 mg/mL were carried out with a 600 seconds' interval from each other, after which the baseline was reached again. The temperature fluctuations indicated by the instrument were below 0.0002 K. Both resin slurries and sample solutions were previously degassed in a degassing station at 420 mm Hg for 10 minutes (TA Instruments).

2.3 THEORY

One of the most important parameters in liquid chromatography is the distribution coefficient, K of a solute defined as

$$K = \frac{C_s}{C} \quad (24)$$

where C_s is the solute concentration in the stationary phase and C is that in the mobile phase.

When the stationary phase is divided into the pore and the surface of the pore, C_s is given by

$$C_s = \varepsilon_p C_p + (1 - \varepsilon_p) C_q \quad (25)$$

where ε_p is the particle porosity, C_p is the solute concentration in the pore and C_q is the solute concentration on the solid surface of the pore. The distribution coefficient between C_p and C_q is defined as K_{pq} . Similarly, $K_p = C_p/C$ is defined.

Then,

$$C_s = \varepsilon_p C_p + (1-\varepsilon_p)C_q = \varepsilon_p C_p + (1-\varepsilon_p)K_{pq}C_p = [\varepsilon_p + (1-\varepsilon_p)K_{pq}]C_p = [\varepsilon_p K_p + (1-\varepsilon_p)K_{pq}K_p]C = KC \quad (26)$$

when there is no adsorption (interaction), $K_{pq}=0$,

$$K = \varepsilon_p K_p = K_C \quad (27)$$

Here, K_C is due to size exclusion by the pore diameter. $K_{ads} = (1-\varepsilon_p)K_{pq}K_p$ is due to adsorption. Then, K is given by

$$K = K_C + K_{ads} \quad (28)$$

2.3.1 Isocratic elution

From the retention volume V_R (mL) measured by isocratic elution experiments, K is determined by

$$K = \frac{V_R - V_0}{V_t - V_0} \quad (29)$$

where V_t is the total packed bed column volume (mL) and V_0 is the column void volume (mL). K_C was determined as the K value at non-binding conditions (>40% ethanol as a mobile phase). K_C values obtained experimentally were 0.7 for both columns used in isocratic elution mode.

2.3.2 Linear gradient elution

Our LGE model was originally developed for ion-exchange chromatography of proteins where the modulator, which controls the distribution between a sample and the stationary phase is a salt such as NaCl. The peak retention modulator concentration (I_R) increases with increasing normalized gradient slope (GH) which can be defined as (Hosono et al. 2012):

$$GH = (gV_0) \left(\frac{V_t - V_0}{V_0} \right) = g(V_t - V_0) \quad (30)$$

Here, g is the gradient slope in %, v/v /mL defined by $g=(I_f-I_0)/V_g$. I_f is the final ethanol concentration (%), I_0 is the initial ethanol concentration (%) and V_g is the gradient volume (mL). In this separation system, the modulator is ethanol. The experimental $GH-I_R$ data can be commonly expressed by the following equation (Yamamoto, Hakoda, et al. 2007; Yamamoto and Kita 2006):

$$GH = \frac{I_R^{B+1}}{A(B+1)} \quad (31)$$

The distribution coefficient of a molecule as a function of I can be then calculated by the following equation (Yamamoto 2005) with the A and B values determined from LGE experiments.

$$K_{LGE} = A \cdot I^{-B} + K_c \quad (32)$$

Although K calculated by equation 32 is the same as the value measured by IE experiments, in this study the subscript LGE is added in order to indicate the value determined by LGE experiments.

2.3.3 Van't Hoff analysis

The distribution coefficient K is related with the change in Gibbs free energy (Δg^{ads}) by the following thermodynamic relation.

$$\Delta g^{ads} = -RT \ln K \quad (33)$$

where R is the universal gas constant ($8.314 \text{ J} \cdot \text{K}^{-1} \cdot \text{mol}^{-1}$) and T is the absolute temperature in Kelvin. With the Gibbs-Helmholtz equation,

$$\Delta g^{ads} = \Delta h^{ads} - T\Delta s^{ads} \quad (34)$$

the following van't Hoff equation is derived.

$$\ln K = \frac{-\Delta h^{ads}}{RT} + \frac{\Delta s^{ads}}{R} \quad (35)$$

Based on this equation, Δh^{ads} and Δs^{ads} can be determined. The most common method is to prepare a plot $\ln K$ against $1/T$, from which Δh^{ads} is obtained from the slope ($-\Delta h^{ads}/R$).

2.3.4 Isothermal titration calorimetry

During an ITC experiment, the incremental heat changes, from each injection are accurately measured and recorded. The heat data (heat change versus time) is usually a tailed Gaussian curve and called “thermogram”. Although a large number of thermograms can be used for the analysis, typical obtained thermograms are as shown in **Figure 2.1**.

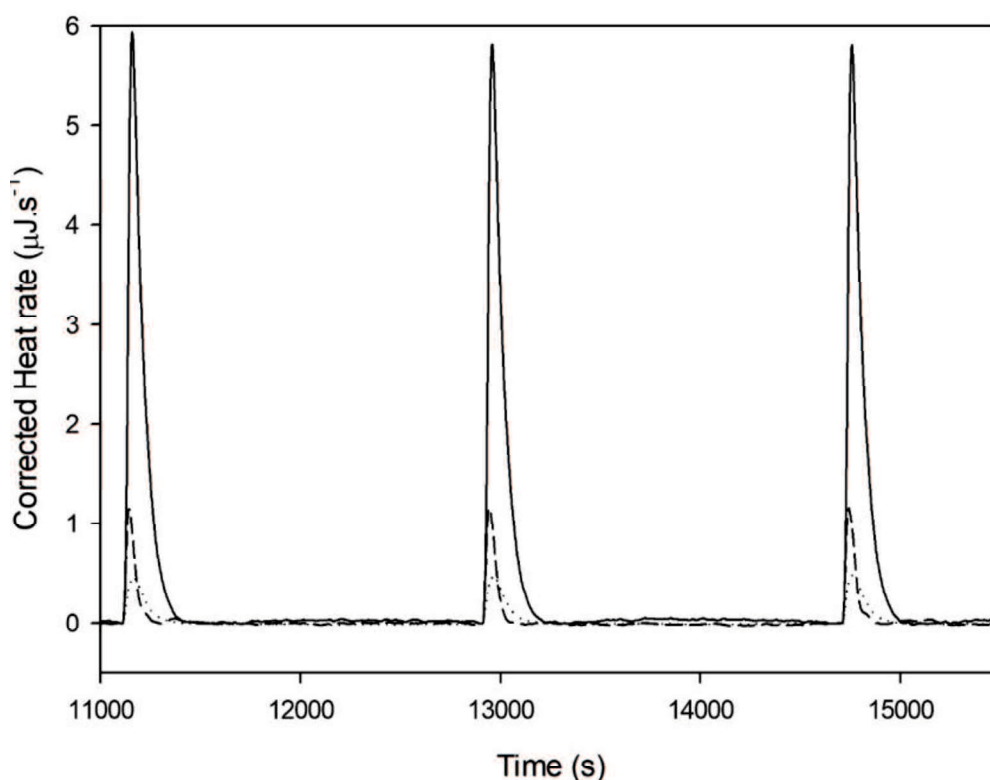


Figure 2.1. Typical thermograms. EGCG in 20% (ethanol-water) injection into PS-DVB resin particles (full line); 20% ethanol injection into PS-DVB (dashed line); and EGCG into 20% ethanol (dotted line). The experiment consists of a total of 10 injections of 10 μL each, the sample cell was stirred at 250 rpm at 288 K.

The first peak of each run was not used in any calculation due to the well-known phenomenon, named “first-peak anomaly” in previous studies (Werner et al. 2012). Thus, the total area under the following nine peaks was averaged and the enthalpic contribution was determined.

During the ITC experiments, a small peak is observed upon injecting the same solution onto itself. This is considered to be due to friction, dilution, dissipation and other effects such as a small mismatch of temperature of the

cell and that of the injected solution. Considerable attention must be given to the design of adequate control experiments to disregard these contributions (Winzor and Jackson 2006b). The enthalpy measured by ITC is divided into several origins:

$$\Delta H^{exp} = \Delta H^{ads} + \Delta H^{dil} + \Delta H^{solv} \quad (36)$$

Here ΔH^{ads} is the effective total heat contribution from the adsorption of the solute into resin. ΔH^{dil} is the contribution of the titrant dilution heat that can be measured by injecting the sample solution into the liquid without resins. Another blank value ΔH^{solv} is obtained by injecting the liquid into the resin slurry.

Furthermore, the average heat correspondent to these blank trials that consisted in a complete set of 9 injections were subtracted from the one obtained titrating the molecule into the resins, and effective heat was obtained. Δh^{ads} was then calculated by the following equation,

$$\Delta h^{ads} = \frac{\Delta H^{ads}}{\Delta m} \quad (37)$$

where Δm is the amount of molecule adsorbed upon injection, which was calculated using the K value from isocratic experiments.

2.4 RESULTS

2.4.1 Elution curves

Typical linear gradient elution curves of catechin and EGCG are shown in **Figure 2.2** at 288, 298 and 308 K. Catechin eluted prior to EGCG at all temperatures, indicating a lower retention and affinity with the PS-DVB resin stationary phase. When the temperature increased, the retention of both molecules decreased, and the peaks became sharper due to faster pore diffusion.

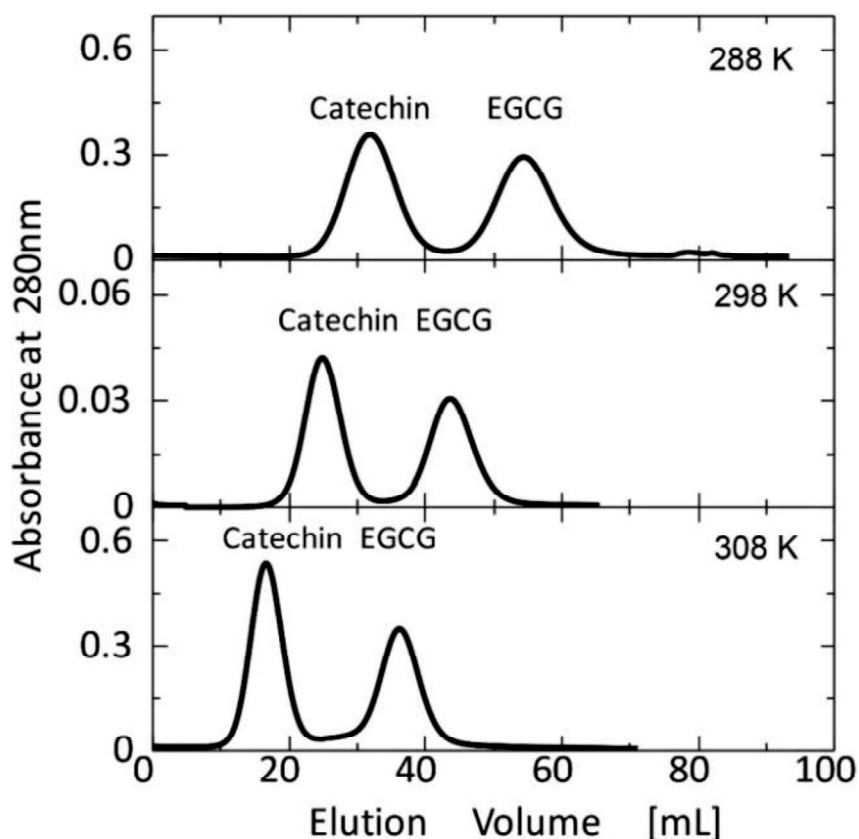


Figure 2.2. Linear gradient elution curves as a function of temperature. Mobile phase A: 10% ethanol; mobile phase B: 40% ethanol; $V_g = 100\text{mL}$. Column size: $Z = 4.1\text{ cm}$, $d_c = 1.1\text{ cm}$, $\epsilon = 0.390$

From LGE experimental data for different gradient slopes at specified temperatures, $GH-I_R$ plots were prepared (Figure 2.3). A and B values determined from $GH-I_R$ curves are summarized in Table 2.1. EGCG showed slightly higher binding site (B) values when compared with the values for catechin. This can be explained by their molecular structures. EGCG molecule is slightly bigger and possesses an extra benzyl group capable of more binding sites with the resin. This will be discussed later with the thermodynamic data. Dong et al. showed that EGCG could bind more strongly to polyvinylpolypyrrolidone (PVPP) than catechin possibly due to the presence of more hydroxyl groups (8 versus 5) (Dong et al. 2011). The temperature effect is much more prominent on A . The A value decreased sharply with increasing temperature whereas the B value did not change considerably. The B value was almost constant for catechin.

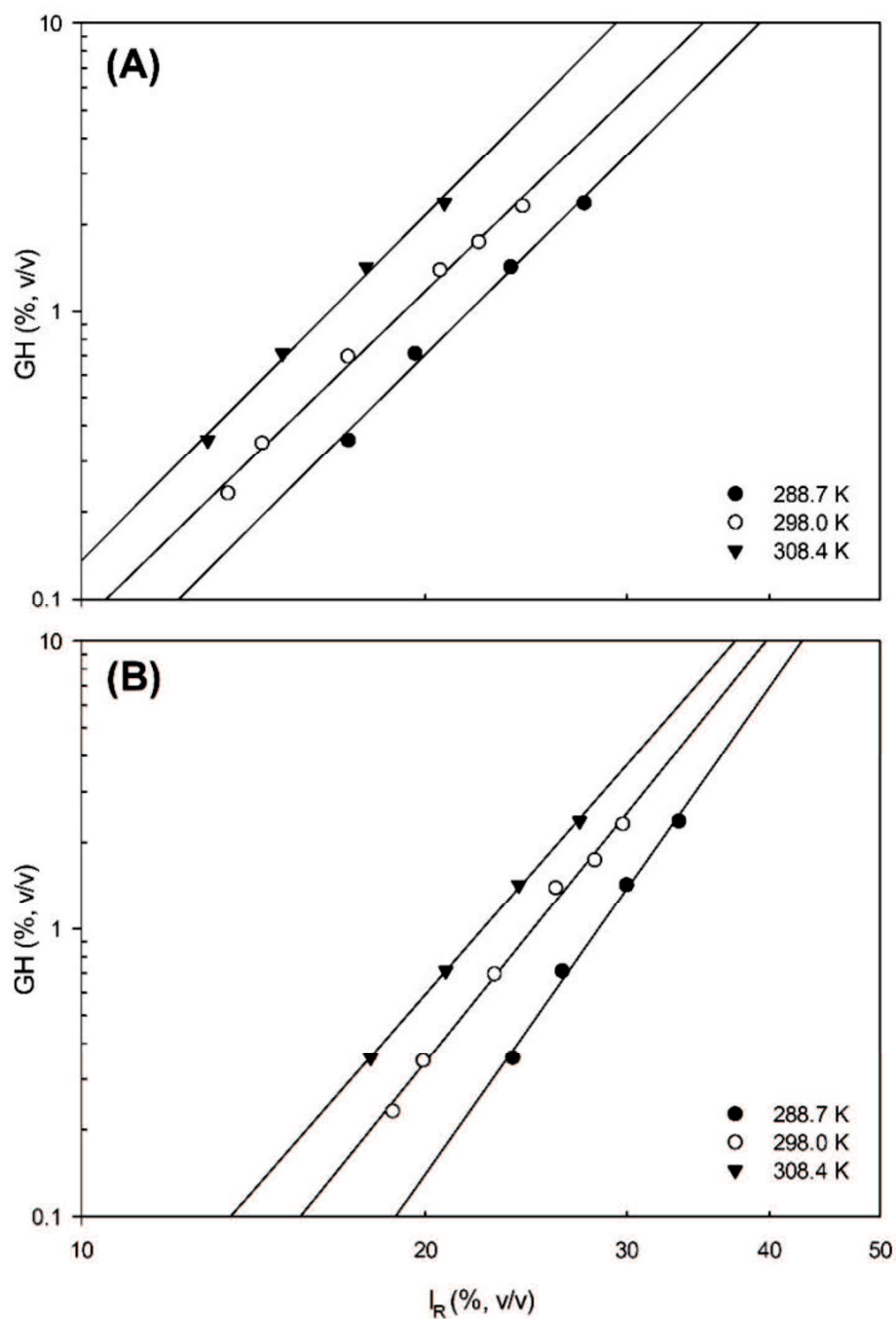


Figure 2.3. GH-IR curves for (A) catechin and (B) EGCG. Note that both axes have a logarithmic scale. The experimental data were fitted to eq. 31 by the least square fitting method, and A and B terms were calculated. Mobile phase A: 10% ethanol; mobile phase B: 40% ethanol; Column size: $Z = 4.1$ cm, $d_c = 1.1$ cm, $\varepsilon = 0.390$

Figure 2.4 represents the isocratic elution curves obtained for both molecules. The peak width became narrower and the retention volume decreased with increasing temperature.

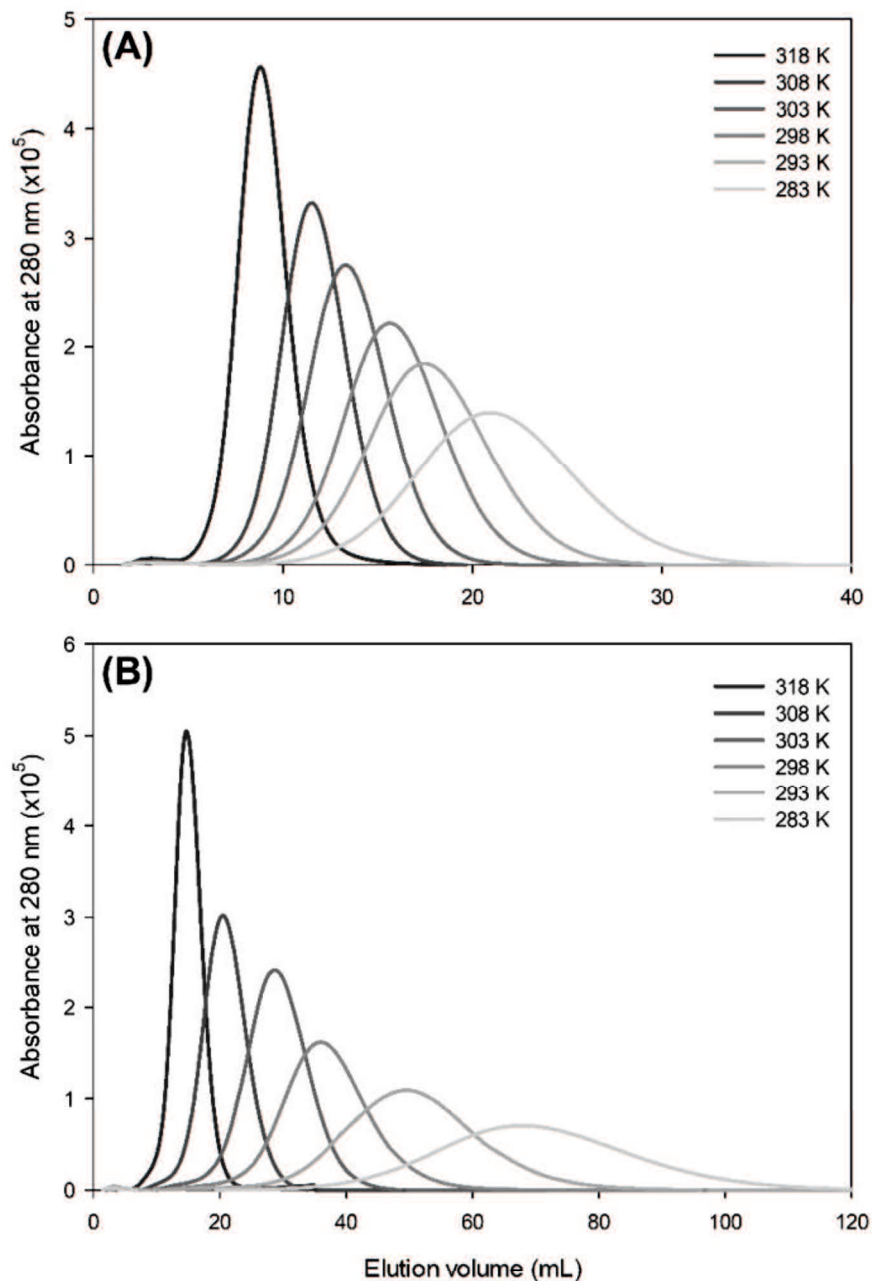


Figure 2.4. Isocratic elution curve profile on HP20SS. Injected sample was (A) catechin, $Z = 4.9$ cm, $\epsilon = 0.378$ and (B) EGCG, $Z = 4.6$ cm, $\epsilon = 0.384$. Injected sample volume was 100 μ L with a concentration of 1 mg/mL. Mobile phase was 20% ethanol with a flow rate of 1 mL/min.

2.4.2 Thermodynamics of adsorption

vH plots were prepared with K from two different elution modes (IE and LGE). K_{LGE} can be obtained as a function of I_R easily by eq. 32 with the A, B and Isocratic elution curve profile on HP20SS. Injected sample was (A) catechin, $Z = 4.9$ cm, $\epsilon = 0.378$ and (B) EGCG, $Z = 4.6$ cm, $\epsilon = 0.384$. Injected sample volume was 100 μ L with a concentration of 1 mg/mL. Mobile phase was 20% ethanol

with a flow rate of 1 mL/min. K_{LGE} values calculated for $I = 20\%$ are shown in **Table 2.1**.

Table 2.1. A and B values obtained from LGE experiments. ¹Calculated at 20% ethanol using eq. 32

T (K)	Catechin			EGCG		
	$A \times 10^4$	B	K_{LGE}^1	$A \times 10^6$	B	K_{LGE}^1
288	4.66	2.93	6.49	26.0	4.62	24.5
298	2.10	2.82	3.75	1.43	3.91	11.1
308	1.81	2.99	2.74	0.29	3.53	6.75

The obtained van't Hoff plots were linear as shown in Fig 5. The K values of EGCG determined by IE and LGE were similar. Therefore, the enthalpy values were comparable. For catechin, we noticed a difference between K_{LGE} and K_{IE} at the highest temperature (308 K). This discrepancy is likely due to the fact that at this temperature, the retention of catechin is so low that I_R is close to the initial ethanol concentration $I_0 = 10\%$. At 308 K, I_R was between 12.9 and 20.8% as shown in **Figure 2.5**.

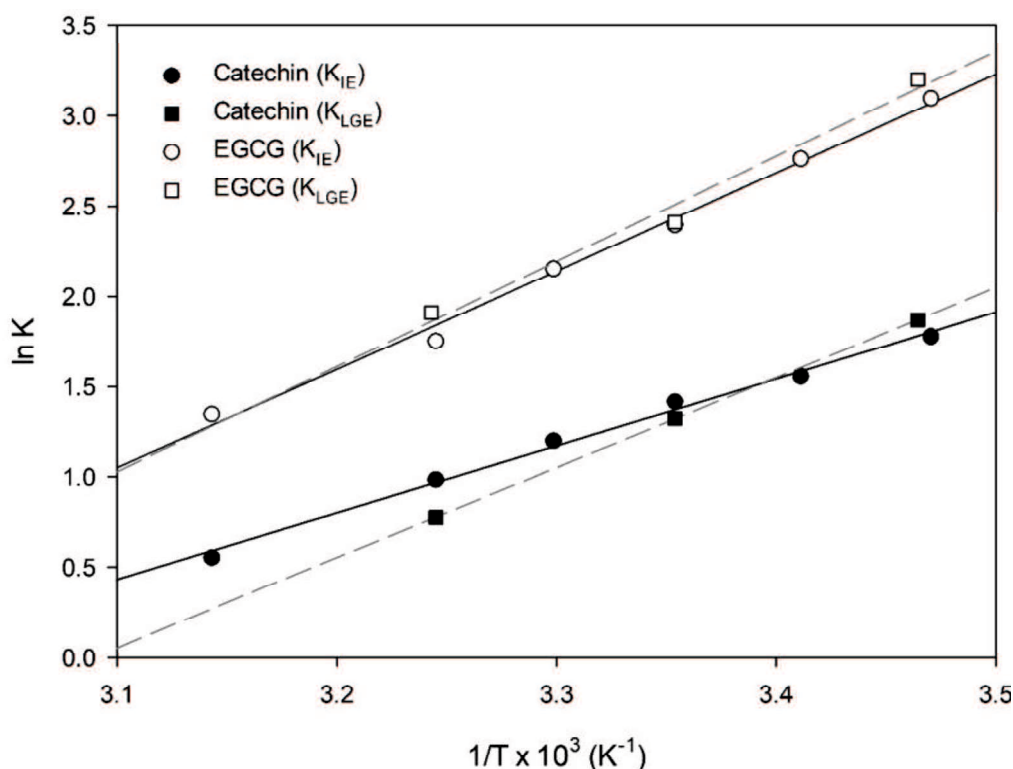


Figure 2.5. van't Hoff plots with K_{IE} and K_{LGE} calculated from isocratic elution curves at 20% ethanol concentration for (●) Catechin and (○) EGCG. Squares represent van't Hoff plots with K_{LGE} calculated from GH-IR curves, (■) Catechin and (□) EGCG. The solid and dashed lines represent the linear regressions for obtaining K_{IE} , and K_{LGE} respectively.

In order to derive equation 31 it is assumed that I_R is significantly higher than I_0 (Yamamoto 2005). This assumption allows for the linearization of $GH-I_R$ plots but in this case, due to the lower distribution coefficient at higher temperatures, this assumption may no longer be valid. This possibly influenced the resulting K_{LGE} , and consequently the catechin adsorption enthalpy. At lower temperatures, no significant differences were observed as catechin I_R values are considerably higher than I_0 .

Figure 2.6 and **Table 2.2** show $\Delta h^{\text{ads,ITC}}$ for both molecules at different temperatures. Temperature did not have a very significant effect in the adsorption enthalpy, already suggested by the linearity of the classic van't Hoff plot. When comparing both molecules, $\Delta h^{\text{ads,ITC}}$ value was slightly more exothermic for the stronger retained solute (EGCG) indicating a stronger interaction. Although the absolute values are slightly different, this trend was observed also for $\Delta h^{\text{ads,vH}}$ in both isocratic and gradient elution modes.

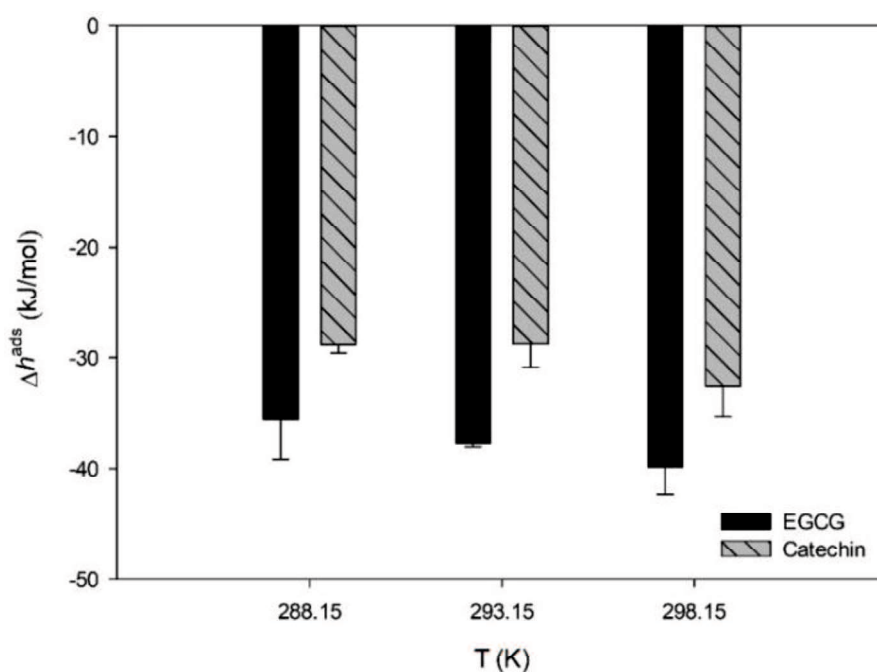


Figure 2.6. Comparison of adsorption enthalpy values determined by isothermal titration calorimetry of EGCG and catechin in 20% ethanol-water onto Polystyrene-divinylbenzene (PS-DVB) resin particles at 288, 293 and 298 K.

Thermodynamic parameters obtained by van't Hoff analysis are shown in **Table 2.3**. It is clearly shown that the process is exothermic ($\Delta h^{ads} < 0$) with negative change in adsorption entropy ($\Delta s^{ads} < 0$). It can be suggested that enthalpy change alone can drive the adsorption. Other researchers also reported an exothermic adsorption enthalpy when studying phenol adsorption onto a polymer adsorbent (Dong et al. 2011; Maity, Payne, and Chipchosky 1991).

Exothermic enthalpy of adsorption together with negative entropy change indicates that the adsorption occurs due to the hydrogen bonding between the polyphenols and the polymeric resin. We can also notice that EGCG adsorption is slightly more exothermic than catechin, indicating that it is capable of more hydrogen bonding with the surface. Molecular dynamic simulations found on the literature indicates that EGCG shows a higher number of formed hydrogen bonds (Sirk et al. 2008, 2009).

Higher temperatures accelerate the movement of the polyphenols into the pores by increasing its diffusion rate in solution, as indicated by sharper peaks in **Figure 2.3**. However, higher temperatures also decrease adsorption spontaneity (Δg^{ads} is less negative), and consequently K decreases. This might be due to an increased rate of desorption at higher temperatures. Δg^{ads} values on **Table 2.3** clearly show that adsorption is favored at lower temperatures. Isocratic elution profiles clearly substantiate these Δg^{ads} values. At lower temperatures, the retention was higher due to adsorption being more exergonic.

Table 2.2. Enthalpy of adsorption obtained with isothermal titration calorimetry at different temperatures.

T (K)	Δh^{ads} (kJ/mol)	
	Catechin	EGCG
288	-28.9 ± 0.8	-35.4 ± 3.6
293	-28.8 ± 2.1	-37.8 ± 0.3
298	-32.6 ± 2.8	-39.9 ± 2.5

Table 2.3. Thermodynamic parameters for adsorption of Catechin and EGCG onto PS-DVB determined using the van't Hoff equation

	EGCG		C	
	Isocratic	Gradient	Isocratic	Gradient
Δh^{ads} (kJ.mol ⁻¹)	-45.24	-48.43	-30.82	-41.59
Δs^{ads} (kJ.mol ⁻¹ .K ⁻¹)	-0.13	-0.14	-0.09	-0.13
Δg^{ads} (kJ.mol ⁻¹)	289 K	-7.28	-4.27	-4.49
	298 K	-6.03	-3.40	-3.27
	308 K	-4.69	-2.46	-1.96
	318 K	-3.39	-1.55	-0.69

Table 2.4. Average enthalpy values obtained by chromatography data (van't Hoff analysis and by ITC) from catechin and EGCG adsorbing onto PS-DVB. $\Delta h^{ads,ITC}$ values are averaged for all temperatures for comparison.

Method	Δh^{ads} (kJ/mol)	
	Catechin	EGCG
Van't Hoff analysis (KLGE)	-41.6 ± 5.0	-48.4 ± 6.4
Van't Hoff analysis (KIE)	-30.8 ± 1.2	-45.2 ± 1.9
Isothermal titration calorimetry	-30.1 ± 1.8	-37.7 ± 1.8

The average $\Delta h^{ads,ITC}$ and $\Delta h^{ads,vH}$ values and compared in **Table 2.4**. In the case of catechin adsorption, $\Delta h^{ads,vH,IE}$ agree well with the $\Delta h^{ads,ITC}$ but LGE and IE show quite different enthalpy values. The reason for this was already discussed in the beginning of this section.

When comparing $\Delta h^{ads,ITC}$ and $\Delta h^{ads,vH}$ in the case of EGCG, discrepancies of about 9.1 kJ/mol were observed between enthalpies (difference between average EGCG's $\Delta h^{ads,ITC}$ and the average between $\Delta h^{ads,vH}$). Discrepancies between vH and ITC methods have been extensively reported in the literature and these are discussed in section 5. We speculate that since ITC directly measures the adsorption enthalpy these might include other equilibria that are not accounted for vH analyses. For example, the equilibria between ethanol and EGCG, water molecules and EGCG, water molecules and PS-DVB, ethanol and PS-DVB, interactions between EGCG molecules and other EGCG molecules are not accounted or assumed to be negligible in $\Delta h^{ads,vH}$. All these equilibria are, however, accounted for and contribute to $\Delta h^{ads,ITC}$. When compared to

catechin, EGCG molecule has more hydroxyl groups that make it more prone to form hydrogen bridges with solvents.

Nevertheless, despite the discrepancy in the absolute values of EGCG Δh^{ads} , the signal of both Δh^{ads} and Δs^{ads} is always negative. On top of that, in a relative comparison, EGCG Δh^{ads} is always more negative than Catechin Δh^{ads} . This is in good accordance when using both vH or ITC. The signals and relative comparison of Δh^{ads} values were the most important aspects when interpreting the thermodynamic driving forces of adsorption in this study. The discrepancy in EGCG's absolute Δh^{ads} values did not have any effect on interpretation of the mechanism of the data because it had no effect on the tendencies and signal of Δh^{ads} determined in this work.

2.5 DISCUSSION

Microcalorimetric techniques have the ability to investigate the driving force of adsorption on liquid chromatography and agree well with retention data. Although $\Delta h^{\text{ads,ITC}}$ and $\Delta h^{\text{ads,vH}}$ showed similar trends, the values were slightly different. Previous authors have extensively reported discrepancies between these two methods. However, the reason of the discrepancy is different from study to study. In general, most authors state that $\Delta h^{\text{ads,ITC}}$ includes other contributions of buffer protonation and desolvation that are not considered in $\Delta h^{\text{ads,vH}}$ (Castellano and Eggers 2013; Chen et al. 2003; Færgeman et al. 1996; Liu and Sturtevant 1995). Liu et al. (Liu and Sturtevant 1995, 1997) associated $\Delta h^{\text{ads,ITC}}$ with the true enthalpy value and associated the van't Hoff analysis results with the apparent enthalpy value because the Gibbs free energy, from which $\Delta h^{\text{ads,vH}}$ is determined, lacks contributions to the system thermodynamics. They also mentioned the possible role of desolvation, which is not included in van't Hoff analyses, while noting the inherent difficulty in measuring changes in hydration. On the other hand, Færgeman, et al. also

noted a discrepancy between $\Delta h^{\text{ads,ITC}}$ and $\Delta h^{\text{ads,vH}}$, and chose to refer to $\Delta h^{\text{ads,vH}}$ as the intrinsic value instead (Færgeman et al. 1996). Also stating that $\Delta h^{\text{ads,ITC}}$ as being the sum of $\Delta h^{\text{ads,vH}}$ and all possible concomitant reactions which may accompany the binding reaction but do not directly influence the intrinsic binding constant K . Horn et al. (Horn et al. 2002) concluded that discrepancies between $\Delta h^{\text{ads,ITC}}$ and $\Delta h^{\text{ads,vH}}$ arise from different experimental conditions, and that for closed systems, in theory, $\Delta h^{\text{ads,ITC}}$ and $\Delta h^{\text{ads,vH}}$ should be the same, regardless of the type or degree of linked equilibrium (e.g., conformational changes, ion binding, dehydration). Other origins of discrepancy between $\Delta h^{\text{ads,vH}}$ and $\Delta h^{\text{ads,ITC}}$ found in the literature include: Protein conformational changes upon adsorption which are not accounted for by van't Hoff analysis in liquid chromatography but are accounted in ITC experiments (Chen et al. 2003; Ueberbacher et al. 2010); that there is no guarantee that the thermodynamic equilibrium is reached, hence the deviation between $\Delta h^{\text{ads,ITC}}$ and $\Delta h^{\text{ads,vH}}$ (Werner et al. 2014); that the usual form of van't Hoff equation does not account for changes in heat capacity with different temperatures (Chaires 1997; Liu and Sturtevant 1995); and that van't Hoff equation overlooks the contribution for total entropy of the system (Weber 1996).

Currently, we are conducting experiments with more complex and bigger molecules, in order to evaluate if these discrepancies are significant to change the mechanism of adsorption data interpretation.

2.6 CONCLUSIONS

Obtaining K_{IE} from isocratic experiments can be an arduous task due to the need of trial and error runs to try to find adequate elution conditions. For example, if the ethanol concentration is too high, there is no retention. If it is too low, the retention becomes so strong that the peak is not observed or broadened very widely. Obtaining K_{LGE} from gradient experiments could be

more straightforward and lowers the need of trial and error runs. This method can still provide an accurate way to compare enthalpy of adsorption using vH curves. Additionally, in this study, K_{LGE} was calculated using GH-IR curves by interpolation at 20% ethanol ($I_R=20$), but could be calculated at, in theory, any ethanol concentration desired. Allowing the study of the thermodynamic parameters at different ethanol concentrations with the same set of experiments. However, we acknowledge the fact that this would need further comparisons and validation using ITC or IE experiments using different buffer compositions.

In summary, the adsorption of two polyphenols, catechin and EGCG, was found to have an exothermic nature and was enthalpically driven. EGCG, the higher retention molecule, shows slightly more exothermic adsorption enthalpy change. $\Delta h^{\text{ads,ITC}}$ and $\Delta h^{\text{ads,vH}}$ were similar despite a minor difference in EGCG adsorption. Since K can be correctly obtained from isocratic elution experiments as well as gradient elution experiments, it is also possible to apply van't Hoff plots to accurately determine the adsorption enthalpy change using both elution modes.

2.7 SUMMARY

Temperature effect on the adsorption enthalpy of polyphenols was analyzed with van't Hoff plots using the distribution coefficient, K , determined with isocratic and gradient elution chromatography. Catechin and epigallocatechin gallate were used as model polyphenols. The stationary phase was polystyrene-divinylbenzene resin particles, and the mobile phase was an ethanol-water mixture. The values of adsorption enthalpy determined by chromatography and isothermal titration calorimetry obtained between the temperature range of 283 and 318 K. The results obtained by van't Hoff plots were consistent with the ones obtained with the isothermal titration

calorimetry (ITC). The interaction between PS-DVB particles and the polyphenols was found to be exothermic with negative values of enthalpy, –30.1 and –37.7 kJ/mol for catechin and EGCG, respectively.

Chapter 3: Adsorption thermodynamics of proteins with similar charge and size onto conventional cation exchange chromatography resins

3.1 INTRODUCTION

Several chromatographic steps are involved in the separation and purification processes of recombinant proteins. The understanding of chromatographic adsorbents is crucial to obtaining a high capacity, selectivity and throughput. These benefits are connected to the nature of protein-resin adsorption mechanism. The mechanism of adsorption is broadly understood and the protein adsorption process at the molecular level as proven to be highly complex (Delgado-Magnero et al. 2014; Dieterle, Blaschke, and Hasse 2008; Gill et al. 1995; Latour 2011; Liang and Fieg 2013; Yu et al. 2015; Zhang and Sun 2010), because protein adsorption involves various interactions between the protein and surface or the ligands attached to the surface (Lin et al. 2001a; Rabe, Verdes, and Seeger 2011; Yu et al. 2015).

Experimental data, mechanistic modeling and computational simulation of chromatography are of utmost importance for a better understanding of the adsorption mechanism, and the rational design of new chromatographic resins, optimization and scale-up of current biotechnology processes. Nowadays, there is a lack of fundamental understanding of the retention mechanisms in ion exchange chromatography (IEC) which leads to an inefficient process design. Only a thorough understanding of the underlying physics will allow the extension of knowledge on the proteins binding behavior (Dieterle et al. 2008).

Microcalorimetric techniques have already proven the ability to directly measure the enthalpy of adsorption, and with that, investigate and enlighten complex adsorption mechanisms in liquid chromatography based on acquired thermodynamic parameters (Blaschke et al. 2013; Ee 1996a; Katiyar et al. 2010; Korfhagen, Dias-Cabral, and Thrash 2010; Lin et al. 2001b; Marques et al. 2014; Thrash and Pinto 2002; Werner et al. 2012).

The design of IEC processes in downstream processing can be very complex, since there are many parameters that affect protein retention. Most studied parameters include ionic strength, temperature (Lin et al. 2001a; Winzor and Jackson 2006b), pH and also protein parameters, like protein size, protein flexibility (Hao et al. 2016), charge and structure (Yao and Lenhoff 2005). Ion exchange chromatography is usually addressed as a technique that can separate proteins based on their charge. However, it was reported that even proteins with similar charge and size can have different adsorption behaviors and retain differently in ionic exchange chromatography (DePhillips and Lenhoff 2001; Yao and Lenhoff 2005). A typical case is that of lysozyme (Lys) and cytochrome c (Cyt). Lys retention volumes were consistently higher than Cyt on a large set on cation exchangers (DePhillips and Lenhoff 2001). Underlying retention mechanisms, and the basis for retention differences among such proteins, remains incompletely understood. The present work aims to extend the knowledge on thermodynamics of this phenomenon by studying the adsorption of Cyt and Lys on two strong cation exchanger resins. We pretend to relate chromatography retention data of both proteins, together with ITC trials, to further elucidate the fundamental adsorption mechanism. Temperature dependence and particle size effect were evaluated. Adsorption energies and adsorption isotherms near the isoelectric point of each protein adsorbing into SPFF in the presence of salt and near the isoelectric point were also evaluated to further investigate the phenomenon.

3.2 MATERIALS AND METHODS

3.2.1 Chemicals

The selected model stationary phases were SP Sepharose Fast Flow (SPFF), SP Sepharose High Performance (SPHP), and SP Sepharose XL (SPXL), these resins are commercially available (GE Healthcare Life Sciences, Sweden). The physical properties of the chromatographic surfaces used in this study are summarized in **Table 3.1**.

Table 3.1. Summary of the chromatography surfaces used in this study along with the physical properties disclosed by the manufacturer.

Commercial name	SP Sepharose FF	SP Sepharose HP	SP Sepharose XL
Ligand	Sulphopropyl	Sulphopropyl	Sulphopropyl
Base matrix structure	Cross-linked 6% agarose	Cross-linked 6% agarose	Cross-linked 6% agarose
Particle size [µm]	45 - 165	24 - 44	45 - 165
Ion Exchange capacity [mmol H⁺/mL]	0.18-0.25	0.15-0.20	0.18-0.25
Ligand attachment chemistry	Conventional type	Conventional type	Grafted ligands. Dextran chains

Cytochrome c from bovine heart (Cyt) Lot# SLBK4245V was obtained from Sigma-Aldrich (St. Louis, MO, USA). Lysozyme from egg white (Lys) Lot# SAH3680 was purchased from Wako (Osaka, Japan). Proteins solvent accessible area were obtained from PDBePISA from Protein Data Bank in Europe. The calculations for the dipole moment for Cyt (PDB-ID: 1HRC) and Lys (PDB-ID:2LYZ) were done according to previous authors (Bharti 2012) by Protein Dipole Moments Server from Weizmann Institute (Felder et al. 2007).

Table 3.2. Summary of model proteins used in this study together with their physical properties. ^aDetermined with PDBePISA bioinformatics tool from Protein Data Bank in Europe. ^bDetermined with Protein Dipole Moments Server, according to previous authors (Bharti 2012). ^cfrom the literature (Yao and Lenhoff 2005).

	Cytochrome c	Lysozyme
Molecular weight (Da)	12384	14307
pI	10.0-10.5	11.35
^aSolvent-accessible area Å²	6364.3	6500.2
Number of residues in surface	102	117
Arginine residues	2	11
Lysine residues	19	6
^bDipole moment (Debye)	267	130
^cNet charge at pH 7	+8.3	+8.1

Two buffers were used as mobile phase in salt gradient elution experiments. 10mM phosphate buffer, 30 mM NaCl at pH 7 was used as the starting buffer (buffer A). The same buffer solution containing 1M NaCl was used as final elution buffer (buffer B).

There is one major difference between ITC conditions and chromatography conditions that cannot be controlled. In the ITC experiments, we study protein adsorption at strong binding conditions, i.e., lower salt conditions. On the other hand, in chromatography experiments, protein adsorbs at lower salt concentrations, but it elutes at higher salt concentrations. By using linear gradient elution chromatography to study protein adsorption, one cannot clearly separate adsorption from desorption. In addition to adsorption conditions, ITC experiments at higher salt concentrations (typical concentrations at elution) were used to find out if there were significant differences in the thermodynamic parameters. In the ITC experiments of proteins near their isoelectric point, 10 mM boric acid with 75 mM NaCl at pH 11 was used in the case of lysozyme. Cytochrome c experiments were carried out with 10 mM boric acid with 200 mM NaCl at pH 10. Salt concentration was chosen based on a normalized value for $K=17$ for both proteins using $K-I_R$ curves explained by previous papers by our group (Yamamoto 2005) and pH were set near the isoelectric point of the proteins.

All salts and buffers used in this work were purchased from Wako (Osaka, Japan) and dissolved in ultrapure deionized water.

3.2.2 Linear Gradient Elution

Chromatography experiments were carried out on a fully automated liquid chromatography system ÄKTA purifier (GE Healthcare Life Sciences, Sweden). Column physical characteristics were the following: column length was 20 cm; porosity was 0.34; and the column internal diameter was 0.9 cm. The column was equilibrated with buffer A. Proteins were dissolved in buffer A at 1 mg/mL and 0.1 mg/mL for Lysozyme and Cytochrome c, respectively. The injection volume was 0.5 mL. The linear gradient was performed by changing the buffer composition linearly from buffer A to buffer B with time. Namely, the salt concentration was increased with time at a constant temperature and pH. Flow rate was kept constant at 1.6 mL/min. Mobile phases, column, sample loop, and injection valve were kept at 15 °C, 25 °C and 35 °C throughout the experiments. The experiments were done in duplicate.

3.2.3 Adsorption isotherm experiments

The resins were washed with ultrapure water and later with the respective buffer solution by decantation. The resins were used in a 50% resin/buffer slurry. Equilibrium adsorption experiments were carried out in falcon centrifuge tubes. First, the tubes were filled with 4 mL of different dilutions of the protein solution. Initial protein concentration was measured by spectrophotometry at 280 nm and 300 nm in a multi-well plate reader PowerWave XS (Biotek, United States of America). Then, 200 µL of resin slurry (50% resin-buffer) was added in each tube and stirred inside a temperature controlling chamber for at least 120 min at 15 °C, 25 °C and 35 °C. Preliminary experiments, in the whole range of tested concentrations, showed that

equilibrium was reached after only 15 minutes (data not shown). After equilibration, tubes were centrifuged at 10 000 RPM for 5 minutes and the liquid equilibrium concentration was determined. From the equilibrium concentration and initial concentration, the surface concentration could be determined by a mass balance. Equilibrium concentration was plotted against the surface concentration calculated. The experiments were done in triplicate. The curves were then fitted with the well-known Langmuir model,

$$C_s = \frac{q_m(KC)}{1 + (KC)} \quad (38)$$

where C_s is the surface concentration of protein in the resin surface, q_m is the maximum static binding capacity, K is the equilibrium coefficient and C is the bulk concentration after equilibrium.

3.2.4 Isothermal titration calorimetry

Microcalorimeter used in this work was ITC SV obtained from TA Instruments (New Castle, DE, USA). The specification of this equipment was as follows. At the beginning of the ITC experiment, the reference cell was filled with previously degassed pure water. The sample cell with a total volume of 1.3 mL was filled with 1.3 mL of the slurry-stationary phase suspension (1.225 mL of buffer A and 0.075 mL of stationary phase). The ITC syringe was filled with protein solution in a concentration of 1 mg/mL in buffer A. After resin sedimentation by gravity in the sample cell, the excess liquid was removed, and the cell was closed and agitated at 300 RPM at 288, 293 and 298K. After a 5400 second timeout, for the thermal equilibrium, ten injections of 10 μ L were titrated with a 100 μ L Hamilton syringe. Injections of 1 mg/mL were carried out with a 600 seconds' interval from each other, after which the baseline was reached again. The temperature fluctuations indicated by the instrument were below 0.0002 K. Both resin slurries and sample solutions were previously

degassed in a degassing station at 420 mm Hg for 10 minutes obtained from TA Instruments (New Castle, DE, USA).

It has been already shown that even small pH differences between the ITC cell and titration solution affects quite significantly the calorimetric results as artifacts in the enthalpy can arise due to buffer protonation effects (Duff et al. 2011). Prior to the experiment, Lys and Cyt solutions were prepared in the respective buffers and exhaustively washed with the respective buffer using AmiconR Ultra-4 10000MW obtained from MilliporeSigma, (Burlington, MA, USA), for 15 min at 7000 RPM. This step was repeated until the conductivity of the buffer solution and protein solution was the same (around 4 to 5 times). Conductivity was checked after every washing step with a portable conductivity meter B-173 Twin Cond acquired from Horiba (Kyoto, Japan).

During the calorimetric measurements, a small signal is observed upon injecting the same solution onto itself. This signal was previously considered to be due to friction, dissipation and other effects like a small mismatch of temperature of the cell and that of the injected solution (Dieterle et al. 2008). Additional contributions to the calorimetric signal can arise from buffer interactions that are independent of the adsorption interactions. These contributions that reflect temperature dependence of buffer ionization as well as of water structure, need to be subtracted from the total measured signal. Considerable attention must be given to the design of adequate control experiments to clarify these contributions (Winzor and Jackson 2006b). The contribution of heat of a protein injection into a resin mixture using ITC can be divided into several origins:

$$\Delta H^{exp} = \Delta H^{ads} + \Delta H^{dil} + \Delta H^{solv} \quad (39)$$

where ΔH^{exp} is the total enthalpy measured by the ITC. ΔH^{ads} is the enthalpy contribution from the adsorption of the protein into resin. ΔH^{dil} is the contribution of the protein solution dilution heat, measured by titrating protein solution into the same buffer that it was diluted into. ΔH^{solv} is caused

by the adsorption of buffer ions and it was determined titrating buffer into the resin slurry. Furthermore, the area correspondent to these blank trials that consisted in a complete set of 10 injections were subtracted from the one obtained titrating the protein into the resins, and effective enthalpic contribution from the protein adsorption was obtained.

The first peak of every trial is not shown and it was not used in any calculation due to the well-known phenomenon, named “first-peak anomaly” in previous studies (Werner et al. 2012). Protein injections and all blank trials were done in duplicate.

Adsorption heats were measured directly by ITC, and molar enthalpy of adsorption Δh^{ads} was then calculated by the following equation:

$$\Delta h^{ads} = \frac{\Delta H^{ads}}{\Delta m} \quad (40)$$

where Δm is the amount of molecule adsorbed upon each injection (mol), which was calculated using a combination of the equilibrium adsorption isotherm and a mass balance.

3.3 THEORY

3.3.1 Thermodynamic analysis

The difference of the molar Gibbs energies in the reference state ($\Delta g^{ads\ ref}$) resulting from the transfer of a molecule from the mobile to the stationary phase is related with the corresponding equilibrium coefficient K at a specific temperature by the following equation,

$$\Delta g^{ads\ ref} = -RT \times \ln(K) \quad (41)$$

where R is the ideal gas constant ($8.314 \text{ J.K}^{-1}.\text{mol}^{-1}$) and T is absolute temperature.

Blaschke et al. (Blaschke et al. 2011, 2013) proposed a simple method to extend the thermodynamics analyses to any state on the equilibrium adsorption isotherm at the concentration of interest. The equilibrium

coefficient K can be determined from the slope of the equilibrium adsorption isotherm at the concentration of interest, previously used by other authors (Blaschke et al. 2011), or by linear gradient elution experiments:

$$K = \frac{\partial C_s}{\partial C} \quad (42)$$

Thus, allowing $\Delta g^{ads ref}$ to be determined for each concentration of interest by equation 41.

By assuming infinite dilution, constant pressure and a closed system, the specific enthalpy of adsorption in the reference state $\Delta h^{ads ref}$ is equal to the value determined in ITC experiment Δh^{ads} at the studied concentrations. In addition, entropic effects $\Delta s^{ads ref}$ can be determined at each concentration using Gibbs-Helmholtz relation:

$$\Delta g^{ads ref} = \Delta h^{ads ref} - T\Delta s^{ads ref} \quad (43)$$

where $\Delta h^{ads ref}$ and $\Delta s^{ads ref}$ are the specific molar enthalpy and entropy of adsorption of the adsorption process in reference state, respectively. The reference state (^{ref}) superscript is omitted for the sake of convenience.

3.4 RESULTS AND DISCUSSION

3.4.1 Gradient elution retention

As shown in **Figure 3.1**, **Figure 3.2** and **Figure 3.3**, Lys retention was higher than Cyt in all tested surfaces and this phenomenon has already been observed before (DePhillips and Lenhoff 2001; Hao et al. 2016). More importantly, we found that the difference between Cyt and Lys peaks (resolution) decreased with increasing temperatures i.e., when the temperature increases, the retention volume of Cyt slightly increases, whereas that of Lys slightly decreased.

Table 3.3 clearly shows these differences with temperature. This behavior was observed for all the three surfaces, despite some differences in the peak shape

when comparing different surfaces. Resulting peaks obtained with SPHP were sharper than the ones obtained with SPFF and SPXL, showing less mass transfer limitations, caused by the smaller particle size. In addition, SPXL showed a higher resolution when compared with the conventional non-grafted resins. At 35 °C, Cyt and Lys peak overlap with each other when using SPFF and SPHP but not when using the dextran modified grafted resin SPXL.

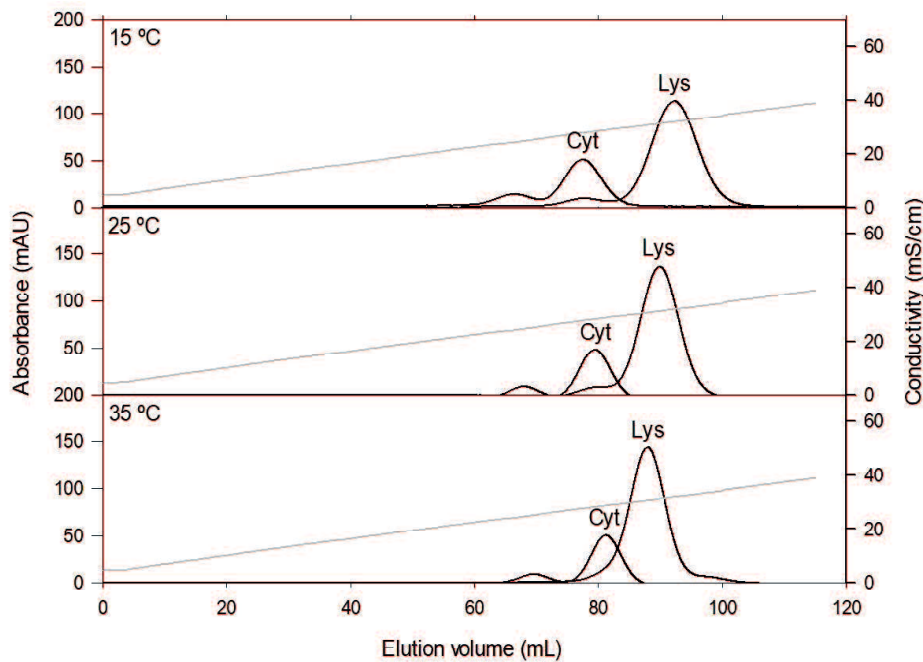


Figure 3.1. Overlapped chromatograms obtained at 15 °C, 25 °C and 35 °C injecting lysozyme and cytochrome c, onto a SP Sepharose FF column. The absorbance was measured at 420 nm and 280 nm in the case of cytochrome c and lysozyme, respectively. The operational parameters were the following: Salt gradient length $v_g = 300$ mL; flow rate 1.6 mL/min; column length $Z = 20$ cm.

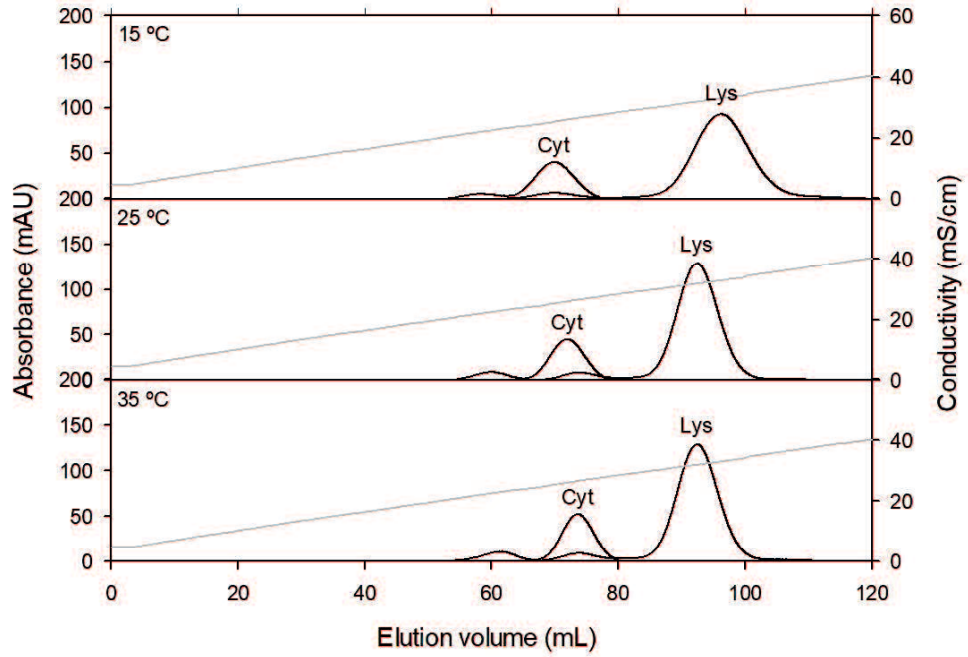


Figure 3.2. Overlapped chromatograms obtained at 15 °C, 25 °C and 35 °C injecting lysozyme and cytochrome *c*, onto a SP Sepharose XL column. The absorbance was measured at 420 nm and 280 nm in the case of cytochrome *c* and lysozyme, respectively. The operational parameters were the following: Salt gradient length $v_g = 300$ mL; flow rate 1.6 mL/min; column length $Z = 20$ cm.

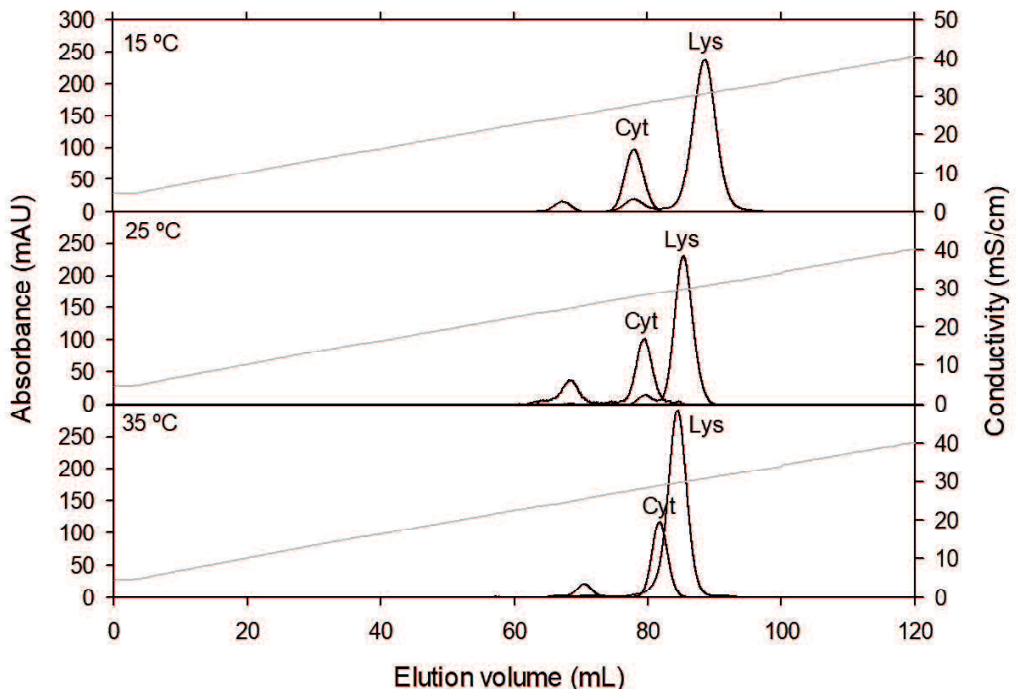


Figure 3.3. Overlapped chromatograms obtained at 15 °C, 25 °C and 35 °C injecting lysozyme and cytochrome *c*, onto a SP Sepharose HP column. The absorbance was measured at 420 nm and 280 nm in the case of cytochrome *c* and lysozyme, respectively. The operational parameters were the following: Salt gradient length $v_g = 300$ mL; flow rate 1.6 mL/min; column length $Z = 20$ cm.

Table 3.3. Retention volumes obtained for cytochrome c and lysozyme. These were determined by linear gradient elution at a constant salt gradient slope of 400 mL.

	Cytochrome c		Lysozyme
	T (°C)	Retention volume (mL)	
SPFF	15	77.52	92.11
	25	79.25	89.87
	35	81.14	87.94
SPHP	15	77.97	88.57
	25	79.36	85.29
	35	81.75	84.47
SPXL	15	69.85	96.29
	25	71.98	94.20
	35	73.53	92.53

3.4.2 Equilibrium adsorption isotherms

Equilibrium adsorption isotherms were used to calculate more precisely the amount of protein adsorbed in each ITC. As indicated in **Figure 3.4**, the temperature effect on the shape of adsorption isotherms curves is not very noticeable except for the case of lysozyme adsorbing onto SPFF. We believe that temperature had small effect on the equilibrium adsorption isotherm shape due to the small range of temperatures tested. However, the temperature effect on adsorption could be clearly seen when looking at chromatographic retention volumes. This indicates that, in this case, the use of salt gradient elution chromatography was more sensitive to study temperature effect on adsorption.

Figure 3.4 shows the equilibrium isotherms obtained at pH 7 with 30mM NaCl with lysozyme (top) and Cytochrome C (bottom) adsorbing onto SPFF, SPHP and SPXL at 15 °C, 25 °C and 35 °C. The chromatographic surfaces were placed in contact with protein solutions and the equilibrium concentration was determined after 16 hours.

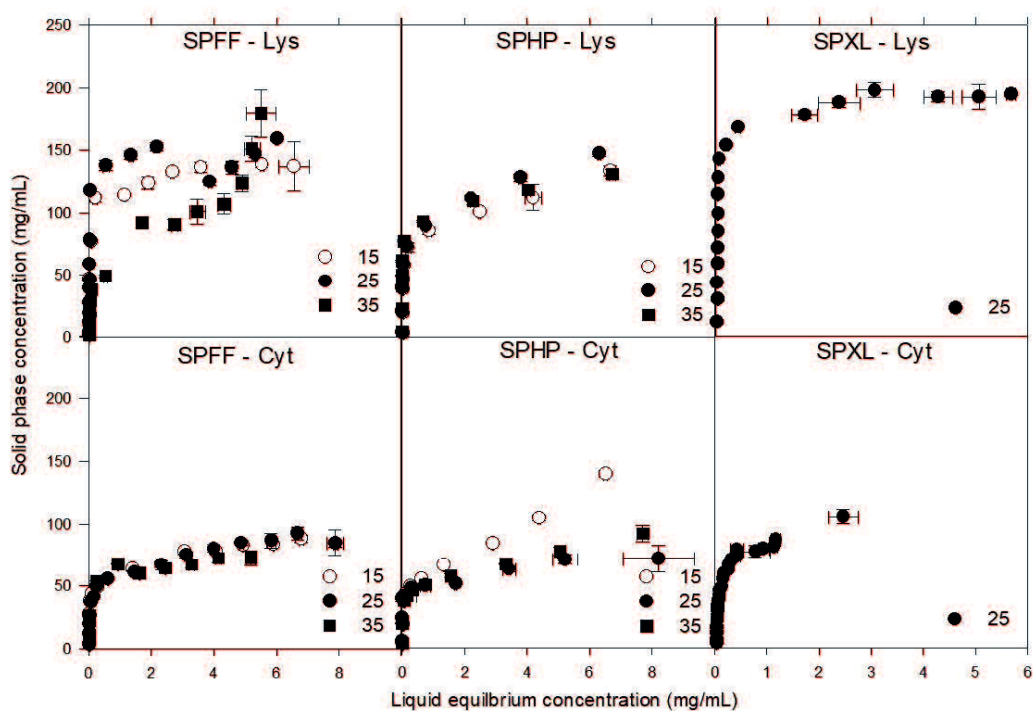


Figure 3.4. Equilibrium isotherms obtained at pH 7 with 30mM NaCl with lysozyme (top) and Cytochrome C (bottom) adsorbing onto SPFF, SPHP and SPXL at 15 °C, 25 °C and 35 °C. The chromatographic surfaces were placed in contact with protein solutions and the equilibrium concentration was determined after 16 hours.

Both proteins have similar molecular weights, and are considered small proteins (Lyz 14307 Da, Cyt 12327 Da). However, lysozyme showed an approximate 60% higher maximum capacity. This difference in the binding capacity was also observed by previous authors, and it was considered that it was due to different amino acid composition (Martin et al. 2005) and protein structural flexibility (Hao et al. 2016). However, due to the different composition and surface location of residues, there is also a significant difference in the dipole moment of both proteins at pH 7 (Lyz: 72 Debye, Cyt: 325 Debye (DePhillips and Lenhoff 2001)). Previous studies (Zhou, Zheng, and Jiang 2004) show that the dipole moment of Cyt proved to be an important factor in its binding orientation in adsorption in charged surfaces. Whereas for lysozyme, the patches of positive and negative charge are distributed uniformly on its surface (low dipole moment), the higher dipole moment of Cyt implies a bipolar distribution of the charge. Hence there will be a tendency for the Cyt molecules to adsorb in an orientation with the positive patches pointing toward the negative surface and the negative charge pointing

outwards (Bharti 2012). Our hypothesis is that due to lysozyme's more uniform charge distribution, the protein-protein repulsion is less likely, leading to a higher packing of the protein in the pores. On the other hand, the higher Cyt-Cyt repulsion, protein orientation and lesser Cyt structural flexibility, seem to be responsible for its lower static binding capacity.

3.4.3 Driving force of adsorption

It can be seen in **Figure 3.5**, **Figure 3.6**, **Figure 3.7** that the specific enthalpy of adsorption of both Cyt and Lys remains constant along the studied surface concentrations, which is not surprising since the studied surface concentrations were in the very beginning of the linear region of the adsorption isotherm. Studying the effect of surface concentration on Δh^{ads} was not the aim of this study. This clearly shows that we are indeed working in infinite dilution conditions, a premise for the use of thermodynamic fundamental equations 41 and 43. Since the surface concentration showed no significant effect on Δh^{ads} , the average values are presented in **Table 3.4** along with the other thermodynamic parameters.

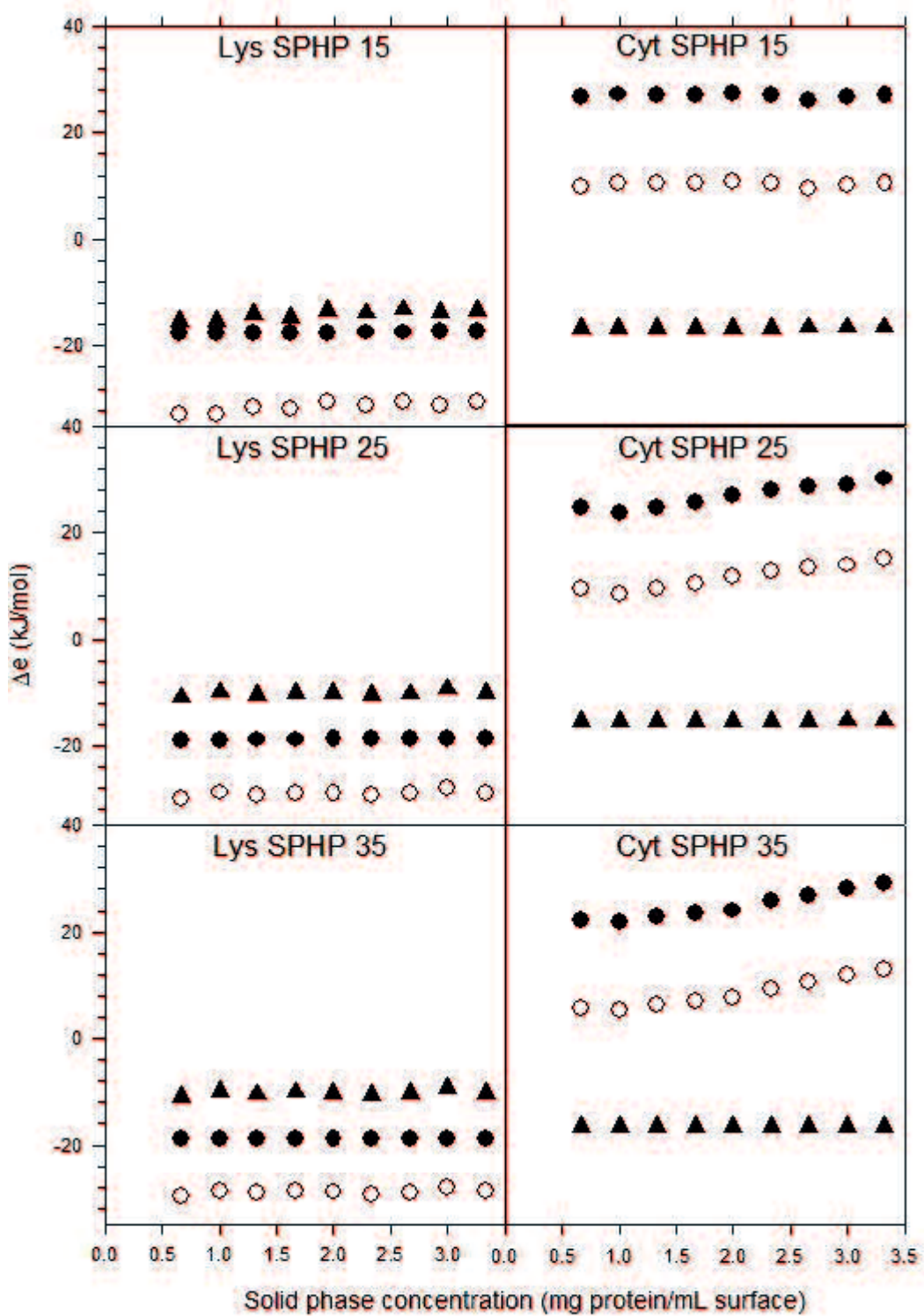


Figure 3.5. Specific thermodynamic parameters of adsorption of both cytochrome c (Right) and lysozyme (Left) onto SPHP at 15 °C, 25 °C and 35 °C with 30mM NaCl pH7. Symbols represent Δh^{ads} (O), Δg^{ads} (▲) and $T\Delta s^{ads}$ (●). Enthalpy values was considered constant along the studied concentrations.

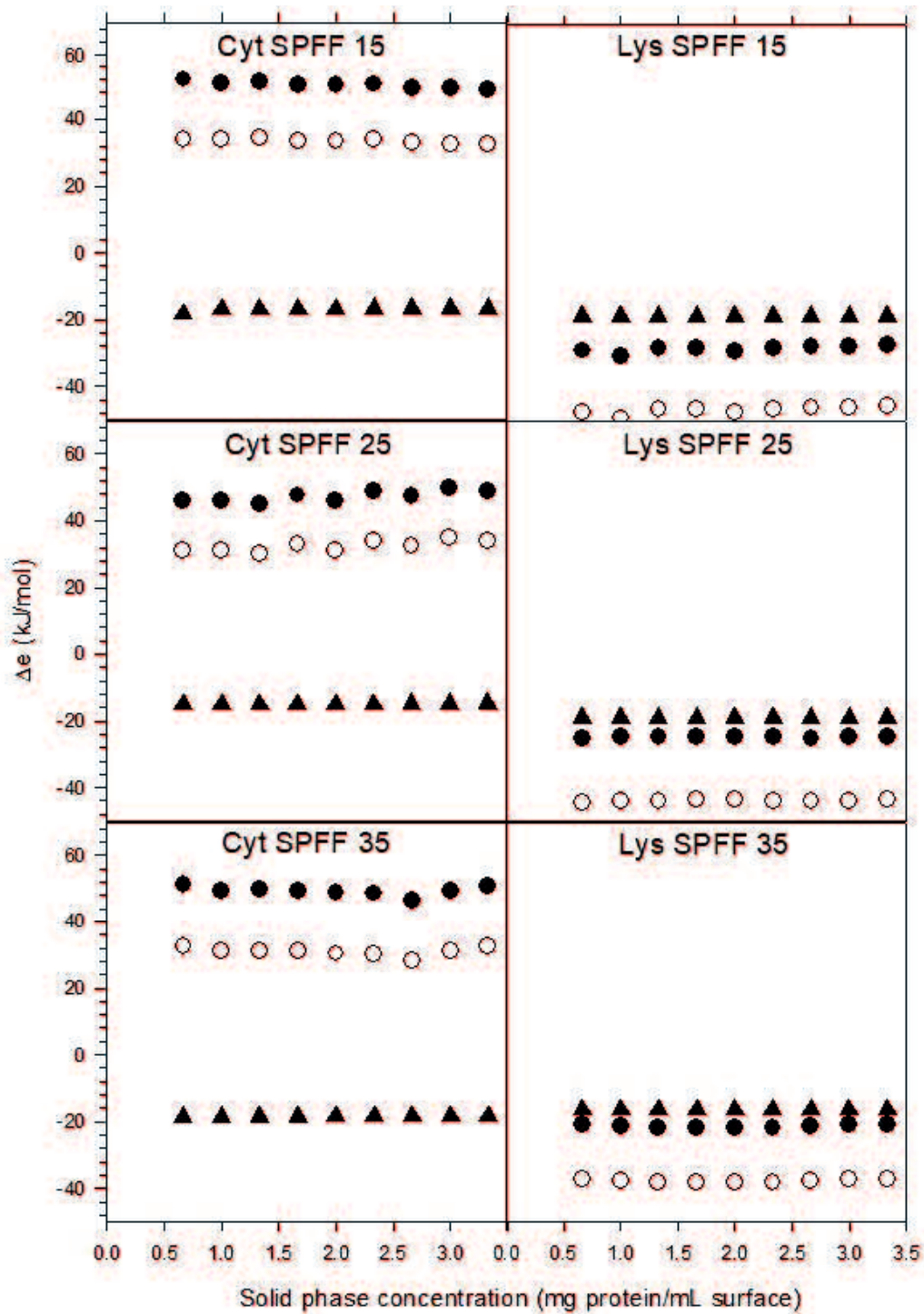


Figure 3.6. Specific thermodynamic parameters of adsorption of both cytochrome c (Left) and lysozyme (Right) onto SPFF at 15 °C, 25 °C and 35 °C with 30mM NaCl pH7. Symbols represent Δh^{ads} (○), Δg^{ads} (▲) and $T\Delta s^{ads}$ (●). Enthalpy values was considered constant along the studied concentrations.

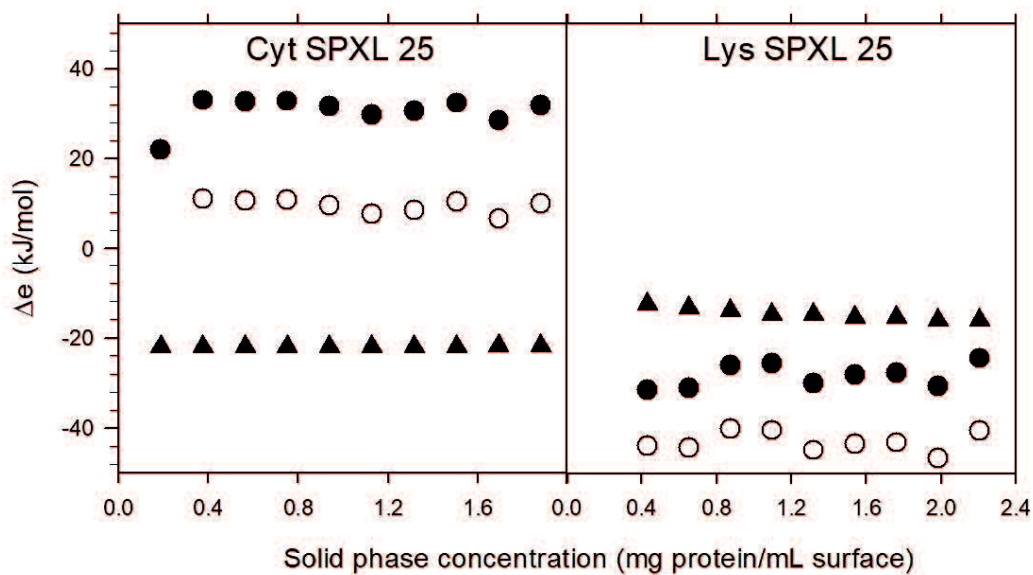


Figure 3.7. Specific thermodynamic parameters of adsorption of both cytochrome *c* (Left) and lysozyme (Right) onto SPXL at 25 °C with 30mM NaCl pH7. Symbols represent Δh^{ads} (○), Δg^{ads} (▲) and $T\Delta s^{ads}$ (●). Enthalpy values was considered constant along the studied concentrations.

Gibbs free energy was found to be, negative as expected, and very similar between all systems studied. Since the adsorption isotherms initial slopes were similar and very high.

We found that Lys adsorption is an exothermal process ($\Delta h^{ads} < 0$) in both resins at these conditions. The adsorption process is enthalpically driven which is in agreement with previous authors' data with lysozyme adsorbing onto other cation exchangers (Blaschke et al. 2011; Silva et al. 2014). This suggests that the major contribution for the adsorption mechanism is electrostatic interaction between the protein and the resin (Blaschke et al. 2013; Lin et al. 2002; Rosa et al. 2018).

Latest nuclear magnetic resonance data (Hao et al. 2016) shows that, during ion exchange chromatography, both Lys and Cyt show structural flexibility, but it was found to be slightly more significant in the case of Lys adsorption. It is known that temperature can affect protein flexibility (Tilton et al. 1992). Temperature increases lead to less energy release upon adsorption i.e. Δh^{ads} is less negative. We believe this happens due to Lys structural flexibility at higher temperatures and there is a slight reduction of the ionic

interactions between the solid phase and protein. This is consistent with the lower retention times of Lys when temperature increases.

Table 3.4. Average of Δh^{ads} , Δg^{ads} and $T\Delta s^{ads}$ obtained for the adsorption of cytochrome c and lysozyme at pH 7 with 30mM NaCl, phosphate buffer. The equilibrium constant K was obtained using equation 42.

T (°C)	Lysozyme			Cytochrome c			
	Δh^{ads} (kJ/mol)	Δg^{ads} (kJ/mol)	$T\Delta s^{ads}$ (kJ/mol)	Δh^{ads} (kJ/mol)	Δg^{ads} (kJ/mol)	$T\Delta s^{ads}$ (kJ/mol)	
SPFF	15	-46.39	-18.3	-28.09	33.46	-16.90	50.35
	25	-43.95	-19.05	-24.91	32.38	-14.87	47.24
	35	-37.15	-16.35	-21.41	30.89	-18.38	49.27
SPHP	15	-31.44	-17.45	-14.00	10.27	-16.46	26.88
	25	-28.96	-18.83	-10.13	11.72	-15.21	26.93
	35	-26.73	-20.34	-6.40	8.55	-16.33	24.97
SPXL	25	-43.08	-14.69	-28.39	9.46	-21.99	31.44

On the other hand, the enthalpy of adsorption of Cyt is endothermic ($\Delta h^{ads} > 0$) which means that, according to equation 7, entropic contribution plays a much more important role. Adsorption of Cyt into SPFF and SPHP is entropically driven. Despite entropically driven adsorption being generally unexpected in ion exchangers, this was reported in literature for different protein ion-exchangers combinations (Blaschke et al. 2013; W.-Y. Chen et al. 2007; Lin et al. 2001a). Entropic increases are often related to protein structural rearrangements (Lin et al. 2002; Norde 1994) and, more importantly, the release of water molecules and counter-ions (Blaschke et al. 2011; Bowen and Moran 1995; Desch et al. 2014; Dias-Cabral et al. 2005; Werner et al. 2012) from the protein and solid phase surface. The disruption of water structures and the subsequent release of the disordered water molecules to the bulk solution is responsible for the large entropy increases in the ion exchange processes. When a reversible equilibrium interaction prevails, for an entropically driven process, the binding strength of the protein with the resin is generally expected, to be enhanced by increases in temperature. When temperature increases, the ordered water molecules structure is diminished (Bowen and Moran 1995;

Duboue-dijon and Laage 2015), making the release of water molecules and counter ions requiring less energy, resulting in a higher protein retention. Nevertheless, this does not mean that electrostatic interactions are not present in Cyt adsorption process. In this case, the entropic effects overlapped the enthalpic ones and the net enthalpy of all present interactions was positive.

In addition, due to the interaction of the grafted layer with water molecules and counter ions, the presence of dextran grafted chains in the SPXL surface affects Cyt adsorption mechanism more than Lys because it is driven by entropy. **Table 3.4** shows a 3-fold decrease on ΔH^{ads} when comparing Cyt adsorption on SPFF and SPXL, while in Lys case there was no perceptible change in the enthalpy of adsorption.

Given these points, the driving force of adsorption of both proteins is different. Despite Lys and Cyt's charge being similar at these conditions, temperature affects retention in an opposite way. Lysozyme adsorption is enthalpically driven while cytochrome c adsorption is entropically driven. However, given that these proteins are similar in net charge and size, what are the physical properties that are responsible for opposite thermodynamic driving forces of adsorption? Our hypothesis is that the different driving forces are due to an interplay of (1) tertiary structure mobility and (2) partial secondary structure denaturation and (3) amino acid composition of the protein. Effect (1) and (2) are undoubtedly correlated with effect (3) because a change in the protein primary structure will likely translate into changes in secondary and tertiary structure. The balance of entropic and enthalpic contributions has been determined to vary significantly between amino acids (Bowen and Moran 1995).

Since the chromatographic surfaces are negatively charged, we assume that basic amino acids play a more important role in the adsorption mechanism. At pH 7, arginine and lysine are mainly responsible for positive charges at protein surface. As shown in **Table 3.2**, there are significant

difference in the basic amino acid composition of both proteins. In Lys there are 11 arginine residues (while only 2 in Cyt). On the other hand, Cyt has 19 lysine residues (while Lys has 6). Recently, combined molecular Monte Carlo and molecular dynamics simulations have indicated that lysine residues (Lys-25, Lys-27, Lys-72 and Lys-79) are responsible for the electrostatic interactions of Cyt with the negatively charged surfaces (Zhou et al. 2004). On the other hand, three arginine residues (Arg-5, Arg-125 and Arg-128) play a critical role on the binding of Lys in cation exchange surfaces (Steudle and Pleiss 2011). There is a quite big difference in the main amino acids involved in these proteins solid phase interaction.

Petrauskas et al. (Petrauskas, Maximowitsch, and Matulis 2015), in a thermodynamic study of positive amino acids binding to negatively charged aspartame, found out that arginine was bound with a more exothermic enthalpy and higher affinity than lysine. The hydrogen bonding formation enthalpy of arginine binding was -6.4 kJ.mol^{-1} whereas with lysine was 3.8 kJ.mol^{-1} . This is correlated with the adsorption energies observed for lysozyme (negative enthalpy, more arginine residues) and cytochrome c (positive enthalpy, more lysine residues). We conclude that positive charges in proteins should not be considered entirely equivalent if carried by lysine or arginine. The effect of the surface particle size on Δh^{ads} was also evaluated. It was observed that enthalpy absolute values slightly decrease when SPHP is used, due to the lower particle sized resin. This indicates that the particle size can interfere with access of the protein to the functional groups and decrease accessibility. The physical structures of resins are quite complex, the pore network contained within are typically a poorly defined collection of spaces of which the shape, cross-section and connectivity that may vary substantially. These structures may have an influence of the patches that proteins have in contact with the resins and subsequently slightly alter the adsorption enthalpy. The decrease of enthalpy absolute value with decrease particle size is observed

for both proteins but it is more notorious for Cyt case (from 30 kJ/mol to 10 kJ/mol). This difference is possibly due to higher repulsion caused the heterogenous charge distribution of Cyt previously explained. Also, when the pore is smaller, the frequency of interaction of proteins in the solution between themselves and with the ones already adsorbed increases, leading to a higher repulsion.

3.4.4 Effect of salt and pH conditions near protein isoelectric point

Adsorption energies and adsorption isotherms near the isoelectric point of each protein adsorbing into SPFF was also evaluated at 25 °C in order to further understand the charge effect on Δh^{ads} . **Table 3.5** and **Figure 3.7** show that Δg^{ads} is less exergonic for both molecules (Lys: from -19.05 to -7.98 kJ.mol⁻¹; Cyt: from -14.87 to -6.01 kJ.mol⁻¹). Adsorption is less spontaneous and energetically less favorable, which is expected when working with high salt concentrations in cation exchange chromatography.

Table 3.5. Average of Δh^{ads} , Δg^{ads} and $T\Delta s^{ads}$ obtained for the adsorption of cytochrome c with 10 mM boric acid with 200 mM NaCl at pH 10. In the case of lysozyme, 10 mM boric acid with 75 mM NaCl at pH 11 was used.

	T (°C)	Lysozyme			Cytochrome c		
		Δh^{ads} kJ/mol	Δg^{ads} kJ/mol	$T\Delta s^{ads}$ kJ/mol	Δh^{ads} kJ/mol	Δg^{ads} kJ/mol	$T\Delta s^{ads}$ kJ/mol
SPFF	25	-31.26	-7.98	-23.28	0.2	-6.19	4.88

Adsorption enthalpy absolute value decreases, which indicates that ionic interactions between the protein and resin are less energetic or masked by the presence of higher salt concentrations. This decrease on Δh^{ads} has already been observed before with lactoglobulin (Lin et al. 2001b) and lysozyme (Silva et al. 2014) adsorption. This is possibly due to: (1) a reduction in the energy necessary for dehydration and release of counter-ions at higher salt concentrations; and (2) the electrostatic attractive force was screened by an increment of the salt concentration leading to a decrease in the exothermic

amount of heat. While effect (1) is more significant in Cyt adsorption, effect (2) is more significant in Lys adsorption mechanism due to their respective difference of the driving forces of adsorption.

All things considered, Lys and Cyt were used in this study as model molecules with the hope that they would represent well what could happen in the adsorption of other proteins. However, we can conclude that is probably too soon to make general theories regarding protein adsorption. Even similar proteins may show completely opposite behaviors in a chromatographic column. There is a need of further fundamental thermodynamic studies on protein adsorption without forgetting molecular dynamics simulations that consider often neglected phenomena, such as, structural rearrangements, release of water molecules and counter-ions. These are needed to address the protein-solvent interaction so that adsorption phenomena can be understood more completely.

3.5 CONCLUSION

In conclusion, the presented study aims to further contribute to the understanding of different behavior Cyt and Lys in cation exchangers from a thermodynamic viewpoint. This study relates thermodynamic parameters with chromatography parameters in order to further understand protein behavior at charged surfaces. Lys adsorption was exothermic while Cyt showed an endothermic adsorption despite the fact that these proteins share several common characteristics. Our data indicates that even when proteins are considered similar, conclusions on their molecular driving force of adsorption should not be generalized.

Each protein behaves differently when adsorbing onto a surface, and more protein adsorption studies are needed in order to have an overarching general model capable of predicting protein behavior in these surfaces.

3.6 SUMMARY

Understanding of the adsorption mechanism of proteins onto chromatography resins is essential for modeling and developing efficient chromatographic processes. In this study, we analyzed the adsorption of model proteins onto ion exchange chromatography (IEC) resins by using isothermal titration calorimetry (ITC) in order to further understand the adsorption mechanism. As a model system, two basic proteins, equine cytochrome c (CytC) and chicken egg-white lysozyme (Lys) adsorbing onto cation-exchange chromatography resins [SP Sepharose Fast Flow and SP Sepharose High Performance] was chosen. In linear gradient elution (LGE) the retention volume of Lys was larger than that of CytC for both SPFF and SPHP. When the temperature increased, the retention volume of CytC slightly increased, whereas that of Lys slightly decreased. The protein binding site values determined by using LGE experimental data (GH-IR plots) did not change with temperature. This indicates that a more complex mechanism of adsorption may be involved. Large exothermal enthalpies of adsorption were observed when Lys adsorbed onto the cation exchanger. The Lys adsorption was found to be enthalpically driven. On the other hand, endothermic enthalpies were dominant for CytC adsorption, which was entropically driven. This indicates that structural rearrangements, dehydration and release of counter-ions plays a major role in CytC adsorption.

Chapter 4: Grafted ligand architecture effect on protein adsorption enthalpy

4.1 INTRODUCTION

One of the most challenging factors on the biomolecule production is its purification from cell culture and most importantly its separation from other similar proteins that are present in the expression systems. Protein chromatography, a technique based on selective adsorption, is able to successfully purify proteins for therapeutic use while following the guidelines required by drug regulatory agencies. Downstream protein processing is now routinely found to be the bottleneck in biopharmaceutical manufacturing because it has not kept pace with upstream production latest improvements. In some cases, the lack of downstream processing capacity can seriously affect the profitability of a new pharmaceutical product and even result in its failure.

In order to increase the capacity and performance of chromatographic surfaces, new ligand types and new technologies have been developed. Maximum binding capacities and mass transfer properties have been the main focus point of optimizations by the chromatography industry (Müller 2005). Chromatography surfaces with grafted ligands have equally charged polymer chains that repel each other providing a three-dimensional space for proteins to travel into the “forest” of the extended polymer chains (Kawai et al. 2003). Hence, increasing the space available for proteins to adsorb and consequently having higher capacity. However, surface with grafted ligands have been commercially available and are used for protein separation but not much attention has been given on the molecular interactions and thermodynamics of the protein adsorption process.

Thermodynamic studies on protein adsorption onto chromatographic resins mainly focus on the molecular and sometimes atomic level interaction between proteins and ligands. Yet, not much attention is given to the relation between chromatographic parameters with thermodynamic parameters. This results in a difficult interpretation of thermodynamic data when applied to protein adsorption studies. If present, these relations would be important to directly make thermodynamic parameters more practical with direct applications to protein chromatography. Important the development of novel adsorption surfaces.

In this work, relations between thermodynamic parameters, in this case, the change in standard molar adsorption enthalpy (Δh^{ads}), and chromatography operational parameters were investigated. Four grafted layer surfaces with different base matrixes were studied. Isothermal titration calorimetry, together with equilibrium adsorption isotherms, were used to directly determine the adsorption enthalpy change (Δh^{ads}) of a model protein, bovine serum albumin (BSA). In addition, a conventional non-grafted surface (Q-Sepharose FF), was also used in order to serve as a comparison to the obtained thermodynamic data with a conventional surface.

4.2 EXPERIMENTAL

4.2.1 Ion exchange chromatography

The selected model stationary phases were Toyopearl GigaCap Q-650M, Toyopearl SuperQ-650M, Toyopearl Q-600C AR (Tosoh Biosciences, Japan) and Q Sepharose FF, Q Sepharose XL (GE Healthcare, USA). The physical properties of the chromatographic adsorption surfaces used in this work are summarized in **Table 4.1**. Bovine serum albumin Lot#037K0765 was purchased from Sigma-Aldrich (USA). Commercial protein composition was approximately 10% dimer and 90% monomer. Before the use of BSA on

isothermal titration calorimetry and equilibrium adsorption isotherms experiments, dimers and monomers were separated using a preparative size exclusion chromatography column Superdex Hiload 26/600, 200 pn (GE Healthcare, USA). BSAm was selected because its protein characteristics are well known and it is extensively used in previous literature as a model protein. All salts and buffers used in this work were purchased from Wako (Japan) and dissolved in ultrapure deionized water.

Table 4.1. Summary of physical properties of chromatographic resins used in this study. Information was given by the manufacturers.

	Q Sepharose FF	Q Sepharose XL	Toyopearl SuperQ 650M	Toyopearl GigaCap Q650M	Toyopearl Q 600C AR
Manufacturer	GE Healthcare	GE Healthcare	Tosoh Biosciences	Tosoh Biosciences	Tosoh Biosciences
Base matrix structure	Cross-linked 6% agarose	Cross-linked 6% agarose	Methacrylic	Methacrylic	Methacrylic
Mean pore size of base matrix [nm]	n.d.	n.d.	100	100	75
Mean particle Size of base matrix [μm]	90	90	65	75	100
Ion Exchange capacity [eq/L gel]	0.18-0.25	0.18-0.26	0.25	0.10-0.20	0.14 – 0.23
Ligand attachment chemistry	Conventional type	Grafted ligands. Dextran chains	Grafted ligands. 2 nd Generation	Grafted ligands. 3 rd Generation	Grafted ligands. 3 rd Generation

Chromatography experiments were carried out on a fully automated liquid chromatography system ÄKTA purifier (GE Healthcare Life Sciences, Sweden). Two buffers were used as mobile phase in salt gradient elution experiments. 10 mM TRIS, 30 mM NaCl at pH 7 (or pH 8.5) was used as the starting buffer (buffer A). The same buffer solution containing 1M NaCl was used as final elution buffer (buffer B). The column was equilibrated with buffer

A. BSA was dissolved in buffer A at 5 mg/mL. The linear gradient was performed by changing the buffer composition linearly from buffer A to buffer B with time. Namely, the salt concentration was increased with time at a constant pressure, temperature and pH. Experiments were done in the linear region of the adsorption isotherm. The experiments were done in duplicate.

For Toyopearl resins the column properties and operational parameters were the following: 1 mL pre-packed Toyoscreen columns were used with a constant flow rate of 1 mL/min. The injection volume was 0.01 mL. The porosity values of the columns were measured with an unretained solute (Vitamin B12) at the same flow rate, these were $\varepsilon = 0.34, 0.33, 0.37$ for GigacapQ, SuperQ and Q600, respectively. On the other hand, Q Sepharose resins were packed with a total column volume of 9.5 mL. 0.1 mL BSA samples were injected and eluted at a constant 3 mL/min. Porosity values were $\varepsilon = 0.37$ and 0.32 for Q Sepharose FF and Q Sepharose XL, respectively.

Since the columns have different dimensions, GH-I_R model was applied in order to normalize the gradient slopes and to determine inherent adsorption parameters. GH-I_R model was originally developed for ion-exchange chromatography of proteins by our group where the modulator, NaCl, is used to elute proteins from a chromatographic surface. The peak retention modulator concentration (I_R) increases with increasing normalized NaCl gradient slope (GH) which can be defined as (Hosono et al. 2012):

$$GH = (gV_0) \left(\frac{V_t - V_0}{V_0} \right) = g(V_t - V_0) \quad (44)$$

here, V_t is the total column volume (mL), V_0 is the retention volume of a totally unretained solute (mL), and g is the gradient slope defined by

$$g = \frac{I_F - I_0}{V_g} \quad (45)$$

where I_F is the final NaCl concentration (M), I_0 is the initial NaCl concentration (M) and V_g is the gradient volume (mL). The experimental GH-I_R data can be commonly expressed by the following equation, detailed in previous

publications (Yamamoto 2005; Yamamoto, Hakoda, et al. 2007; Yamamoto and Kita 2006):

$$GH = \frac{I_R^{B+1}}{A(B+1)} \quad (46)$$

In this expression, I_R is the elution salt concentration, B is the protein binding site number, and A is given by the following expression:

$$A = K_e \cdot \Lambda^B \quad (47)$$

where K_e is the reaction constant for ion exchange reaction and Λ is the effective ionic capacity of the surface. Using $GH-I_R$ model, protein adsorption/desorption parameters can be compared using chromatographic columns with different physical characteristics and I_R can be determined at any given GH .

4.2.2 Equilibrium adsorption isotherms

Batch equilibrium adsorption isotherms were obtained to determine more accurately the amount of protein adsorbed with each isothermal titration injection, explained later in this section. The chromatographic resins were washed with ultrapure water and later with the respective buffer solution by decantation. Equilibrium adsorption experiments were carried out in 96-well acrylic plates. First, each well was filled with 0.3 mL of BSA monomer (BSAm) at concentration varying from 0 to 20. Initial protein concentration was measured by spectrophotometry at 280 nm and 300 nm in a multi-well plate reader PowerWave XS (Biotek, USA). BSA calibration curves were determined in preliminary experiments using 0.2 and 0.3 volume in each well. Then, 20 μ L of resin slurry (50% resin-buffer) was added in each well and stirred inside a temperature controlling chamber for at least 8 hours at 25 °C. Preliminary experiments, in the whole range of tested concentrations, showed that equilibrium was reached after only 15 minutes (data not shown). After equilibration, the contents of the wells were transferred to a 96-well filter plate

and centrifuged for 3 minutes at 2000 RPM onto a new acrylic 96-well plate. 0.2 mL of the filtered solution was transferred to analogous wells in order to keep the solution pathlength constant in each well. The equilibrium concentration was determined using the same method as the initial concentrations. From the equilibrium concentration and initial concentration, the surface concentration could be determined by a mass balance. Equilibrium concentration was plotted against the surface concentration calculated. The experiments were done in duplicate. The adsorption equilibrium isotherms were not obtained to study the fitted parameters, but to determine the adsorbed amount in each isothermal titration injection. For this goal, any equation can be used, even lacking physical meaning, as discussed by previous authors (Blaschke et al. 2011; Hackemann and Hasse 2017). In this study, the curves were fitted with the well-known Langmuir model,

$$C_s = \frac{q_m K C}{1 + K C} \quad (48)$$

where C_s is the surface concentration of protein in the resin surface, q_m is the maximum static binding capacity, K is the equilibrium coefficient and C is the bulk concentration after equilibrium.

4.2.3 Isothermal titration calorimetry

Microcalorimeter used in this work was Nano ITC from TA Instruments (Delaware, USA). It has been already shown that even small pH mismatches between the ITC cell and titration solution affects quite significantly the calorimetric results as artifacts in the enthalpy can arise due to buffer protonation effects (Duff et al. 2011). Prior to the experiment, BSA_m solutions were prepared in the respective buffers and exhaustively washed with the respective buffer using AmiconR Ultra-4 10000MW (Milipore Sigma, USA), for 15 min at 7000 RPM.

In the beginning of the calorimetric titration experiment, the reference cell was filled with distilled degassed water. The main cell was filled with 1.8 mL of a 50% (buffer/resin) slurry suspension. The syringe was filled with BSA solution at 20 mg/mL. The cell was closed and agitated at 300 RPM at 25 °C. After a 5400 seconds' timeout, for the thermal equilibrium can be reached, ten injections of 10 µL were titrated with the 100 µL syringe from the ITC equipment. Injections were carried out with a 600 seconds' interval from each other. The temperature fluctuations indicated by the instrument were below 0.0002 K. Both resin slurries and protein solutions were previously degassed in a degassing station at 400 mmHg for 10 minutes (TA Instruments, Delaware, USA).

During the calorimetric measurements, a small signal is observed upon injecting the same solution onto itself. This signal was previously considered to be due to friction, dissipation and other effects like a small mismatch of temperature of the cell and that of the injected solution (Dieterle et al. 2008). Additional contributions to the calorimetric signal can arise from buffer interactions that are independent of the adsorption interactions. These contributions that reflect temperature dependence of buffer ionization as well as of water structure, need to be subtracted from the total measured signal. Considerable attention must be given to the design of adequate control experiments to clarify these contributions (Winzor and Jackson 2006b). The contribution of heat of a protein injection into a resin mixture using ITC can be divided into several origins:

$$\Delta H^{exp} = \Delta H^{ads} + \Delta H^{dil} + \Delta H^{solv} \quad (49)$$

where ΔH^{exp} is the total enthalpy measured by the ITC. ΔH^{ads} is the enthalpy contribution from the adsorption of the protein into resin. ΔH^{dil} is the contribution of the protein solution dilution heat, measured by titrating protein solution into the same buffer that it was diluted into. ΔH^{solv} is caused by the adsorption of buffer ions and it was determined titrating buffer into the

resin slurry. **Table 4.1** shows a typical thermogram and the respective blank trials. Furthermore, the area correspondent to these blank trials that consisted in a complete set of 10 injections were subtracted from the one obtained titrating the protein into the resins, and effective enthalpic contribution from the protein adsorption was obtained.

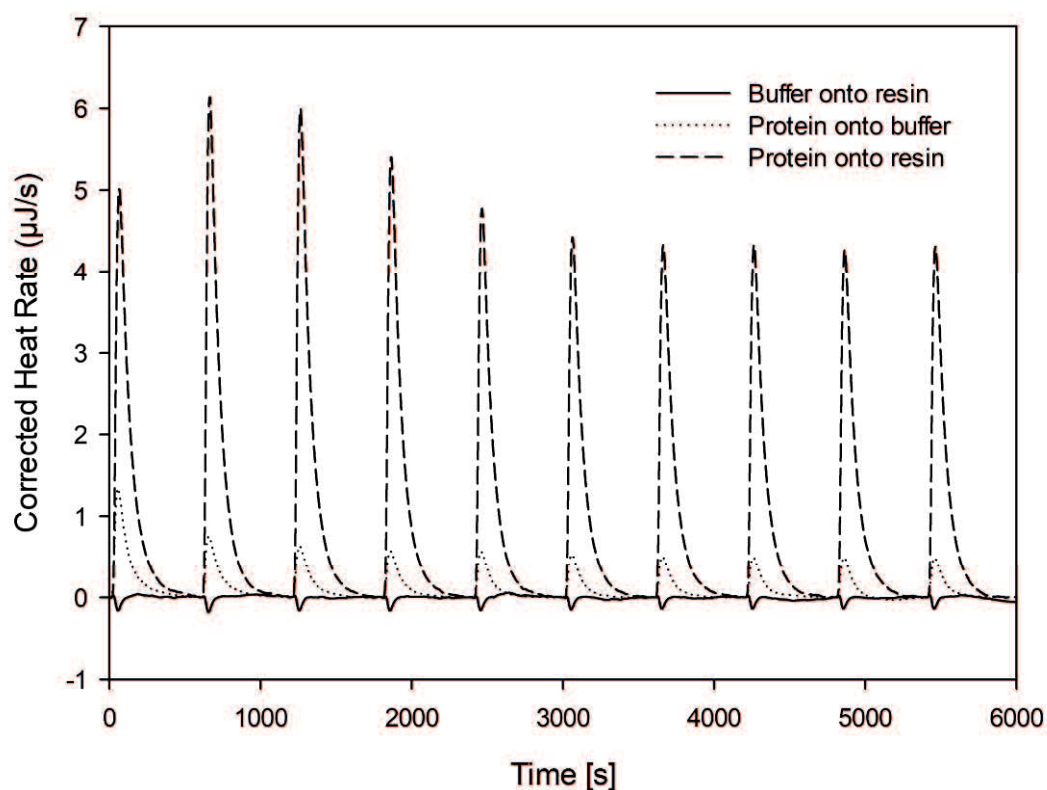


Figure 4.1. Typical thermogram obtained titrating BSA monomer at 20 mg/mL onto Toyopearl Q600AR and the respective blank trials. Buffer was 10 mM TRIS, 30 mM NaCl at pH 7, 25°C.

The first peak of every trial is not shown and it was not used in any calculation due to the well-known phenomenon, named “first-peak anomaly” in previous studies (Werner et al. 2012). Protein injections and all blank trials were done in duplicate.

Adsorption heats are measured directly by ITC, and molar enthalpy of adsorption Δh^{ads} was then calculated by the following equation:

$$\Delta h^{ads} = \frac{\Delta H^{ads}}{\Delta m} \quad (50)$$

where Δm is the amount of molecule adsorbed upon each injection (mol). Since ITC is a closed system, it is impossible to measure the concentration in real time. Hence, the amount of adsorbed BSAm in each injection was calculated using a combination of the equilibrium adsorption isotherm and a mass balance.

Since protein adsorption can be considered a reversible spontaneous reaction in these conditions, Gibbs-Helmoltz relation is valid to be used in protein adsorption:

$$\Delta g^{ads} = \Delta h^{ads} - T\Delta s^{ads} < 0 \quad (51)$$

where T is the absolute temperature, Δg^{ads} and Δs^{ads} are the standard molar change in Gibbs free energy and standard molar change in entropy, respectively.

4.3 RESULTS AND DISCUSSION

4.3.1 Linear gradient chromatography and equilibrium adsorption isotherms

Chromatography was conducted using a linear gradient elution to understand the retention profiles of BSAm onto these anion exchangers. GH-I_R model allows for the elucidation and comparison of the molecular mechanism of protein adsorption (Rüdt et al. 2015; Urmann et al. 2010; Yamamoto, Nakamura, et al. 2007). From the slope of these curves we can determine the protein binding sites number (B-number). After the application of the GH-I_R model, **Figure 4.2A** clearly shows that changing the chromatographic surface did not drastically change the B number as the slopes of GH-I_R plots were quite similar. **Table 4.2** shows that the B-number appears to be constant when using different grafted resin, indicating that the protein binding sites did not change significantly between chromatographic resins. The B-number is more sensitive to protein changes than changes in the surface physical properties. In addition, since BSAm isoelectric point is approximately pI = 4.7, when increasing pH

from 7 to 8.5 we are inducing more charges on the surface amino acids by getting further from the pI, leading to a modest increase in the B-number with pH.

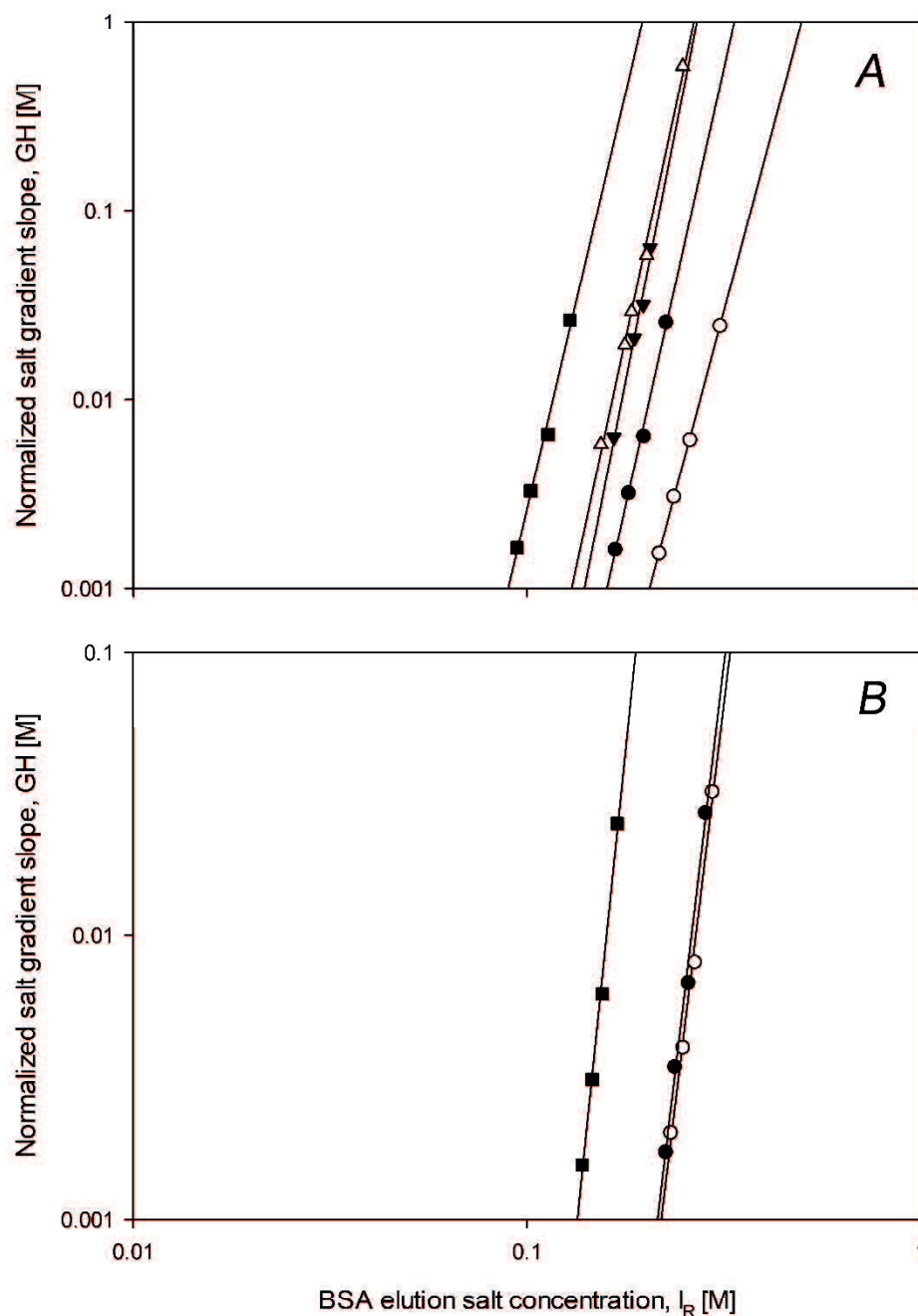


Figure 4.2. GH-IR curves for all the tested chromatographic surfaces at pH 7 (A) and pH 8.5 (B); Q Sepharose FF (Δ), Q Sepharose XL (\blacktriangledown), Toyopearl Q600-AR (O), Toyopearl SuperQ-650M (\blacksquare), Toyopearl GigacapQ 650M (\bullet). Note that both axes have a logarithmic scale. The experimental data were fitted using GH-IR model equation (Yamamoto 2005), and A and B values were calculated. Mobile phase A: 10 mM TRIS, 30 mM NaCl; mobile phase B: 10 mM TRIS, 1M NaCl.

Although Toyopearl resins share the same base metacrylate base matrix, A-values suggest that the disposition of the ligands (or ligands themselves) are different between these resins. When considering equation 47, A-parameter is directly proportional to the specific surface ligand density. The ligand density obtained from retention data will of course be different from the values disclosed by the manufacturers due to inherent differences in the method of determination. While the prior is determined from elution profiles and it is specific for each condition and adsorbed molecule, the former is measured with a direct pH titration not specifying the adsorbed molecule. The second-generation grafted ligand, Toyopearl SuperQ 650M, shows the lowest A-value, i.e. lowest specific ligand density, when compared with the other chromatography surfaces. The disposition of ligands capable of protein adsorption appear to be lower than the others, if we consider the ligand density from the protein point of view. However, the ionic capacity values published by the manufacturer are quite similar to other grafted ligand resins, this suggests that some ligands may be forming a denser “forest” inside pores that are hardly accessed by BSA_m and do not contribute for protein adsorption. This also results in a lower binding capacity of SuperQ.

When pH increases from 7 to 8.5, A-value decreases for all resins, but this decrease is more significant in Q600 and SuperQ (more than 500-fold decrease), than in GigaCapQ (around 3-fold decrease). This suggests that despite all possessing quaternary amine ligands (as indicated by the manufacturer), there are significant differences in the Q-ligand structure of both resins probably induced by the chemical modifications of the grafted chains. This pH effect on toyopearl resins was also observed in the equilibrium adsorption isotherms.

Equilibrium adsorption isotherms were mainly used to determine the protein adsorbed amount in the ITC cell. Nevertheless, important information can be derived from these curves. Surprisingly, despite being grafted, SuperQ

shows a very low capacity when compared to other grafted ligand surfaces showing slightly lower capacities than the conventional model surface Q Sepharose FF (**Figure 4.3A**). With the exception of SuperQ, grafted ligand surfaces show higher binding capacities for BSA_m when compared with the non-grafted surface. Our data suggests that SuperQ behaves similarly with a resin without grafted chains. Pezzini et al. (Pezzini, Cabanne, and Santarelli 2009), by analyzing the profile of breakthrough curves, consider Toyopearl SuperQ 650M as a non-grafted chromatographic surface despite the manufacturers catalog indicating that it is a 2nd generation ligand with a carbon spacer network between the bead surface and the ligand.

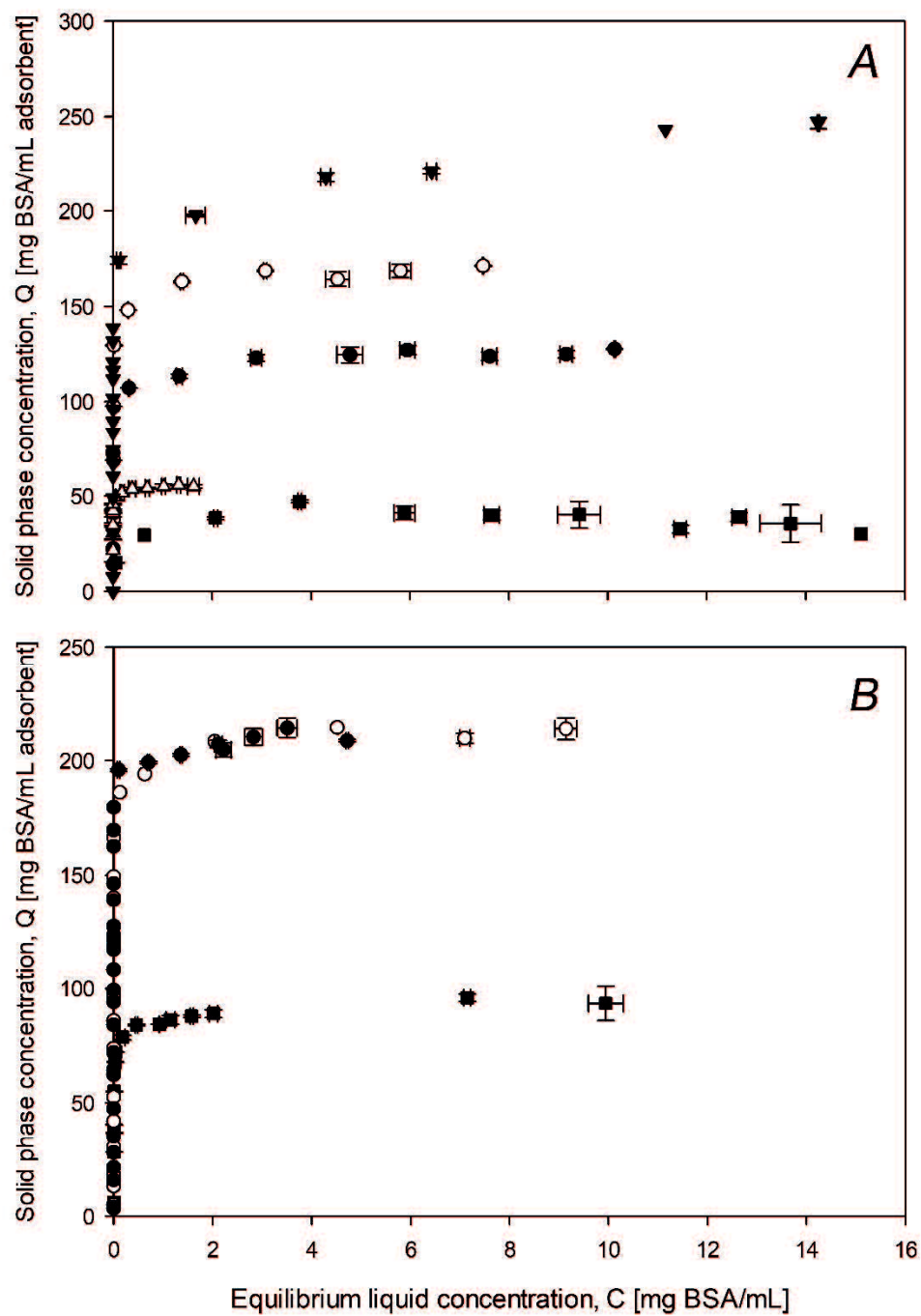


Figure 4.3. Equilibrium adsorption isotherms obtained at 25 °C at pH 7 (A) and pH 8.5 (B); Q Sepharose FF (Δ), Q Sepharose XL (▼), Toyopearl Q600-AR (○), Toyopearl SuperQ-650M (■), Toyopearl GigacapQ 650M (●). 10 mM TRIS, 30 mM NaCl.

Ordered from higher to lower maximum binding capacities: Sepharose XL, Q600, GigaCapQ, Sepharose FF and SuperQ. When pH increases from 7 to 8.5, SuperQ's maximum binding capacity increases significantly more than the other chromatography surfaces. If this would be solely due to changes in the

protein, then the change in capacity would be comparable between different resins. As it is not, and due to SuperQ's ligands being more dependent on pH than other methacrylate resins, as shown by the A-value 550-fold decrease at pH 8.5, it can be suggested that the resins ligands responsible for the protein adsorption may not be composed of solely quaternary amines.

Table 4.2. Summary of chromatographic retention data and change in adsorption enthalpy.

	Toyopearl SuperQ650M		Toyopearl Q600C AR		Toyopearl GigaCap Q650M		Q Sepharose XL	Q Sepharose FF
pH	7.0	8.5	7.0	8.5	7.0	8.5	7.0	7.0
A ($\times 10^7$)	0.72	0.0013	5800	11	45	17.2	1.1	2.8
B	7.7	12.5	6.7	9.4	8.3	10.5	9.5	8.7
Salt needed to cause desorption¹ [mol/L]	0.127	0.171	0.307	0.291	0.227	0.283	0.191	0.182
Δh^{ads} (kJ/mol)	49.65	14.73	-134.06	-25.45	-55.55	-18.91	-25.06	73.43

¹at GH = 0.025

4.3.2 Thermodynamic analysis

Isothermal titration calorimetry shows that BSA_m adsorption was exothermic ($\Delta h^{ads} < 0$) for almost all grafted ligand resins (Table 4.2). Exothermic enthalpies of adsorption are commonly found when studying protein adsorption onto ion exchange chromatography surfaces (Blaschke et al. 2011; Bowes et al. 2012; Dieterle et al. 2008; Lin et al. 2001b; Silva et al. 2014), indicating that the major driving force of adsorption are attractive ionic interactions between the ligands and the protein. The most exothermic values were observed for Q600, followed by GigaCapQ and lastly Q Sepharose XL. On the other hand, SuperQ, once again, shares more properties with the conventional model resin. Both SuperQ and Q Sepharose FF adsorption is endothermic, indicating that the enthalpy change itself is not promoting

adsorption spontaneity (i.e. a positive effect on Δg^{ads} in equation 51). In these surfaces, BSAm adsorption is entropically driven indicating that the entropy gains overcome the gain in enthalpy and are likely to drive the adsorption process. This does not mean, however, that ionic interactions don't play a role in this mechanism but that these interactions were masked by the higher entropically driven subprocesses. In protein adsorption, the subprocesses that are characterized by increases in entropy are (1) dehydration and release of counter-ions from the ligands and grafted chains, (2) dehydration and release of counter-ions from the protein surface, (3) conformational changes of the protein. Protein conformational changes may differ with different ligand attachment technologies, being more likely to occur in some surfaces more than others. Since ITC only measures the total change of enthalpy, it is impossible to isolate the energetics of the complex subprocesses of protein adsorption. However, it is clear that the ligand attachment technique affects how the ligand and chain interact with counter-ions and water molecules, thus confirming the existence and importance of water release in ion-exchange adsorption applications. Assuming that SuperQ surface possesses a grafted layer, Toyopearl SuperQ's grafted ligand layer may hold a higher number of orders water molecules and counter-ions. The increased degrees of freedom gained by these small molecules upon release, i.e., entropic gains, are the main driving force for the adsorption.

GH- I_R plots allow us to normalize the salt gradient slope of any column size using any flow rate. Although columns used in this experiment have different sizes, porosity and they were operated in slightly different conditions, the salt required for BSAm elution (I_R) can be determined by interpolation of the GH- I_R model at any given salt gradient slope. **Table 4.2** shows the I_R value for each surface at GH = 0.025. A new relation has been found between the change of adsorption enthalpy Δh^{ads} and I_R , represented in **Figure 4.4A**. It is clear that this relation was only true for the grafted layer resins as Sepharose

FF, the only resin without grafted chains, is the clear outlier for this trend. This linear trend was also observed at pH 8.5 (**Figure 4.4B**), despite not showing the same slope. This new relation is very significant for the future interpretation of adsorption thermodynamics parameters, it is a small step to the demystification of thermodynamics applied to the study of protein adsorption.

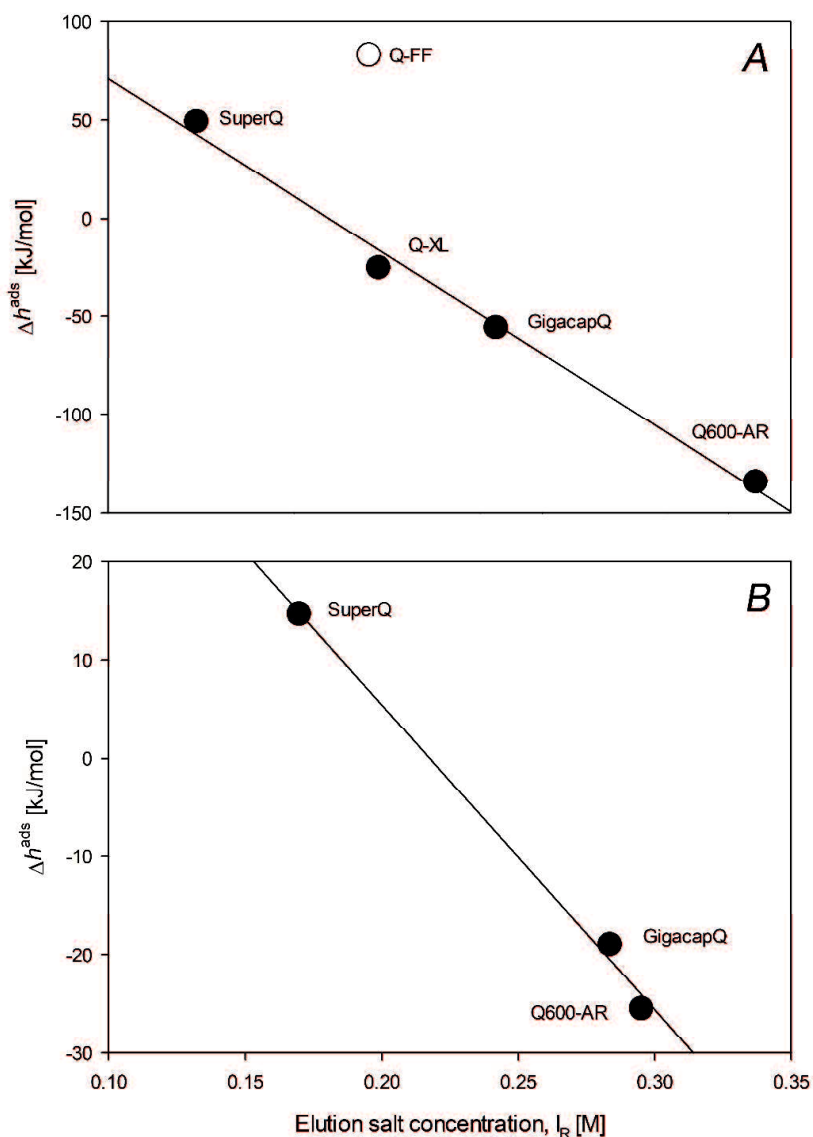


Figure 4.4. Linear relations between the change in adsorption enthalpy (Δh^{ads}) directly measured by ITC and the BSAm elution salt concentration (I_R) determined with linear gradient chromatography. (A) pH 7, (B) pH 8.5. Grafted layer chromatographic surfaces are represented with black circle while the model conventional non-grafted surface is represented with an open circle.

4.4 CONCLUSION

Linear gradient elution chromatography and isothermal titration calorimetry have been applied to the study of BSA_m adsorption onto chromatography surfaces with grafted layer ligands.

Different ligand architectures changed the signal of Δh^{ads} . The adsorption of BSA_m was endothermic indicating that the entropic events like dehydration, release of counter-ions, conformational changes are more important for adsorption in second generation grafted ligands (Toyopearl SuperQ 650M). On the other hand, the other two grafted surfaces display exothermic signals indicating attractive ionic interactions.

A new linear relation has been found between I_R and Δh^{ads} , proving there is a strong correlation between attractive forces during adsorption and the salt required for protein desorption. This may provide new resources to the rational design of future chromatographic surfaces and new downstream process units.

ITC is a powerful technique that can be successfully applied to chromatography. However, nowadays, the obtention of the thermodynamic parameters by itself is not enough in order to further help us understand adsorption mechanisms. Also, these relations between measured thermodynamic quantities and properties with a physical meaning are necessary for the future application of ITC in more fields.

4.5 SUMMARY

Thermodynamic studies on protein adsorption onto chromatographic surfaces mainly focus on the molecular level interaction between proteins and ligands. Yet, not much attention is given to the study of grafted ligand architecture effect on thermodynamic parameters, nor to the relation between chromatographic parameters with the directly obtained thermodynamic

parameters. These relations are needed in order to confer meaning and to ease future data interpretation of thermodynamic studies of protein adsorption. In this study, bovine serum albumin monomer (BSAm) was adsorbed onto chromatographic surfaces with grafted ligands and adsorption was studied from a thermodynamic point of view together with chromatographic data. Isothermal titration calorimetry (ITC) results showed that BSA_m adsorption is exothermic ($\Delta h^{\text{ads}} < 0$) when adsorbs onto Toyopearl GigaCapQ 650M, Toyopearl Q600AR, and Q Sepharose XL, but endothermic ($\Delta h^{\text{ads}} > 0$) when adsorbs onto Toyopearl SuperQ and Q Sepharose FF, showing clear differences in the adsorption driving forces caused by different ligand architectures. In addition, we found a new linear relation between the salt required for protein elution and the change in adsorption enthalpy (Δh^{ads}), intrinsically connecting both adsorption and desorption mechanisms.

General conclusions

Despite the controversy surrounding the discrepancies found between indirect and direct methods for thermodynamic parameters determination, this study did not find significant discrepancies. This was probably due to the fact that the model system was too simple, as the molecules were too small when compared to proteins.

van't Hoff analysis is usually applied to the chromatography using isocratic elution data. However, this mode can be quite time consuming because the optimal K values are searched based in trial and error. In addition, van't Hoff application to IE only allows for the calculation of thermodynamic parameters at once salt concentration. Further experiments are needed at different salt concentrations to re-calculate those parameters.

This thesis, more precisely in chapter 2, shows that is also possible to apply van't Hoff analysis to linear elution data. This mode of operation not only does not require trial and error searches for optimal K values but theoretically allows for the determination of the thermodynamic parameters at any given salt concentration with the same set of experiments.

Another important conclusion in this study is that the amino acid composition of proteins seems to be the cause for different driving forces of adsorption. Even two very similar proteins, like lysozyme and cytochrome *c*, show opposite temperature-dependent behaviors. Proteins like, lactoalbumin, serum albumin, cytochrome, lysozyme, ribonuclease and so on, are often used as model proteins in adsorption studies. However, our data suggests that the use of model proteins in thermodynamic studies has its merit. It allows us to compare and compile large amounts of data obtained from different techniques. But, at the time of the writing of this thesis, it is still impossible to find an overarching model that explains every single protein adsorption

mechanism. In our study, we hypothesize that lysozyme and cytochrome c adsorption onto charged sepharose beads is connected with the protein amino acid sequence. This complicates any theory or model that tries to predict the binding energetics based on protein physical properties. In thermodynamic studies of adsorption, each case is a different one, and it is too soon to make general conclusions about all proteins.

In addition, thermodynamic studies on protein adsorption onto chromatographic surfaces mainly focus on the molecular level interaction between proteins and ligands. However, not much attention is given to the relation between chromatographic operational parameters with the directly obtained thermodynamic parameters. These relations are needed to confer meaning and to ease future data interpretation of applied thermodynamic studies of protein adsorption.

In this study we present a novel linear relation between the salt concentration needed for protein elution (I_R) and the adsorption enthalpy (Δh^{ads}). This intrinsically connects both adsorption and desorption mechanisms and allows a more rational design of new chromatographic surfaces and downstream processes.

We hope this study helps to shed more light into the fundamental properties of protein adsorption.

List of Publications

Proceedings

Masataka Hamachi, Simoes Cardoso Joao Carlos, Noriko Yoshimoto, Shuichi Yamamoto, "Retention and Diffusion Behaviours of Large Biomacromolecules in Chromatography Solid Phase", 3rd International Symposium on Multiscale Multiphase Process Engineering – Toyama – Japan, 2017

Joao Simoes-Cardoso, Nanako Hoshino, Noriko Yoshimoto, Shuichi Yamamoto, "Isothermal titration calorimetry application to the study of the protein adsorption onto ion exchange chromatographic materials", Asian Pacific Confederation of Chemical Engineering – Sapporo – Japan, 2019. (Submitted)

Full length articles

Joao Simoes-Cardoso, Noriko Yoshimoto, Shuichi Yamamoto, "Thermodynamic analysis of polyphenols retention in polymer resin chromatography by van't Hoff plot and isothermal titration calorimetry". Journal of Chromatography A, July 2019, In Press. DOI: 10.1016/j.chroma.2019.460405

Joao Cardoso, Noriko Yoshimoto, Shuichi Yamamoto, "Methods for thermodynamic analysis of temperature dependence of chromatography separation". Japan Journal of Food Engineering, September 2019, Vol. 20, No. 3, pp 99-105. DOI: 10.11301/jsfe.19550T

Joao Carlos Simoes-Cardoso, Hiroshi Kojo, Noriko Yoshimoto, Shuichi Yamamoto, "Thermodynamic analysis of the adsorption of lysozyme and cytochrome c onto cation exchange chromatography resins". (Submitted, In Peer Review)

Joao Carlos Simoes-Cardoso, Nanako Hoshino, Noriko Yoshimoto, Shuichi Yamamoto, "Surface grafted ligand architecture effect on protein adsorption enthalpy". (To be submitted)

List of Figures

Figure 1.1. Adsorption equilibria. This is a simplified scheme of the equilibriums and interactions that are present on protein adsorption onto an anionic surface. Despite most adsorption models taking into consideration some of the overall equilibriums, overarching general mechanistic models are still lacking.....	4
Figure 1.2. Pores of grafted chromatography surface beads. (A) conventional type with charged ligands covalently bound to the pore walls, (B) grafted polymers as spacers, (C) cross-linked gel polymer network.....	9
Figure 1.3. van't Hoff plot. By plotting $\ln K$ versus $1/T$, standard enthalpy change can be directly determined from the slope of the obtained curve ($-\Delta H^0/R$), and standard entropy change from ordinate intercept ($\Delta S^0/R$).	14
Figure 1.4. Isothermal titration calorimeter scheme. reference cell is usually filled with distilled degassed water (Solution B). The main cell is filled with slurry resin suspension, i.e., chromatography resin mixed with buffer (Solution A). The titration syringe is containing the protein solution (Solution C) which then is injected periodically	17
Figure 1.5. Typical thermogram for a reaction with a moderate K value. The enthalpy of adsorption can be directly determined from the area of the first peaks. The area of the smaller, later peaks occur due to dilution heat.....	19
Figure 1.6. Typical thermogram for a reaction with a high K value. Thermograms obtained titrating BSA monomer at 20 mg/mL onto Toyopearl Q600AR and the respective blank trials. Buffer was 10 mM TRIS, 30 mM NaCl at pH 7, 25°C.....	20
Figure 1.7. Flow chart of the present study	25
Figure 1.8. Summary schematics of the present study	26

Figure 2.1. Typical thermograms. EGCG in 20% (ethanol-water) injection into PS-DVB resin particles (full line); 20% ethanol injection into PS-DVB (dashed line); and EGCG into 20% ethanol (dotted line). The experiment consists of a total of 10 injections of 10 μ L each, the sample cell was stirred at 250 rpm at 288 K.	34
Figure 2.2. Linear gradient elution curves as a function of temperature. Mobile phase A: 10% ethanol; mobile phase B: 40% ethanol; $V_g = 100$ mL. Column size: $Z = 4.1$ cm, $d_c = 1.1$ cm, $\epsilon = 0.390$	36
Figure 2.3. GH-IR curves for (A) catechin and (B) EGCG. Note that both axes have a logarithmic scale. The experimental data were fitted to eq. 8 by the least square fitting method, and A and B terms were calculated. Mobile phase A: 10% ethanol; mobile phase B: 40% ethanol; Column size: $Z = 4.1$ cm, $d_c = 1.1$ cm, $\epsilon = 0.390$	37
Figure 2.4. Isocratic elution curve profile on HP20SS. Injected sample was (A) catechin, $Z = 4.9$ cm, $\epsilon = 0.378$ and (B) EGCG, $Z = 4.6$ cm, $\epsilon = 0.384$. Injected sample volume was 100 μ L with a concentration of 1 mg/mL. Mobile phase was 20% ethanol with a flow rate of 1 mL/min.	38
Figure 2.5. Van't Hoff plots with KIE and KLGE calculated from isocratic elution curves at 20% ethanol concentration for (●) Catechin and (○) EGCG. Squares represent van't Hoff plots with KLGE calculated from GH-IR curves, (■) Catechin and (□) EGCG. The solid and dashed lines represent the linear regressions for obtaining KIE, and KLGE respectively.	39
Figure 2.6. Comparison of adsorption enthalpy values determined by isothermal titration calorimetry of EGCG and catechin in 20% ethanol-water onto Polystyrene-divinylbenzene (PS-DVB) resin particles at 288, 293 and 298 K.....	40
Figure 3.1. Overlapped chromatograms obtained at 15 $^{\circ}$ C, 25 $^{\circ}$ C and 35 $^{\circ}$ C injecting lysozyme and cytochrome c, onto a SP Sepharose FF column. The absorbance was measured at 420 nm and 280 nm in the case of cytochrome c and lyzosime, respectively. The operational paramteres were the following: Salt gradient length $v_g = 300$ mL; flow rate 1.6 mL/min; column length $z = 20$ cm.	56

Figure 3.2. Overlapped chromatograms obtained at 15 °C, 25 °C and 35 °C injecting lysozyme and cytochrome c, onto a SP Sepharose XL column. The absorbance was measured at 420 nm and 280 nm in the case of cytochrome c and lyzosime, respectively. The operational paramteres were the following: Salt gradient length $v_g = 300$ mL; flow rate 1.6 mL/min; column length $z = 20$ cm.	57
Figure 3.3. Overlapped chromatograms obtained at 15 °C, 25 °C and 35 °C injecting lysozyme and cytochrome c, onto a SP Sepharose HP column. The absorbance was measured at 420 nm and 280 nm in the case of cytochrome c and lyzosime, respectively. The operational paramteres were the following: Salt gradient length $v_g = 300$ mL; flow rate 1.6 mL/min; column length $z = 20$ cm.	57
Figure 3.4. Equilibrium isotherms obtained at pH 7 with 30mM NaCl with lysozyme (top) and Cytochrome C (bottom) adsorbing onto SPFF, SPHP and SPXL at 15 °C, 25 °C and 35 °C. The chromatographic surfaces were placed in contact with protein solutions and the equilibrium concentration was determined after 16 hours.	59
Figure 3.5. Specific thermodynamic parameters of adsorption of both cytochrome c (Right) and lysozyme (Left) onto SPHP at 15 °C, 25 °C and 35 °C with 30mM NaCl pH7. Symbols represent Δh^{ads} (O), Δg^{ads} (▲) and $T\Delta s^{ads}$ (●). Enthalpy values was considered constant along the studied concentrations.	61
Figure 3.6. Specific thermodynamic parameters of adsorption of both cytochrome c (Left) and lysozyme (Right) onto SPFF at 15 °C, 25 °C and 35 °C with 30mM NaCl pH7. Symbols represent Δh^{ads} (O), Δg^{ads} (▲) and $T\Delta s^{ads}$ (●). Enthalpy values was considered constant along the studied concentrations.	62
Figure 3.7. Specific thermodynamic parameters of adsorption of both cytochrome c (Left) and lysozyme (Right) onto SPXL at 25 °C with 30mM NaCl pH7. Symbols represent Δh^{ads} (O), Δg^{ads} (▲) and (●). Enthalpy values was considered constant along the studied concentrations.	63

Figure 4.1. Typical thermogram obtained titrating BSA monomer at 20 mg/mL onto Toyopearl Q600AR and the respective blank trials. Buffer was 10 mM TRIS, 30 mM NaCl at pH 7, 25°C. 78

Figure 4.2. $GH-I_R$ curves for all the tested chromatographic surfaces at pH 7 (A) and pH 8.5 (B).; Q Sepharose FF (Δ), Q Sepharose XL (\blacktriangledown), Toyopearl Q600-AR (O), Toyopearl SuperQ-650M (\blacksquare), Toyopearl GigacapQ 650M (\bullet). Note that both axes have a logarithmic scale. The experimental data were fitted using $GH-I_R$ model equation (Yamamoto 2005), and A and B values were calculated. Mobile phase A: 10 mM TRIS, 30 mM NaCl; mobile phase B: 10 mM TRIS, 1M NaCl. 80

Figure 4.3. Equilibrium adsorption isotherms obtained at 25 °C at pH 7 (A) and pH 8.5 (B); Q Sepharose FF (Δ), Q Sepharose XL (\blacktriangledown), Toyopearl Q600-AR (O), Toyopearl SuperQ-650M (\blacksquare), Toyopearl GigacapQ 650M (\bullet). 10 mM TRIS, 30 mM NaCl. 83

Figure 4.4. Fig. 4. Linear relations between the change in adsorption enthalpy (Δh^{ads}) directly measured by ITC and the BSA_m elution salt concentration (I_R) determined with linear gradient chromatography. (A) pH 7, (B) pH 8.5. Grafted layer chromatographic surfaces are represented with black circle while the model conventional non-grafted surface is represented with an open circle. 86

List of Tables

Table 1.1. Various fields or events in which adsorption of proteins onto solid surfaces plays an important role. The open circle symbol (○) indicates the factors that are primarily important in the function or efficiency of the events. Adapted and transformed from (Nakanishi, Sakiyama, and Imamura 2001).....	2
Table 1.2. Summary of main techniques that can be used to study adsorption. Adapted from (Nakanishi, Sakiyama, and Imamura 2001). ¹ Search results obtained on scopus.com by searching the technique name followed by the word “adsorption” from 1989 to 2019.	5
Table 1.3. Adsorption mechanisms subtopics applied to chromatography	8
Table 1.4. Assumptions for linear van’t Hoff expression in chromatography	14
Table 1.5. Summary of discrepancies found in literature between indirect and direct methods for enthalpy determination. Note that not all of them apply to adsorption studies.	24
Table 2.1. A and B values obtained from LGE experiments. ¹ Calculated at 20% ethanol using eq. 32.....	39
Table 2.2. Enthalpy of adsorption obtained with isothermal titration calorimetry at different temperatures.	41
Table 2.3. Thermodynamic parameters for adsorption of Catechin and EGCG onto PS-DVB determined using the van’t Hoff equation	42
Table 2.4. Average enthalpy values obtained by chromatography data (van’t Hoff analysis and by ITC) from catechin and EGCG adsorbing onto PS-DVB. $\Delta h^{ads,ITC}$ values are averaged for all temperatures for comparison.	42
Table 3.1. Summary of the chromatography surfaces used in this study along with the physical properties disclosed by the manufacturer.....	49

Table 3.2. Summary of model proteins used in this study together with their physical properties. ^a Determined with PDBePISA bioinformatics tool from Protein Data Bank in Europe. ^b Determined with Protein Dipole Moments Server, according to previous authors (Bharti n.d.). ^c from the literature (Yao and Lenhoff 2005).	50
Table 3.3. Retention volumes obtained for cytochrome c and lysozyme. These were determined by linear gradient elution at a constant salt gradient slope of 400 mL.....	58
Table 3.4. Average of Δh_{ads} , Δg_{ads} and $T\Delta s_{ads}$ obtained for the adsorption of cytochrome c and lysozyme at pH 7 with 30mM NaCl, phosphate buffer. The equilibrium constant K was obtained using equation 42	64
Table 3.5. Average of Δh_{ads} , Δg_{ads} and $T\Delta s_{ads}$ obtained for the adsorption of cytochrome c with 10 mM boric acid with 200 mM NaCl at pH 10. In the case of lysozyme, 10 mM boric acid with 75 mM NaCl at pH 11 was used.	67
Table 4.1. Summary of physical properties of chromatographic resins used in this study. Information was given by the manufacturers.....	73
Table 4.2. Summary of chromatographic retention data and change in adsorption enthalpy. ¹ at $GH=0.025$	84

List of Common Abbreviations

BSAm	Monomer bovine serum albumin
Cyt	Equine cytochrome c
EDL	Electrical double layer
EGCG	Epigallocatechin Gallate
FMC	Flow microcalorimetry/calorimeter
IE	Isocratic elution
IEC	Ion exchange chromatography
ITC	Isothermal titration calorimetry
LGE	Linear gradient elution
Lys	Chicken egg-white lysozyme
PS-DVB	Polystyrene-divinylbenzene
SPFF (QFF)	SP(Q) Sepharose Fast Flow
SPHP	SP Sepharose High Performance
SPXL(QXL)	SP(Q) Sepharose XL

References

- Aguilar, Marie-Isabel and Milton T. W. Hearn. 1996. "High-Resolution Reversed-Phase High-Performance Liquid Chromatography of Peptides and Proteins." Elsevier.
- Aguilar, P., A. Twarda, F. Sousa, and A. C. Dias-Cabral. 2014. "Thermodynamic Study of the Interaction between Linear Plasmid Deoxyribonucleic Acid and an Anion Exchange Support under Linear and Overloaded Conditions." *Journal of Chromatography A* 1372:166–73.
- Alberts, Bruce, Alexander Johnson, Julian Lewis, Martin Raff, Keith Roberts, and Peter Walter. 2002. *Analyzing Protein Structure and Function*. Garland Science.
- Arima, Yusuke and Hiroo Iwata. 2007. "Effects of Surface Functional Groups on Protein Adsorption and Subsequent Cell Adhesion Using Self-Assembled Monolayers." *Journal of Materials Chemistry* 17(38):4079.
- Atkins, P. W. and Julio. De Paula. 2010. *Atkins' Physical Chemistry*. Oxford University Press.
- Baker, B. M. and K. P. Murphy. 1996. "Evaluation of Linked Protonation Effects in Protein Binding Reactions Using Isothermal Titration Calorimetry." *Biophysical Journal* 71(4):2049–55.
- Bernard Cohen, I. 1958. *Isaac Newton's Papers and Letters on Natural Philosophy*. Cambridge, Massachusetts: Harvard University Press.
- Beyer, Beate and Alois Jungbauer. 2018. "Conformational Changes of Antibodies upon Adsorption onto Hydrophobic Interaction Chromatography Surfaces." *Journal of Chromatography A* 1552:60–66.
- Bharti, Bhuvnesh. 2012. *Adsorption, Aggregation and Structure Formation in Systems of Charged Particles: From Colloidal to Supracolloidal Assembly*. Springer.
- Blaschke, Tim, Jefferson Varon, Albert Werner, and Hans Hasse. 2011. "Microcalorimetric Study of the Adsorption of PEGylated Lysozyme on a Strong Cation Exchange Resin." *Journal of Chromatography A* 1218(29):4720–26.

- Blaschke, Tim, Albert Werner, and Hans Hasse. 2013. "Microcalorimetric Study of the Adsorption of Native and Mono-PEGylated Bovine Serum Albumin on Anion-Exchangers." *Journal of Chromatography. A* 1277:58–68.
- Bowen, W. Richard and Enda B. Moran. 1995. "Ion Exchange of Amino Acids at a Natural Organic Ion Exchanger: Thermodynamics and Energetics." *Biotechnology and Bioengineering* 48(6):559–72.
- Bowes, B. D., S. J. Traylor, S. M. Timmick, K. J. Czymmek, and A. M. Lenhoff. 2012. "Insights into Protein Sorption and Desorption on Dextran-Modified Ion-Exchange Media." *Chemical Engineering and Technology* 35(1):91–101.
- Castellano, Brian M. and Daryl K. Eggers. 2013. "Experimental Support for Desolvation Energy Term in Governing Equations for Binding Equilibria." *The Journal of Physical Chemistry. B* 117(27):8180–88.
- Chaires, Jonathan B. 1997. "Possible Origin of Differences between van't Hoff and Calorimetric Enthalpy Estimates." *Biophysical Chemistry* 64(1–3):15–23.
- Chen, Wen-Yih, Ming-Shen Lin, Po-Hsun Lin, Pei-Shun Tasi, Yung Chang, and Shuichi Yamamoto. 2007. "Studies of the Interaction Mechanism between Single Strand and Double-Strand DNA with Hydroxyapatite by Microcalorimetry and Isotherm Measurements." *Colloids and Surfaces A: Physicochemical and Engineering Aspects* 295(1–3):274–83.
- Chen, Wen Yih, Hsiang Ming Huang, Chien Chen Lin, Fu Yung Lin, and Yu-Chia Chan. 2003. "Effect of Temperature on Hydrophobic Interaction between Proteins and Hydrophobic Adsorbents: Studies by Isothermal Titration Calorimetry and the van't Hoff Equation." *Langmuir* 19(22):9395–9403.
- Chen, Wen Yih, Ming Shen Lin, Po Hsun Lin, Pei Shun Tasi, Yung Chang, and Shuichi Yamamoto. 2007. "Studies of the Interaction Mechanism between Single Strand and Double-Strand DNA with Hydroxyapatite by Microcalorimetry and Isotherm Measurements." *Colloids and Surfaces A: Physicochemical and Engineering Aspects* 295(1–3):274–83.
- Cherry, John P. 1988. *Methods for Protein Analysis*. The American Oil Chemists Society.
- Cliff, Matthew J., Aldo Gutierrez, and John E. Ladbury. 2004. "A Survey of the Year

- 2003 Literature on Applications of Isothermal Titration Calorimetry.” *Journal of Molecular Recognition* 17(6):513–23.
- Connelly, P. R., R. a Aldape, F. J. Bruzzese, S. P. Chambers, M. J. Fitzgibbon, M. a Fleming, S. Itoh, D. J. Livingston, M. a Navia, and J. a Thomson. 1994. “Enthalpy of Hydrogen Bond Formation in a Protein-Ligand Binding Reaction.” *Proceedings of the National Academy of Sciences of the United States of America* 91(5):1964–68.
- Delgado-Magnero, Karelia H., Pedro A. Valiente, Miriam Ruiz-Peña, Aurora Pérez-Gramatges, and Tirso Pons. 2014. “Unraveling the Binding Mechanism of Polyoxyethylene Sorbitan Esters with Bovine Serum Albumin: A Novel Theoretical Model Based on Molecular Dynamic Simulations.” *Colloids and Surfaces B: Biointerfaces* 116:720–26.
- DePhillips, Peter and Abraham M. Lenhoff. 2001. “Determinants of Protein Retention Characteristics on Cation-Exchange Adsorbents.” *Journal of Chromatography A* 933(1–2):57–72.
- Desch, Rebecca J., Jungseung Kim, and Stephen W. Thiel. 2014. “Interactions between Biomolecules and an Iron-Silica Surface.” *Microporous and Mesoporous Materials* 187:29–39.
- Dias-Cabral, A. C., A. S. Ferreira, J. Phillips, J. A. Queiroz, and Neville G. Pinto. 2005. “The Effects of Ligand Chain Length, Salt Concentration and Temperature on the Adsorption of Bovine Serum Albumin onto Polypropyleneglycol-Sepharose.” *Biomedical Chromatography* 19(8):606–16.
- Dias-Cabral, A. C., J. A. Queiroz, and N. G. Pinto. 2003. “Effect of Salts and Temperature on the Adsorption of Bovine Serum Albumin on Polypropylene Glycol-Sepharose under Linear and Overloaded Chromatographic Conditions.” *Journal of Chromatography A* 1018(2):137–53.
- Dieterle, Michael, Tim Blaschke, and Hans Hasse. 2008. “Microcalorimetric Study of Adsorption of Human Monoclonal Antibodies on Cation Exchange Chromatographic Materials.” *Journal of Chromatography A* 1205(1–2):1–9.
- Dong, Zhan-Bo, Yue-Rong Liang, Fang-Yuan Fan, Jian-Hui Ye, Xin-Qiang Zheng, and Jian-Liang Lu. 2011. “Adsorption Behavior of the Catechins and Caffeine

- onto Polyvinylpolypyrrolidone.” *Journal of Agricultural and Food Chemistry* 59(8):4238–47.
- Duboue-dijon, Elise and Damien Laage. 2015. “Characterization of the Local Structure in Liquid Water by Various Order Parameters.” *The Journal of Physical Chemistry B* 26(119):8406–18.
- Duff, Michael R., Jordan Grubbs, and Elizabeth E. Howell. 2011. “Isothermal Titration Calorimetry for Measuring Macromolecule-Ligand Affinity.” *Journal of Visualized Experiments* (55):2796–2800.
- Ee, J. Iunn W. U. L. 1996a. “Microcalorimetric Studies of the Interactions of Imidazole with Immobilized Cu (II): Effects of PH Value and Salt Concentration.” *Journal of Colloid and Interface Science* 242(190):236–41.
- Ee, J. Iunn W. U. L. 1996b. “Microcalorimetric Studies of the Interactions of Lysozyme with Immobilized Cu(II): Effects of PH Value and Salt Concentration.” *Journal of Colloid and Interface Science* 242(190):49–54.
- Elofsson, Ulla M., Marie A. Paulsson, and Thomas Arnebrant. 1997. “Adsorption of β -Lactoglobulin A and B: Effects of Ionic Strength and Phosphate Ions.” *Colloids and Surfaces B: Biointerfaces* 8(3):163–69.
- Esquibel-King, Maria A., Ana Cristina Dias-Cabral, Joao A. Queiroz, and Neville G. Pinto. 1999a. “Study of Hydrophobic Interaction Adsorption of Bovine Serum Albumin under Overloaded Conditions Using Flow Microcalorimetry.” *Journal of Chromatography A* 865(1–2):111–122.
- Esquibel-King, Maria A., Ana Cristina Dias-Cabral, Joao A. Queiroz, and Neville G. Pinto. 1999b. “Study of Hydrophobic Interaction Adsorption of Bovine Serum Albumin under Overloaded Conditions Using Flow Microcalorimetry.” *Journal of Chromatography A* 865(1–2):111–22.
- Færgeman, Nils Joakim, Bent W. Sigurskjold, Birthe B. Kragelund, Kim V. Andersen, and Jens Knudsen. 1996. “Thermodynamics of Ligand Binding to Acyl-Coenzyme A Binding Protein Studied by Titration Calorimetry.” *Biochemistry* 35(45):14118–26.
- Felder, Clifford E., Jaime Prilusky, Israel Silman, and Joel L. Sussman. 2007. “A Server and Database for Dipole Moments of Proteins.” *Nucleic Acids Research*

35:W512-521.

- Freiburger, Lee A., Karine Auclair, and Anthony K. Mittermaier. 2012. "Van 't Hoff Global Analyses of Variable Temperature Isothermal Titration Calorimetry Data." *Thermochimica Acta* 527:148–57.
- Freire, Ernesto, Obdulio L. Mayorga, and Martin Straume. 1990. "Isothermal Titration Calorimetry." *Analytical Chemistry* 62(18):950A-959A.
- Ganazzoli, Fabio and Giuseppina Raffaini. 2019. "Classical Atomistic Simulations of Protein Adsorption on Carbon Nanomaterials." *Current Opinion in Colloid & Interface Science* 41:11–26.
- Gill, D., D. Roush, K. Shick, and R. Willson. 1995. "Microcalorimetric Characterization of the Anion-Exchange Adsorption of Recombinant Cytochrome B5 and Its Surface-Charge Mutants." *Journal of Chromatography A* 715(1):81–93.
- Hackemann, Eva and Hans Hasse. 2017. "Influence of Mixed Electrolytes and PH on Adsorption of Bovine Serum Albumin in Hydrophobic Interaction Chromatography." *Journal of Chromatography A* 1521:73–79.
- Haidacher, D., A. Vailaya, and C. Horváth. 1996. "Temperature Effects in Hydrophobic Interaction Chromatography." *Proceedings of the National Academy of Sciences of the United States of America* 93(6):2290–95.
- Hao, Dongxia, Jia Ge, Yongdong Huang, Lan Zhao, Guanghui Ma, and Zhiguo Su. 2016. "Microscopic Insight into Role of Protein Flexibility during Ion Exchange Chromatography by Nuclear Magnetic Resonance and Quartz Crystal Microbalance Approaches." *Journal of Chromatography A* 1438:65–75.
- Horn, James R., John F. Brandts, and Kenneth P. Murphy. 2002. "Van't Hoff and Calorimetric Enthalpies II: Effects of Linked Equilibria." *Biochemistry* 41(23):7501–7.
- Hosono, M., R. Maeda, N. Yoshimoto, and S. Yamamoto. 2012. "Rational Method for Designing Efficient Chromatography Processes Based on the Iso-Resolution Curve." *Chemical Engineering & Technology* 35(1):198–203.
- Huang, Hm, Fy Lin, Wy Chen, and Rc Ruaan. 2000. "Isothermal Titration Microcalorimetric Studies of the Effect of Temperature on Hydrophobic

- Interaction between Proteins and Hydrophobic Adsorbents.” *Journal of Colloid and Interface Science* 229(2):600–606.
- Huang, Junfeng, Fangjun Wang, Mingliang Ye, and Hanfa Zou. 2014. “Enrichment and Separation Techniques for Large-Scale Proteomics Analysis of the Protein Post-Translational Modifications.” *Journal of Chromatography. A* 1372:1–17.
- Kabiri, Maryam and Larry D. Unsworth. 2014. “Application of Isothermal Titration Calorimetry for Characterizing Thermodynamic Parameters of Biomolecular Interactions: Peptide Self-Assembly and Protein Adsorption Case Studies.” *Biomacromolecules* 15:3463–73.
- Kalasin, Surachate and Maria M. Santore. 2009. “Non-Specific Adhesion on Biomaterial Surfaces Driven by Small Amounts of Protein Adsorption.” *Colloids and Surfaces B: Biointerfaces* 73(2):229–36.
- Katiyar, Amit, Stephen W. Thiel, Vadim V Guliants, and Neville G. Pinto. 2010. “Investigation of the Mechanism of Protein Adsorption on Ordered Mesoporous Silica Using Flow Microcalorimetry.” *Journal of Chromatography. A* 1217(10):1583–88.
- Kaufman, Eric D., Jennifer Belyea, Marcus C. Johnson, Zach M. Nicholson, Jennifer L. Ricks, Pavak K. Shah, Michael Bayless, Torbjörn Pettersson, Zsombor Feldotö, Eva Blomberg, Per Claesson, and Stefan Franzen. 2007. “Probing Protein Adsorption onto Mercaptoundecanoic Acid Stabilized Gold Nanoparticles and Surfaces by Quartz Crystal Microbalance and ζ -Potential Measurements.” 21(11):6053–62.
- Kawai, Tomomi, Kyoichi Saito, and William Lee. 2003. “Protein Binding to Polymer Brush, Based on Ion-Exchange, Hydrophobic, and Affinity Interactions.” *Journal of Chromatography B* 790(1–2):131–42.
- Komatsu, Yoshihiro, Shinichi Suematsu, Yoshihiro Hisanobu, Hideaki Saigo, Ryoko Matsuda, and Kyoko Hara. 1993. “Effects of PH and Temperature on Reaction Kinetics of Catechins in Green Tea Infusion.” *Bioscience, Biotechnology, and Biochemistry* 57(6):907–10.
- Korfhagen, Joseph, Ana C. Dias-Cabral, and Marvin E. Thrash. 2010. “Nonspecific Effects of Ion Exchange and Hydrophobic Interaction Adsorption Processes.”

Separation Science and Technology 45(14):2039–50.

- Ladisch, Michael R. 2001. *Bioseparations Engineering: Principles, Practice, and Economics*. Wiley.
- Latour, R. 2011. “Molecular Simulation Methods to Investigate Protein Adsorption Behavior at the Atomic Level.” *Comprehensive Biomaterials* 1:171–92.
- Liang, Juan and Georg Fieg. 2013. “A Combination of Experiments and Molecular Dynamics Simulation for the Investigation of the Ion-Exchange Adsorption of Biological Macromolecules.” *Computer Aided Chemical Engineering* 1:25–30.
- Lin, Fu-Yung, Chin-Sung Chen, Wen-Yih Chen, and Shuichi Yamamoto. 2001a. “Microcalorimetric Studies of the Interaction Mechanisms between Proteins and Q-Sepharose at PH near the Isoelectric Point (PI): Effects of NaCl Concentration, PH Value, and Temperature.” *Journal of Chromatography A* 912(2):281–89.
- Lin, Fu-Yung, Chin-Sung Chen, Wen-Yih Chen, and Shuichi Yamamoto. 2001b. “Microcalorimetric Studies of the Interaction Mechanisms between Proteins and Q-Sepharose at PH near the Isoelectric Point (PI).” *Journal of Chromatography A* 912(2):281–89.
- Lin, Fu-Yung, Wen-yih Chen, and Milton T. W. Hearn. 2002. “Thermodynamic Analysis of the Interaction between Proteins and Solid Surfaces : Application to Liquid Chromatography.” *Journal of Molecular Recognition* 15:55–93.
- Lin, Fu Yung, Wen Yih Chen, Ruoh Chyu Ruaan, and Hsiang Ming Huang. 2000. “Microcalorimetric Studies of Interactions between Protein and Hydrophobic Ligands in Hydrophobic Interaction Chromatography: Effects of Ligand Chain Length, Density, and the Amount of Bound Protein.” *Progress in Biotechnology* 16(C):59–62.
- Liu, Yongfeng, Qingqing Bai, Song Lou, Duolong Di, Jintian Li, and Mei Guo. 2012. “Adsorption Characteristics of (–)-Epigallocatechin Gallate and Caffeine in the Extract of Waste Tea on Macroporous Adsorption Resins Functionalized with Chloromethyl, Amino, and Phenylamino Groups.” *Journal of Agricultural and Food Chemistry* 60(6):1555–66.
- Liu, Yufeng and Julian M. Sturtevant. 1995. “Significant Discrepancies between van’t Hoff and Calorimetric Enthalpies. II.” *Protein Science* 4(2):2559–61.

- Liu, Yufeng and Julian M. Sturtevant. 1997. "Significant Discrepancies between van't Hoff and Calorimetric Enthalpies. III." *Biophysical Chemistry* 64(1-3):121-26.
- Lu, Jian R., Xiubo Zhao, and Mohammed Yaseen. 2007. "Protein Adsorption Studied by Neutron Reflection." *Current Opinion in Colloid & Interface Science* 12(1):9-16.
- Maity, Nirmalya, Gregory F. Payne, and Jennifer L. Chipchosky. 1991. "Adsorptive Separations Based on the Differences in Solute-Sorbent Hydrogen-Bonding Strengths." *Industrial & Engineering Chemistry Research* 30(11):2456-63.
- Makhatadze, G. I. and P. L. Privalov. 1993. "Contribution of Hydration to Protein Folding Thermodynamics. I. The Enthalpy of Hydration." *Journal of Molecular Biology* 232(2):639-59.
- Marques, F. S., G. L. Silva, M. E. Thrash, and A. C. Dias-Cabral. 2014. "Lysozyme Adsorption onto a Cation-Exchanger: Mechanism of Interaction Study Based on the Analysis of Retention Chromatographic Data." *Colloids and Surfaces. B, Biointerfaces* 122:801-7.
- Marston, Andrew, Maryse Hostettmann, and Kurt Hostettmann. 1986. *Preparative Chromatography Techniques*. Springer-Verlag.
- Martin, Cristina, Gunter Iberer, Antonio Ubiera, and Giorgio Carta. 2005. "Two-Component Protein Adsorption Kinetics in Porous Ion Exchange Media." *Journal of Chromatography A* 1079(1-2):105-15.
- Matsuda, Ryan, Jeanethe Anguizola, K. S. Joseph, and David S. Hage. 2012. "Analysis of Drug Interactions with Modified Proteins by High-Performance Affinity Chromatography: Binding of Glibenclamide to Normal and Glycated Human Serum Albumin." *Journal of Chromatography A* 1265:114-22.
- McCann, Nichola, Marcel Maeder, and Hans Hasse. 2011. "A Calorimetric Study of Carbamate Formation." *The Journal of Chemical Thermodynamics* 43(5):664-69.
- Mirani, Mohammad Reza and Farshad Rahimpour. 2015. "Thermodynamic Modelling of Hydrophobic Interaction Chromatography of Biomolecules in the Presence of Salt." *Journal of Chromatography A* 1422:170-77.
- Mizoue, Laura S. and Joel Tellinghuisen. 2004. "Calorimetric vs. van't Hoff Binding

- Enthalpies from Isothermal Titration Calorimetry: Ba²⁺-Crown Ether Complexation.” *Biophysical Chemistry* 110(1–2):15–24.
- Moo-Young, Murray. 2011. *Comprehensive Biotechnology*. Elsevier.
- Müller, E. 2005. “Properties and Characterization of High Capacity Resins for Biochromatography.” *Chemical Engineering & Technology* 28(11):1295–1305.
- Müller, Egbert. 2003. “Comparison between Mass Transfer Properties of Weak-Anion-Exchange Resins with Graft-Functionalized Polymer Layers and Traditional Ungrafted Resins.” *Journal of Chromatography A* 1006(1–2):229–40.
- Naghibi, H., A. Tamura, and J. M. Sturtevant. 1995. “Significant Discrepancies between van’t Hoff and Calorimetric Enthalpies.” *Proceedings of the National Academy of Sciences of the United States of America* 92(12):5597–99.
- Nakanishi, Kazuhiro, Takaharu Sakiyama, and Koreyoshi Imamura. 2001. “On the Adsorption of Proteins on Solid Surfaces, a Common but Very Complicated Phenomenon.” *Journal of Bioscience and Bioengineering* 91(3):233–44.
- Norde, W. and J. Lyklema. 1979. “Theory with Special Reference to the Adsorption of Human Plasma Albumin and Bovine Pancreas Ribonuclease at Polystyrene Surfaces.” *Journal of Colloid and Interface Science* 71(2):350–66.
- Norde, Willem. 1994. “Protein Adsorption at Solid Surfaces: A Thermodynamic Approach.” *Pure and Applied Chemistry* 66(3):491–96.
- Oberholzer, Matthew R. and Abraham M. Lenhoff. 1999. “Protein Adsorption Isotherms through Colloidal Energetics.” *Langmuir* 15(11):3905–14.
- Peterson, Elbert A. and Herbert A. Sober. 1956. “Chromatography of Proteins. I. Cellulose Ion-Exchange Adsorbents.” *Journal of the American Chemical Society* 78(4):751–55.
- Petrauskas, Vytautas, Eglė Maximowitsch, and Daumantas Matulis. 2015. “Thermodynamics of Ion Pair Formations Between Charged Poly(Amino Acid)S.” *The Journal of Physical Chemistry B* 119(37):12164–71.
- Pezzini, Jerome, Charlotte Cabanne, and Xavier Santarelli. 2009. “Comparative Study of Strong Anion Exchangers: Structure-Related Chromatographic

- Performances.” *Journal of Chromatography B* 877(24):2443–50.
- Phillips, Jessica M. and Neville G. Pinto. 2004. “Calorimetric Investigation of the Adsorption of Nitrogen Bases and Nucleosides on a Hydrophobic Interaction Sorbent.” *Journal of Chromatography A* 1036(1):79–86.
- Pogany, George A. 1985. “The Methodology of Industrial Research Author” edited by J. Worrall and G. Currie. *The British Journal for the Philosophy of Science* 36(3):309–13.
- Rabe, Michael, Dorinel Verdes, and Stefan Seeger. 2011. “Understanding Protein Adsorption Phenomena at Solid Surfaces.” *Advances in Colloid and Interface Science* 162(1–2):87–106.
- Röcker, Carlheinz, Matthias Pötzl, Feng Zhang, Wolfgang J. Parak, and G. Ulrich Nienhaus. 2009. “A Quantitative Fluorescence Study of Protein Monolayer Formation on Colloidal Nanoparticles.” *Nature Nanotechnology* 4(9):577–80.
- Rodler, Agnes, Rene Ueberbacher, Beate Beyer, and Alois Jungbauer. 2019. “Calorimetry for Studying the Adsorption of Proteins in Hydrophobic Interaction Chromatography.” *Preparative Biochemistry and Biotechnology* 49(1):1–20.
- Rosa, Sara A. S. L., C. L. da Silva, M. Raquel Aires-Barros, A. C. Dias-Cabral, and Ana M. Azevedo. 2018. “Thermodynamics of the Adsorption of Monoclonal Antibodies in Phenylboronate Chromatography: Affinity versus Multimodal Interactions.” *Journal of Chromatography A* 1569:118–27.
- Rowe, Gerald E., Hafida Aomari, Tatiana Chevaldina, Martin Lafrance, and Sylvie St-Arnaud. 2008. “Thermodynamics of Hydrophobic Interaction Chromatography of Acetyl Amino Acid Methyl Esters.” *Journal of Chromatography A* 1177(2):243–53.
- Rüdt, Matthias, Florian Gillet, Stefanie Heege, Julian Hitzler, Bernd Kalbfuss, and Bertrand Guélat. 2015. “Combined Yamamoto Approach for Simultaneous Estimation of Adsorption Isotherm and Kinetic Parameters in Ion-Exchange Chromatography.” *Journal of Chromatography A* 1413:68–76.
- Salim, Malinda, Brian O’Sullivan, Sally L. McArthur, and Phillip C. Wright. 2007. “Characterization of Fibrinogen Adsorption onto Glass Microcapillary Surfaces by ELISA.” *Lab Chip* 7(1):64–70.

- Seitz, R., R. Brings, and R. Geiger. 2005. "Protein Adsorption on Solid–Liquid Interfaces Monitored by Laser-Ellipsometry." *Applied Surface Science* 252(1):154–57.
- Servoli, Eva, Devid Maniglio, Maria Rosa Aguilar, Antonella Motta, Julio San Roman, Laurence A. Belfiore, and Claudio Migliaresi. 2008. "Quantitative Analysis of Protein Adsorption via Atomic Force Microscopy and Surface Plasmon Resonance." *Macromolecular Bioscience* 8(12):1126–34.
- Silva, G. L., F. S. Marques, M. E. Thrash, and A. C. Dias-Cabral. 2014. "Enthalpy Contributions to Adsorption of Highly Charged Lysozyme onto a Cation-Exchanger under Linear and Overloaded Conditions." *Journal of Chromatography. A* 1352:46–54.
- Sirk, Timothy W., Eugene F. Brown, Mendel Friedman, and Amadeu K. Sum. 2009. "Molecular Binding of Catechins to Biomembranes: Relationship to Biological Activity." 57(15):6720–28.
- Sirk, Timothy W., Eugene F. Brown, Amadeu K. Sum, and Mendel Friedman. 2008. "Molecular Dynamics Study on the Biophysical Interactions of Seven Green Tea Catechins with Lipid Bilayers of Cell Membranes." *Journal of Agricultural and Food Chemistry* 56(17):7750–58.
- Steudle, Alexander and Jürgen Pleiss. 2011. "Modelling of Lysozyme Binding to a Cation Exchange Surface at Atomic Detail: The Role of Flexibility." *Biophysical Journal* 100(12):3016–24.
- Thrash, Marvin E. and Neville G. Pinto. 2001. "Flow Microcalorimetric Measurements for Bovine Serum Albumin on Reversed-Phase and Anion-Exchange Supports under Overloaded Conditions." *Journal of Chromatography A* 908(1–2):293–99.
- Thrash, Marvin E. and Neville G. Pinto. 2002. "Characterization of Enthalpic Events in Overloaded Ion-Exchange Chromatography." *Journal of Chromatography A* 944(1–2):61–68.
- Tilton, Robert F., John C. Dewan, and Gregory A. Petsko. 1992. "Effects of Temperature on Protein Structure and Dynamics: X-Ray Crystallographic Studies of the Protein Ribonuclease-A at Nine Different Temperatures from 98 to 320K."

Biochemistry 31(9):2469–81.

Tsai, De-Hao, Frank W. DelRio, Athena M. Keene, Katherine M. Tyner, Robert I. MacCuspie, Tae Joon Cho, Michael R. Zachariah, and Vincent A. Hackley. 2011. “Adsorption and Conformation of Serum Albumin Protein on Gold Nanoparticles Investigated Using Dimensional Measurements and in Situ Spectroscopic Methods.” *Langmuir* 27(6):2464–77.

Ubiera, Antonio R. and Giorgio Carta. 2006. “Radiotracer Measurements of Protein Mass Transfer: Kinetics in Ion Exchange Media.” *Biotechnology Journal* 1(6):665–74.

Ueberbacher, Rene, Agnes Rodler, Rainer Hahn, and Alois Jungbauer. 2010. “Hydrophobic Interaction Chromatography of Proteins: Thermodynamic Analysis of Conformational Changes.” *Journal of Chromatography A* 1217(2):184–90.

Urmann, Marina, Heiner Graalfs, Matthias Joehnck, Lothar R. Jacob, and Christian Frech. 2010. “Antibodies: Characterisation of a Novel Stationary Phase Designed for Production-Scale Purification Characterization of a Novel Stationary Phase Designed for Production-Scale Purification Cation-Exchange Chromatography of Monoclonal Antibodies.” *MAbs* 0862(4):395–404.

Ustinov, Eugene. 2019. “Kinetic Monte Carlo Approach for Molecular Modeling of Adsorption.” *Current Opinion in Chemical Engineering* 24:1–11.

Verlaan, Jan P. J., Jan P. C. Bootsma, and G. Challa. 1982. “Immobilization of a Homogeneous Macromolecular Copper Catalyst for the Oxidative Coupling of Phenols.” *Journal of Molecular Catalysis* 14(2):211–18.

Vlachakis, Dimitrios, Elena Bencurova, Nikitas Papangelopoulos, and Sophia Kossida. 2014. “Current State-of-the-Art Molecular Dynamics Methods and Applications.” *Advances in Protein Chemistry and Structural Biology* 94:269–313.

Vuong, T. and P. A. Monson. 1996. “Monte Carlo Simulation Studies of Heats of Adsorption in Heterogeneous Solids.” *Langmuir* 12(22):5425–32.

Wang, Dongze, Xuemei Li, Xiangqun Jin, and Qiong Jia. 2019. “Design of Cucurbit[6]Uril-Based Hypercrosslinked Polymers for Efficient Capture of

- Albendazole.” *Separation and Purification Technology* 216:9–15.
- Weber, G. 1996. “Persistent Confusion of Total Entropy and Chemical System Entropy in Chemical Thermodynamics.” *Proceedings of the National Academy of Sciences* 93(15):7452–53.
- Weber, Gregorio. 1995. “Van’t Hoff Revisited: Enthalpy of Association of Protein Subunits.” *Journal of Physical Chemistry* 99(3):1052–59.
- Werner, Albert, Tim Blaschke, and Hans Hasse. 2012. “Microcalorimetric Study of the Adsorption of PEGylated Lysozyme and PEG on a Mildly Hydrophobic Resin: Influence of Ammonium Sulfate.” *Langmuir* 28(31):11376–83.
- Werner, Albert, Eva Hackemann, and Hans Hasse. 2014. “Temperature Dependence of Adsorption of PEGylated Lysozyme and Pure Polyethylene Glycol on a Hydrophobic Resin: Comparison of Isothermal Titration Calorimetry and van’t Hoff Data.” *Journal of Chromatography A* 1356:188–96.
- Willemsen, Oscar H., Margot M. E. Snel, Alessandra Cambi, Jan Greve, Bart G. De Groot, and Carl G. Figdor. 2000. “Biomolecular Interactions Measured by Atomic Force Microscopy.” *Biophysical Journal* 79(6):3267–81.
- Winzor, Donald J. and Craig M. Jackson. 2006a. “Interpretation of the Temperature Dependence of Equilibrium and Rate Constants.” *Journal of Molecular Recognition* 19(5):389–407.
- Winzor, Donald J. and Craig M. Jackson. 2006b. “Interpretation of the Temperature Dependence of Equilibrium and Rate Constants.” *Journal of Molecular Recognition : JMR* 19(August):389–407.
- Wiseman, Thomas, Samuel Williston, John F. Brandts, and Lung-Nan Lin. 1989. “Rapid Measurement of Binding Constants and Heats of Binding Using a New Titration Calorimeter.” *Analytical Biochemistry* 179(1):131–37.
- Yamamoto, S. and A. Kita. 2006. “Rational Design Calculation Method for Stepwise Elution Chromatography of Proteins.” *Food and Bioproducts Processing* 84(1):72–77.
- Yamamoto, Shuichi. 2005. “Electrostatic Interaction Chromatography Process for Protein Separations: Impact of Engineering Analysis of Biorecognition Mechanism on Process Optimization.” *Chemical Engineering and Technology*

28(11):1387–93.

- Yamamoto, Shuichi, Masashi Hakoda, Takahiro Oda, and Mareto Hosono. 2007. “Rational Method for Designing Efficient Separations by Chromatography on Polystyrene-Divinylbenzene Resins Eluted with Aqueous Ethanol.” *Journal of Chromatography A* 1162(1):50–55.
- Yamamoto, Shuichi, Masashi Nakamura, Christina Tarmann, and Alois Jungbauer. 2007. “Retention Studies of DNA on Anion-Exchange Monolith Chromatography Binding Site and Elution Behavior.” *Journal of Chromatography A* 1144:155–60.
- Yang, Zhen. 2009. “Hofmeister Effects: An Explanation for the Impact of Ionic Liquids on Biocatalysis.” *Journal of Biotechnology* 144(1):12–22.
- Yao, Yan and Abraham M. Lenhoff. 2005. “Electrostatic Contributions to Protein Retention in Ion-Exchange Chromatography . 2 . Proteins with Various Degrees of Structural Differences.” 77(7):2157–65.
- Yu, Linling, Lin Zhang, and Yan Sun. 2015. “Protein Behavior at Surfaces: Orientation, Conformational Transitions and Transport.” *Journal of Chromatography A* 1382:118–34.
- Zhang, Junfang, M. B. Clennell, D. N. Dewhurst, and Keyu Liu. 2014. “Combined Monte Carlo and Molecular Dynamics Simulation of Methane Adsorption on Dry and Moist Coal.” *Fuel* 122:186–97.
- Zhang, Lin and Yan Sun. 2010. “Molecular Simulation of Adsorption and Its Implications to Protein Chromatography: A Review.” *Biochemical Engineering Journal* 48(3):408–15.
- Zhao, XiuBo, Fang Pan, and Jian R. Lu. 2009. “Interfacial Assembly of Proteins and Peptides: Recent Examples Studied by Neutron Reflection.” *Journal of The Royal Society Interface* 6(5):659–70.
- Zhou, Feng, Mengmeng Wang, Lin Yuan, Zhenping Cheng, Zhaoqiang Wu, and Hong Chen. 2012. “Sensitive Sandwich ELISA Based on a Gold Nanoparticle Layer for Cancer Detection.” *The Analyst* 137(8):1779.
- Zhou, Jian, Jie Zheng, and Shaoyi Jiang. 2004. “Molecular Simulation Studies of the Orientation and Conformation of Cytochrome c Adsorbed on Self-Assembled

Monolayers.” *Journal of Physical Chemistry B* 108(45):17418–24.

Acknowledgments

The author is indebted to Prof. Dr. Hiromori Tsutsumi, Prof. Dr. Rinji Akada, Prof. Dr. Kenjiro Onimura and Prof. Dr. Kazuhiro Tanaka (Department of Applied Chemistry, Graduate School of Sciences and Technology for Innovation, Yamaguchi University) for the valuable comments and critics during the completion of this work.

The author is sincerely grateful to Prof. Dr. Shuichi Yamamoto (Department of Applied Chemistry, Graduate School of Sciences and Technology for Innovation, Yamaguchi University) for the helpful guidance that led to the completion of this work. The author is greatly indebted to Prof. Dr. Noriko Yoshimoto (Department of Applied Chemistry, Graduate School of Sciences and Technology for Innovation, Yamaguchi University) for the enormous amount of time she spent for day-to-day supervision, support, critical thoughts, revision and everything else. The author would like to thank both of his supervisors for allowing work flexibility that permitted the author to grow as an independent researcher.

The author gratefully acknowledges the financial support by the Ministry of Education, Culture, Sports, Science and Technology of Japan for supporting the stay at Yamaguchi University.

The author is also indebted to Prof. Dr. Ales Podgornik, Prof. Dr. Cristina Dias-Cabral and Prof. Dr. Giorgio Carta for the help and support for the development of this thesis.

The author is thankful to MSc Hiroshi Kojo, MSc Shumpei Yamamoto and MSc Suriah Ali for their kind words of encouragement and companionship throughout their stay in Yamaguchi University.

The author would also like to thank Nanako Hoshino and Makoto Nakashima for their work on side projects closely related to the work presented here. Any PhD thesis represent the work of more than one researcher. This thesis is no exception.

The author would like to thank all the great colleagues in the Bio-processes Lab: Watanabe T., Tanaka M., Yuko N., Kishi Y, Arakawa Y., Ono Y., Yoshizaki Y., Ando K., Ikeda K., Kenta N., Tanaka T., Matsuzaki T., Chyi-Shin C., Tanaka D..

The author also thanks Paloma Ortiz Albo, Hu Liang Jun, Catarina Nunes, Tsuji Tatsumi and Naoya Senokuchi for playing a tremendous role on both personal and academic life in Japan.

The author is grateful to Catarina Lima, Patrícia Aguilar, Filipa Pires, Gregory Dutra and Lam Kin Man for all the encouragement.

Finally, the author would to thank his parents for their continuous and heartily encouragement.

